

**HOLISTIC WATERSHED MANAGEMENT FOR EXISTING AND FUTURE LAND  
USE DEVELOPMENT ACTIVITIES: OPPORTUNITIES FOR ACTION FOR LOCAL  
DECISION MAKERS: PHASE 1 – MODELING AND DEVELOPMENT OF FLOW  
DURATION CURVES (FDC 1 PROJECT)**

**SUPPORT FOR SOUTHEAST NEW ENGLAND PROGRAM (SNEP)  
COMMUNICATIONS STRATEGY AND TECHNICAL ASSISTANCE**

**TASK 6 TECHNICAL MEMO**

**JULY 26, 2021**

Prepared for:

**U.S. EPA Region 1**



Prepared by:

**Paradigm Environmental**



**Great Lakes Environmental Center**



Blanket Purchase Agreement: BPA-68HE0118A0001-0003

Requisition Number: PR-R1-20-00322

Order: 68HE0121F0001

---

## Table of Contents

1	Introduction .....	5
2	LSPC Model Configuration, Calibration, and Validation .....	6
2.1	Configuration .....	6
2.1.1	Sub-watersheds .....	6
2.1.2	Channel Geometry .....	9
2.1.3	Baseline Boundary Conditions .....	11
2.1.4	Climate Change Scenarios .....	11
2.1.5	Point Source Withdrawals .....	13
2.2	Calibration and Validation .....	13
2.3	HRU Based Water Quality Calibration .....	20
3	Modeling Results .....	22
3.1	Baseline Unit-Area Analysis .....	22
3.2	Relationships Between Impervious Cover and Watershed Function .....	26
3.2.1	Land-use Scenarios .....	34
3.2.2	Pollutant Export .....	44
3.2.3	Climate Change Scenarios .....	44
3.3	Carbon Sequestration .....	55
3.4	Conclusions .....	59
4	Updates To Opti-Tool .....	59
4.1	SCM Groundwater Recharge .....	60
4.2	Flow Duration Curve Evaluation .....	63
5	Next Steps .....	65
5.1	GIS Screening to Identify SCM Opportunities .....	65
5.2	SCM Modeling with FDC Optimization Objective .....	67
5.3	Final Project Report .....	67
5.4	Outreach Materials .....	67
6	References .....	68

## Figures

Figure 1. HSPF/LSPC subbasins for the Wading River, used for calibration and validation. ....	7
Figure 2. LSPC sub-watersheds for the Wading River, used for scenario testing. ....	8
Figure 3. Wading River Cross Section (SWS 4) in LSPC. ....	9
Figure 4. Location of dams and study sub-watersheds. ....	10
Figure 5. Representative Concentration Pathways for climate change analysis (International Institute for Applied Systems Analysis, 2009). ....	12
Figure 6. Comparison of Observed and Predicted Daily Flows for the Calibration (top), Validation (middle), and Baseline (bottom) periods, Wading River, MA. ....	17
Figure 7. Comparison of Observed and Predicted Normalized Monthly Streamflow for the Calibration (top), Validation (middle), and Baseline (bottom) periods, Wading River, MA. ....	18
Figure 8. Comparison of Observed and Predicted Flow Duration Curves for the Calibration (top), Validation (middle), and Baseline (bottom) periods, Wading River, MA. ....	19
Figure 9. Performance Metric Summary for the Calibration (top), Validation(middle), and Baseline (bottom) periods, Wading River, MA. ....	20
Figure 10. Water Balance for LSPC Hydrological Response Units, Summarized by Land Use. Baseline Simulation 2000-2020. ....	23
Figure 11. Water Balance for LSPC Hydrological Response Units, Summarized by Soil Group. Baseline Simulation 2000-2020. ....	24
Figure 12. Water Balance for LSPC sub-watersheds. ....	25
Figure 13. Standard FDC (top) and Normalized FDCs [ <i>daily flow ft<sup>3</sup>watershed area ft<sup>2</sup></i> ] (bottom) for the three study watersheds. ....	27
Figure 14. Ecosurplus and Ecodeficit for Upper Hodges compared to Lower Hodges. ....	28
Figure 15. Average monthly discharge and runoff depth for the three study watersheds. ....	29
Figure 16. Monthly Water Balance with standard (top) and logarithmic (bottom) for the three study watersheds. ....	30
Figure 17. Richard Baker Flashiness Index for the 20-year baseline simulation for the three study sub-watersheds. ....	31
Figure 18. Comparison of Richard Baker Flashiness Index for the 20-year baseline simulation for the three study sub-watersheds. ....	32
Figure 19. Flow Duration Curves for Upper Hodges Brook watershed for baseline, predevelopment, EIA=TIA, and EIA=0 conditions. Baseline FDC is black with a yellow highlight. ....	35
Figure 20. High flow (top) and low flow (bottom) sections of the FDC-presented in Figure 19. Baseline FDC is black with a yellow highlight. ....	36
Figure 21. Water balances and Ecosurplus and Ecodeficit for Upper Hodges Brook watershed for baseline and EIA=TIA conditions. EIA=TIA reflects an increase in directly connected impervious surfaces. Black dots indicate places where FDCs cross. ....	37
Figure 22. Water balances and Ecosurplus for Upper Hodges Brook watershed for baseline and forested/pre-development conditions. Ecosurplus calculated relative to forested/pre-development conditions. ....	38
Figure 23. Water balances and Ecosurplus/Ecodeficit for Upper Hodges Brook watershed for baseline and EIA = 0 (all existing impervious surfaces disconnected). Ecosurplus/Ecodeficit calculated relative to baseline/existing condition. Black dots indicate places where FDCs cross ....	39
Figure 24. Average (top) and minimum (bottom) monthly flows for land use scenarios. Minimum flows are presented on a logarithmic scale. ....	40
Figure 25. Three-day minimum (top) and maximum (bottom) flow for land-use scenarios. ....	41
Figure 26. Richard-Baker Flashiness Index for land-use scenarios. ....	42
Figure 27. Pollutant export comparisons across land-use scenarios. ....	44
Figure 28. Ensemble results for ecosurplus and ecodeficits. ....	45
Figure 29. Ecodeficit FDCs at the Wading River USGS Gage (01109000) under baseline and climate change scenarios for RCP 8.5 (top) and RCP 4.5 (bottom). ....	46
Figure 30. Ecosuplus FDCs at the Wading River USGS Gage (01109000) under baseline and climate change scenarios for RCP 8.5 (top) and RCP 4.5 (bottom). ....	47

---

Figure 31. Results for the wet, median, and dry models for ecodeficits based on an RCP 4.5 scenario. Results are for the Wading River USGS Gage (01109000) under comparing baseline (2000-2020) to future climate scenarios (2079-2099).....	48
Figure 32. Results for the wet, median, and dry models for ecodeficits based on an RCP 8.5 scenario. Results are for Wading River USGS Gage (01109000) comparing baseline (2000-2020) to future climate scenarios (2079-2099). ....	49
Figure 33. Results for the wet, median, and dry models for ecosurpluses based on an RCP 4.5 scenario. Results are for Wading River USGS Gage (01109000) comparing baseline (2000-2020) to future climate scenarios (2079-2099).....	50
Figure 34. Results for the wet, median, and dry models for ecosurpluses based on an RCP 8.5 scenario. Results are for the Wading River USGS Gage (01109000) comparing baseline (2000-2020) to future climate scenarios (2079-2099).....	51
Figure 35. Aquifer information option in Opti-Tool.....	60
Figure 36. The number of aquifers option under Watershed Information window. ....	61
Figure 37. Aquifer Information user interface window.....	61
Figure 38. Aquifer selection under BMP Information user interface window. ....	62
Figure 39. Aquifer selection under Stream/Conduit Properties user interface window.....	62
Figure 40. Aquifer selection under Junction Properties user interface window. ....	63
Figure 41. Flow Duration Curve selection under Optimization Setup user interface window. ....	64
Figure 42. Flow Duration Curve evaluation factor.....	65

## Tables

Table 1. Summary of climate data input requirements by LSPC module.....	11
Table 2. Summary of Public Water Supply (PWS) and Non-Public Water Supply (NPWS) water use data incorporated into LSPC Wading River Model.....	13
Table 3. Summary of Permitted Groundwater Discharge data incorporated into the LSPC Wading River Model.....	13
Table 4. Calibration and Validation Simulation Periods for the LSPC Wading River Model.....	13
Table 5. Summary of performance metrics used to evaluate hydrology calibration .....	15
Table 6. Summary of annual average pollutant loading rate calibrated to HRU type for the study area....	21
Table 7. 3-day minimum and maximum flows for the three study watersheds .....	31
Table 8. Ecological and human risks associated with changing water tables/base flow. Adapted from Bhaskar et al., 2016.....	33
Table 9. Land-use Scenarios simulated using Upper Hodges Brook sub-watershed.....	34
Table 10. Comparison of average 3-day minimum and maximum flows for baseline and land-use scenarios .....	42
Table 11. Summary of average monthly flows and percent differences for land-use scenarios.....	43
Table 12. Selected models from ensemble results .....	45
Table 13. Summary of ecosurpluses and ecodeficits (millions of gallons per year) for RCP 8.5 and 4.5 scenarios .....	52
Table 14. Percent change in 3-day minimum and maximum flows for RCP 8.5 and 4.5 scenarios compared to baseline simulation .....	53
Table 15. Dry days and days with precipitation for the selected future climate scenarios compared to the historical, observed conditions.....	53
Table 16. Percent change for average annual and monthly precipitation for future climate scenarios compared to the historical, observed conditions.....	54
Table 17. Percent change for average maximum consecutive dry days for the future climate scenarios compared to the historical, observed conditions.....	54
Table 18. Percent change in average maximum daily temperature for the selected future climate scenarios compared to the historical, observed conditions.....	54
Table 19. Percent change in average minimum daily temperature for the selected future climate scenarios compared to the historical, observed conditions.....	55
Table 20. Percent change in average daily temperature for the selected future climate scenarios compared to the historical, observed conditions .....	55
Table 21. Carbon benefits and associated activities, indicators, and calculation methods (Brill et.al., 2021) .....	56
Table 22. Carbon pool default dataset by land use/land cover type in InVEST carbon model .....	57
Table 23. Cross-walk table for mapping HRU categories with land use/land cover type in Carbon pool dataset.....	58
Table 24. InVEST carbon model results for three pilot sub-watersheds .....	59
Table 25. Site suitability criteria for stormwater management categories.....	66

---

# 1 INTRODUCTION

---

The purpose of this technical memo is to present hydrological modeling results to quantify the changes to watershed functions associated with landscape conversion to impervious cover. An EPA Loading Simulation Program – C++ (LSPC) model was calibrated for the Wading River Watershed in Massachusetts and the most recent twenty-year period, 2000-2020 was used for baseline conditions. The analysis included unit-area modeling at the Hydrologic Response Unit (HRU) level to elucidate differences in the water balance for various land uses and soil types. The model results for three sub-watersheds with varying degrees of imperviousness were compared. Further investigation on the impact of imperviousness was conducted by varying the land use of one of the three study sub-watersheds over a range of development, from pre-development/forested conditions to fully connected impervious surfaces. Future climate conditions were simulated and the impact to flow metrics and water balances were quantified. Several graphics are presented that can be incorporated into factsheets to facilitate outreach and communication of the impact that impervious surfaces can have within a watershed.

The results support many well-established concepts about how impervious surfaces influence streamflow, especially stormflows. Additionally, the results suggest that the impact development has on baseflows can vary depending on the intensity of development. Compared to pre-development/forested conditions, development, including development that includes disconnected impervious surfaces, increased baseflows. However, baseflows fell below pre-development conditions when the amount of connected impervious surfaces was substantially increased. The results highlight four major mechanisms for flow duration curve (FDC) alteration: removal of vegetation, increase in impervious surfaces, conveyance of impervious surface runoff immediately to receiving waters, and conveyance of impervious surface runoff to infiltration based SCMs. The initial impact of development within a watershed is often the removal of vegetation. Evapotranspiration (ET) plays an important role in ‘natural’ flow regimes and as watershed development increases, the associated reduction in ET throughout the landscape can result in higher flows across the FDC. The loss of vegetative cover (forests), as well as an increase in impervious surfaces, shifts the water balance towards higher flows. As impervious surfaces increase, baseflows may again start to fall due to more water being conveyed immediately to receiving waters with fewer opportunities for infiltration. Additionally, point sources can also impact flows, although the study watersheds had minimal water withdrawals or discharges. The implementation of Stormwater Control Measures (SCMs) that disconnect existing impervious surfaces can reduce high flows and increase baseflows. The results provide important to extent to which restore predevelopment stream flows and improve watershed functions. While SCM implementation can mitigate some of the impacts of impervious surfaces, it may be difficult to attain pre-development watershed functions without landscape-level changes that promote additional evapotranspiration. The results support the findings of previous research efforts into the impact of development on stream flows, although other studies have found contradictory results. Results may be impacted by the geography and climate of the study area. The results of Task 7 are expected to improve our understanding of how various stormwater management approaches may impact the FDC under various land use and climate change scenarios.

This memo also describes updates to the Opti-Tool that were implemented to simulate groundwater recharge from SCMs and to optimize SCM implementation based on FDC evaluation. The modeling results of this task were discussed with the technical steering committee (TSC) members to get their expert opinion and guidance on interpreting the results in such a meaningful way that is easy to understand and communicate with the wider audience for outreach purposes.

---

## 2 LSPC MODEL CONFIGURATION, CALIBRATION, AND VALIDATION

---

### 2.1 Configuration

---

#### 2.1.1 *Sub-watersheds*

The domain of the Wading River LSPC model consisted of 43 square miles of watershed area and 27.6 miles of modeled stream reaches. The watersheds used in calibration were previously delineated for a previous modeling effort (Barbaro and Sorenson, 2013) in the Taunton watershed (Figure 1). The original HSPF model configuration, including hydrology parameter values, was transferred to the LSPC model. LSPC is based on HSPF algorithms but includes additional functionality, including easy linkage to Opti-Tool.

The original HSPF model included virtual reaches to represent the presence of wetlands in specific drainage areas. Generally, virtual wetland reaches were developed for watersheds in which wetlands composed 20 percent or more of the area (Barbaro and Sorenson, 2013). The Wading River LSPC model included one virtual reach for the representation of wetlands. The virtual reach represents the combined storage of all the non-forested wetlands in watershed 4 (Figure 1). Compared to stream reaches, discharge in virtual reach was configured to be low and increased substantially less as storage increased.

While the Wading River watersheds were included in the Taunton model calibrated by Barbaro and Sorenson, (2013), no Wading River gages were used during the calibration of that model. Therefore, while the calibrated HSPF model was obtained and converted to LSPC, additional calibration occurred to improve agreement between observed and predicted flows at the Wading River gage (0110900), calibration and validation are discussed in section 2.2.

After calibration and validation, a set of three smaller sub-watersheds (Figure 2) were used to quantify the impact of impervious surfaces and climate change on flow characteristics. The sub-watersheds were delineated using National Hydrography Dataset (NHD) watershed boundaries. As discussed in the previous memo (Task 5), the sub-watersheds were selected based on their representation of a range of watershed imperviousness. Pilot Tributary, Lower Hodges Brook, and Upper Hodges Brook have impervious surface areas comprising 4%, 20%, and 32% of the total sub-watershed area, respectively.



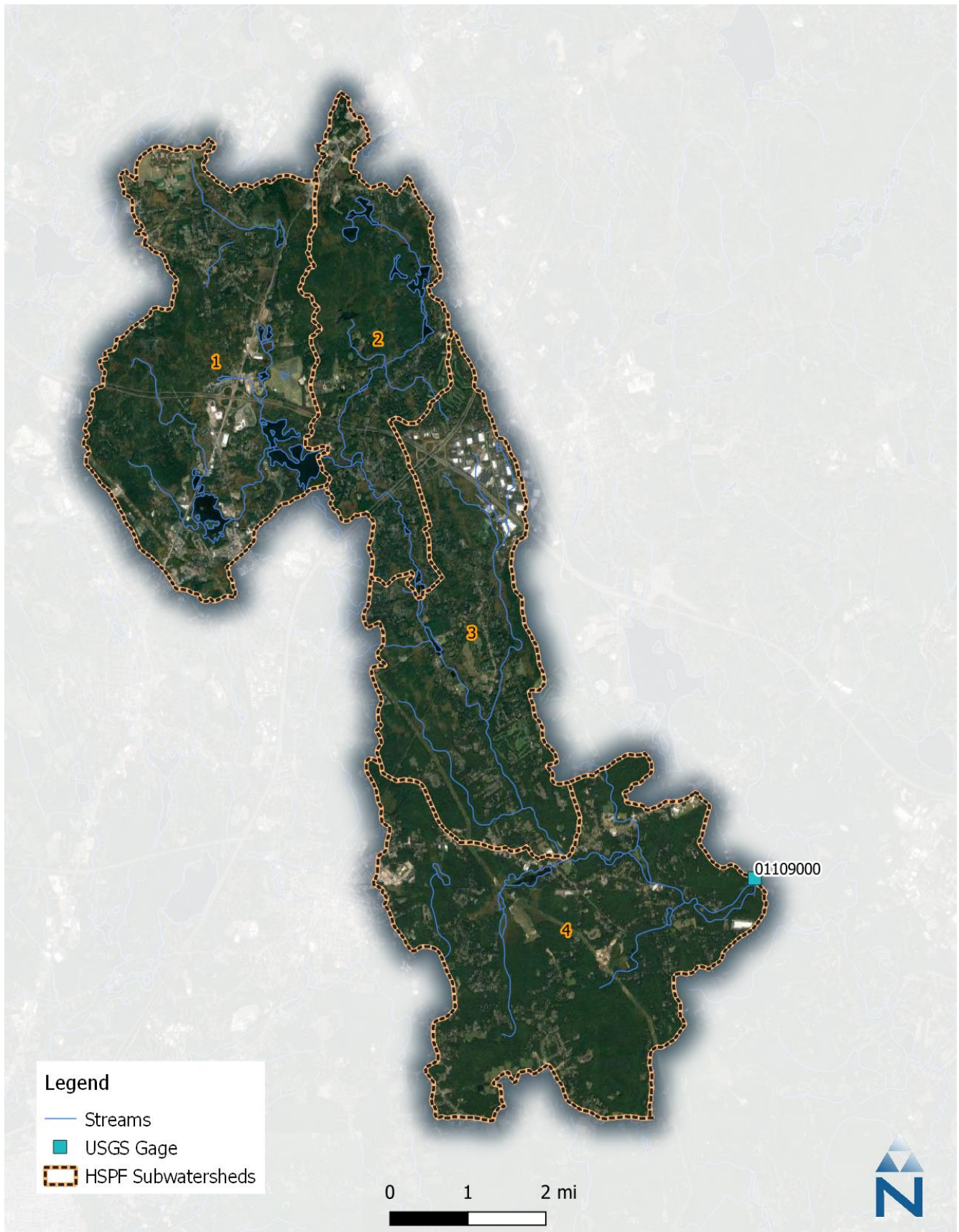


Figure 1. HSPF/LSPC subbasins for the Wading River, used for calibration and validation.



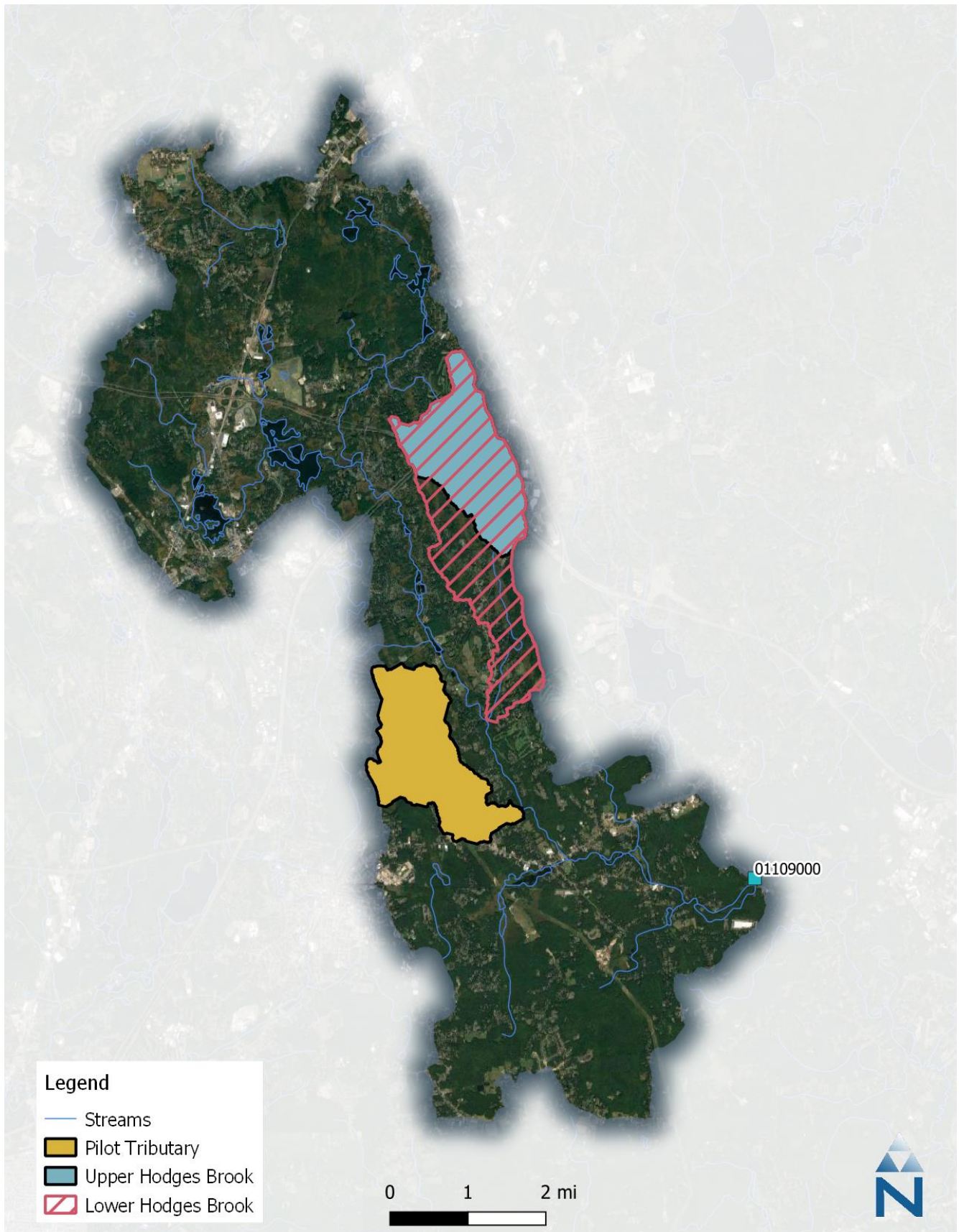


Figure 2. LSPC sub-watersheds for the Wading River, used for scenario testing.

### 2.1.2 Channel Geometry

LSPC routes streamflow and contaminants downstream using stage-storage-discharge relationships defined using an FTABLE (functional table). The basic channel geometry is a trapezoid, an example cross-section from the LSPC model is presented in Figure 3. By altering the stage, the cross-sectional geometry of the mainstem segments represented in LSPC affects the shape of the hydrograph through each sub-catchment. The majority of the original HSPF FTABLES were based on relationships between drainage areas, bankfull width, and bankfull depth (Leopold, 1994). The LSPC FTABLES were updated using more recent channel geometry equations (Bent and Waite, 2013) as follows:

$$\text{Bankfull width (ft)} = 10.6640 [\text{Drainage area (mi}^2\text{)}]^{0.3935} [\text{Mean basin slope (\%)}]^{0.1751} \tag{1}$$

$$\text{Bankfull mean depth (ft)} = 0.7295 [\text{Drainage area (mi}^2\text{)}]^{0.2880} [\text{Mean basin slope (\%)}]^{0.1346} \tag{2}$$

During calibration (Section 2.2), the FTABLES were revised to reflect the observed attenuation in the system, likely due in part to the proliferation of small dams and ponds in the area. However, Equations 1 and 2 were still used for the smaller study sub-watersheds given the lack of dams in those areas (Figure 4).

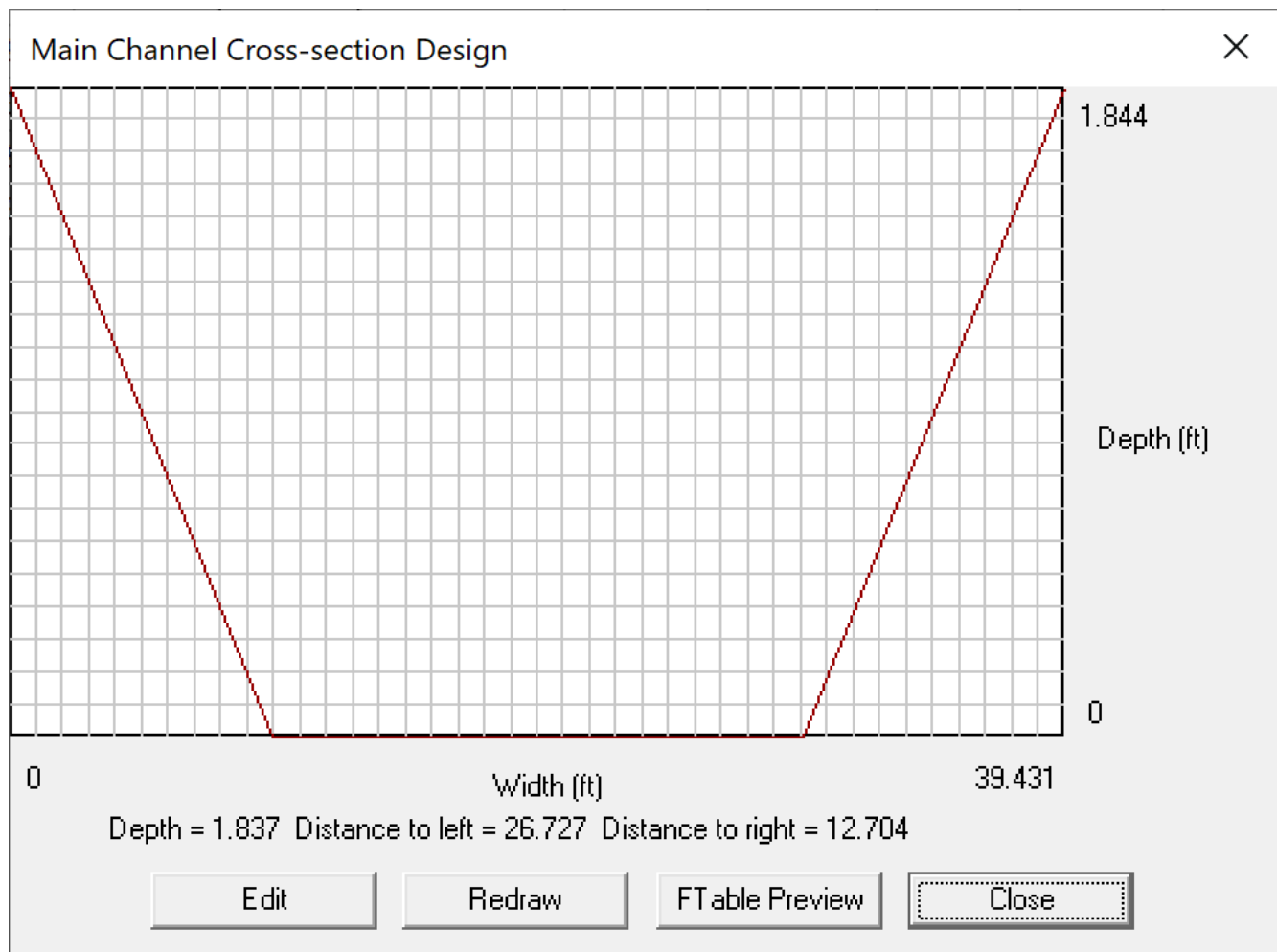


Figure 3. Wading River Cross Section (SWS 4) in LSPC.



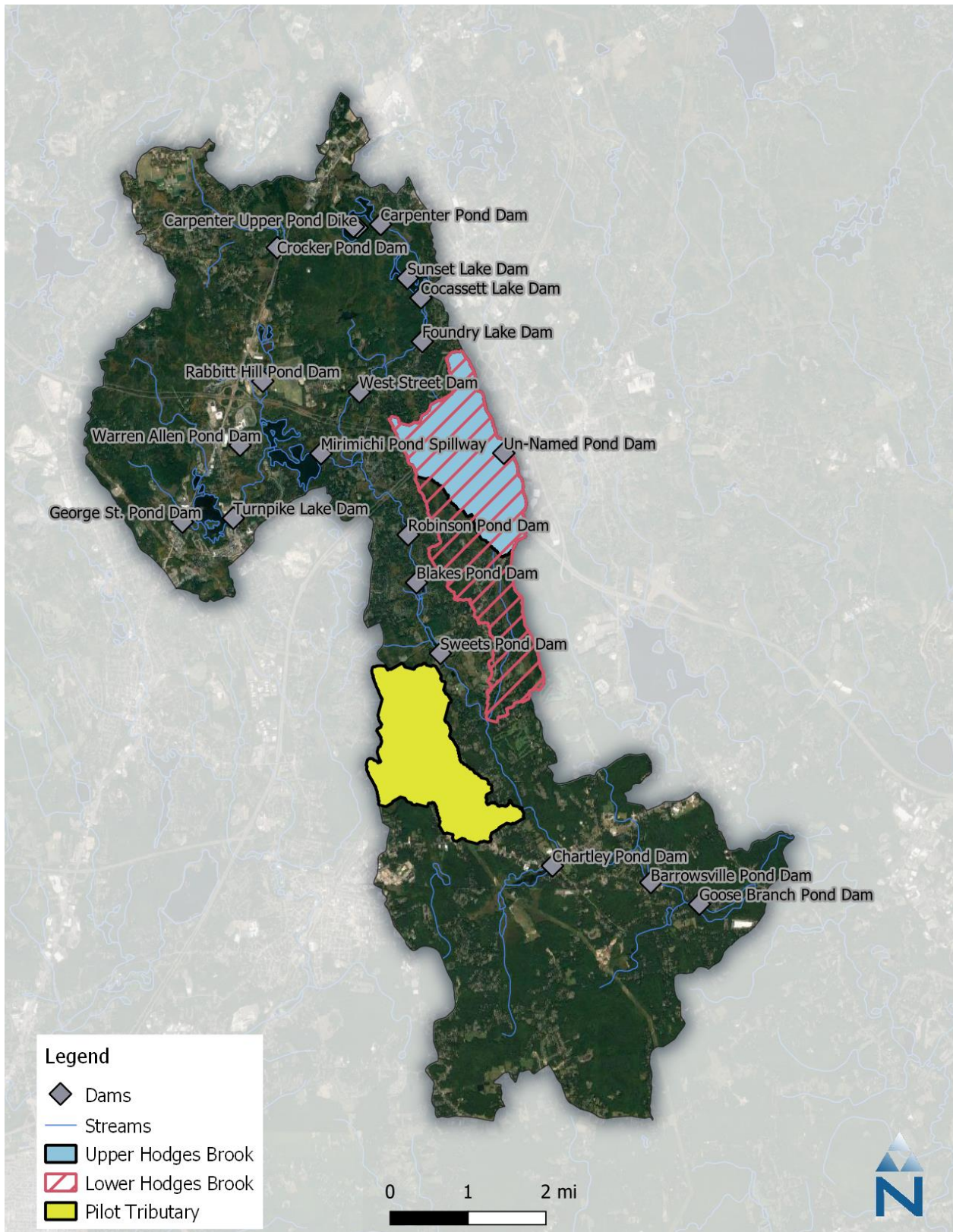


Figure 4. Location of dams and study sub-watersheds.

### 2.1.3 Baseline Boundary Conditions

Precipitation is the primary input to the LSPC water budget. Precipitation discharges to modeled reaches through overland flow, interflow, and active groundwater. The water budget in LSPC resolves the partitioning of rainfall to total actual evapotranspiration (TAET), interflow, groundwater, and overland flow determined for each watershed on an HRU-basis. The amount of TAET is in part determined by potential evapotranspiration (PET), a user input. The interaction of model parameters ultimately determines how much PEVT becomes TAET. Sources of evapotranspiration include groundwater outflow, interception storage, and soil moisture storage. Interflow and overland flow are then determined based on HRU characteristics, including soil infiltration rate, surface roughness, and slope. Precipitation and potential evapotranspiration drive the water balance for the snow accumulation/melt module. Table 1 presents a summary of the LSPC modules activated for the Wading River model. The Task 5 memo presents a detailed review of meteorological inputs.

**Table 1. Summary of climate data input requirements by LSPC module**

LSPC Module	Precipitation	Potential Evapotranspiration	Temperature	Dew Point	Wind Speed	Solar Radiation	Cloud Cover <sup>1</sup>
Snow Accumulation/Melt	●	●	●	●	●	●	--
Hydrology	●	●	--	--	--	--	--
Water Quality (GQUAL)	●	●	--	--	--	--	--

<sup>1</sup> While not required for any of the modules described in the above table, cloud cover inputs were included in the LSPC watershed model to provide flexibility for enhancing the model.

### 2.1.4 Climate Change Scenarios

The impact of climate change was assessed by downscaling available information from several General Circulation Models (GCMs). The future projection scenarios were based on 32 separate GCMs, each of which forecasted a future climate time series based on two Representative Concentration Pathways (RCPs). The RCP 4.5 predicts a stabilization of carbon emissions by 2100 while RCP 8.5 represents a scenario in which carbon emissions continue to climb at historical rates (Figure 5). However, current and pledged carbon emission reduction policies may mean that an RCP 8.5 scenario may be highly unlikely.

Generally, GCM climate change predictions are in the form of forecasted future time series at a daily timescale resolution. Because precipitation exhibits significant temporal variability, it can be challenging to create realistic predictions of future continuous (hourly) precipitation datasets needed for the dynamic hydrology model. However, various techniques have been developed to downscale hourly precipitation (Hwang and Graham, 2014). Localized Constructed Analogs (LOCA) have been used to downscale daily meteorological data, such as precipitation and wind velocity data to hourly resolution. Recently, the approach was successfully used to generate downscaled hourly precipitation for Los Angeles County in support of the County's Watershed Management Modeling System 2.0 ([WMMS2](#)) climate change study. Because of its effectiveness with such datasets, LOCA was selected to downscale hourly precipitation for the Wading River watershed.

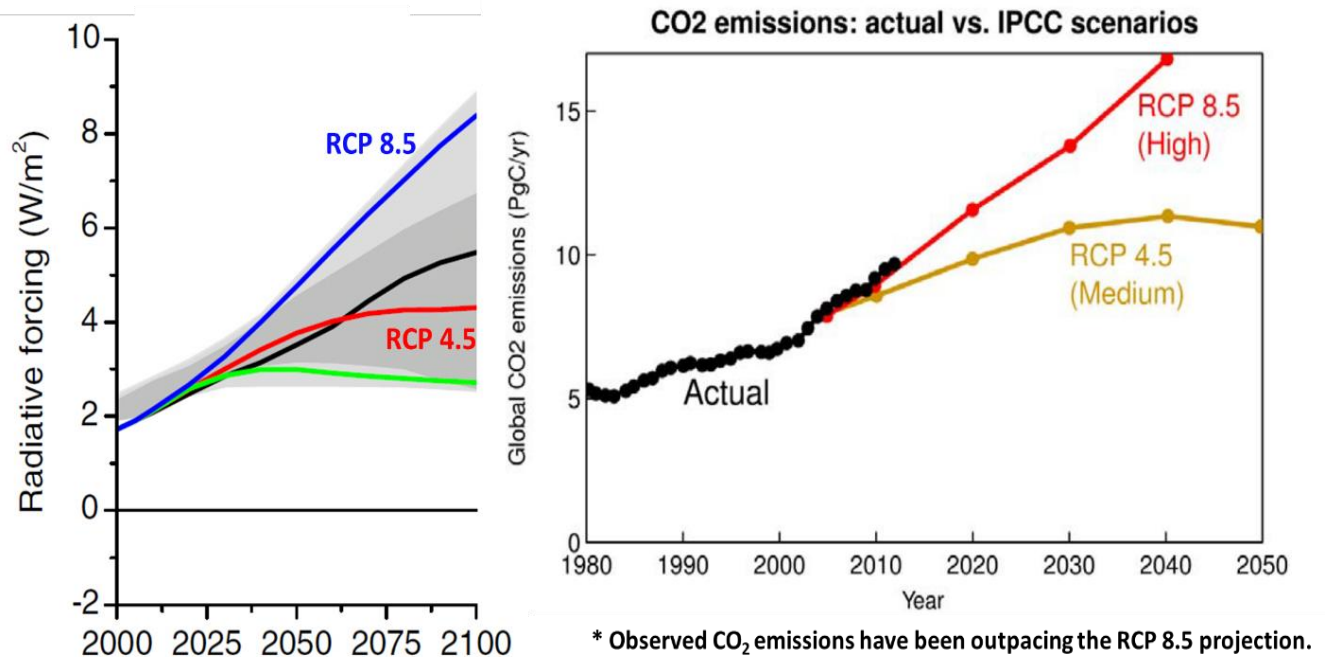


**Figure 5. Representative Concentration Pathways for climate change analysis (International Institute for Applied Systems Analysis, 2009).**

For a given day in the GCM climate model time series, the LOCA algorithm extracts GCM rainfall in the day preceding and following to create a three-day time series of daily rainfall. Then, it searches through the same observed rainfall time series used for the baseline boundary conditions to find the three days with the most similar rainfall. It extracts the second day from the most similar time series and scales it so that its total rainfall is equal to the daily rainfall from the climate model time series. This process repeats every day in the climate model time series. The result of this process was 64 hourly datasets (32 GCMs, 2 RCPs) of precipitation over the Wading River from 2005-2100, suitable for dynamic, continuous hydrologic modeling.

Similar downscaling techniques were applied to other meteorological variables, including temperature, potential evapotranspiration, wind speed, solar radiation, and dew point. Temperature, potential evapotranspiration, solar radiation, and dew point are all much less variable temporally than precipitation, and thus could be downscaled with simpler algorithms. For each future day, the daily average or daily total value for each variable was calculated, and then a historical diurnal cycle was fit to the daily value to create an hourly time series. While wind speed is temporally variable, the model is less sensitive to its impacts, which meant that a simple downscaling technique could be applied to the wind as well. To create an hourly wind time series, the hourly average wind was assumed to be equal to the daily average wind.

The above processes and algorithms were implemented in Python and converted to LSPC format for use as weather files. The Wading River LSPC model was ran using each of these 62 climate change datasets for the years 2005-2100, a total of 5,890 years of simulated rainfall and streamflow at a daily timestep. The resulting outputs were highly complex and varied in many ways. For example, a time series could vary over time, with higher flows later in the century, and different GCM/RCP scenarios could have different characteristics, such as shorter, more intense storms in one GCM compared to another. Often, the size of downscaled GCM datasets can be overwhelming when analyzing hydrologic impacts. This presented a challenge—the size and number of datasets required a screening and selection process to identify a manageable subset of scenarios, but the complexity and richness of the data made summarizing such a complex dataset inherently difficult. To resolve this challenge, the screening of future climate scenarios was based on the ecosurpluses and deficits that they produced. The approach identified which models produced



the 20th, 50th and 80th percentile ecosurpluses and ecodeficits for RCP 4.5 and 8.5 scenarios. Therefore, a total of 12 potential models were selected for further analysis: three models for ecosurpluses at RCP 4.5, three models for ecodeficits at RCP 4.5, three models for ecosurpluses at RCP 8.5, and three models for ecodeficits at RCP 8.5. Section 3.2.3 presents the results of the process and the ecodeficits and ecosurpluses associated with the selected models.

### 2.1.5 Point Source Withdrawals

Table 2 presents a summary of the available water supply information that was incorporated into the LSPC model as daily time series. To quantify the impact of water withdrawals and groundwater discharge on the water balance, 5 years from 10/1/2015 – 9/30/2020 were assessed. During this time, the amount of water withdrawn for both PWS and NPWS purposes was approximately 0.25% of the water budget while water returned to the system via permitted groundwater discharge was approximately 0.05% of the water budget.

**Table 2. Summary of Public Water Supply (PWS) and Non-Public Water Supply (NPWS) water use data incorporated into LSPC Wading River Model**

Supply	Observed data
Foxboro PWS Wells	Jan 2009 - Dec 2019
Mansfield PWS Wells	Jan 2009 - Dec 2019
Foxboro PWS Wells	Jan 2009 - Dec 2019
Foxboro NPWS Wells	Jan 2017 - Jan 2018
Wrentham PWS Wells	Jan 2009 - Dec 2019

**Table 3. Summary of Permitted Groundwater Discharge data incorporated into the LSPC Wading River Model**

Permit #	Observed data
632	Jan 2017 – Dec 2020
973	Jan 2019 – Dec 2020

## 2.2 Calibration and Validation

The study design for this modeling project used 20 years of observed precipitation and streamflow, separated into a 10-year calibration and a 10-year validation period (Table 4). Hydrological Modeling studies often split measured data into two datasets, one used for calibration, and one used for validation. Generally, model calibration involves minimizing the deviation between model output and corresponding measured data by adjusting model parameter values (Jewell et al., 1978).

**Table 4. Calibration and Validation Simulation Periods for the LSPC Wading River Model**

Period	Observed data
Calibration	10/01/2010 – 09/30/2020
Validation	10/01/2000 – 09/30/2010

The model was calibrated manually whereby parameters were adjusted individually to improve the performance. Calibrated parameters were adjusted to maintain consistency with watershed characteristics that they describe and kept within the ranges reported in the literature. Manual calibration contrasts with automatic calibration which uses optimization routines to estimate “best” values for parameters within user-defined upper and lower bounds.

Calibration was assessed using a combination of visual assessments and computed statistical evaluation metrics. The visual assessment involved reviewing panels of simulated vs observed graphical outputs including hydrographs and flow duration curves. For statistical assessment of model performance, the agreement between LPSC outputs and observed data was assessed using performance metrics based on those recommended by (Moriassi et al., 2015). The performance thresholds established by Moriassi et al. (2015) were modified based on performance criteria established by Donigian (2000) to assess targeted conditions based on season and flow rate. Moriassi et al. (2015) only provided metrics for the evaluation of all conditions across the model time series. Donigian (2000) included metrics for model predictions within flow regimes, such as the highest 10% of flows and baseflow. The thresholds suggested by Donigian (2000) essentially shifted the categories one column to the left, so that the threshold 'Very Good' became the threshold for 'Good'. This approach was applied to the Moriassi et al. 2015 to maintain reasonable performance metrics for the flow regime and seasonal conditions. Moriassi et al. (2015) anticipated such adjustments to their thresholds: "these [thresholds] can be adjusted within acceptable bounds based on additional considerations, such as quality and quantity of available measured data, spatial and temporal scales, and project scope and magnitude, and updated based on the framework presented herein." Table 5 presents a summary of performance metrics used in calibration.

While the project is largely focused on flow duration curves, calibrating only to a visual comparison of observed and predicted flow duration curves would limit the ability to fully assess model performance. Quantitative statistics of model calibration help to elucidate error and uncertainty in model predictions and can highlight conditions and seasons associated with varying predictive performance. A set of calibration metrics based on published references on catchment-scale, continuous simulation model performance evaluations were used to assess hydrological calibration. Performance across flow regimes and seasons was evaluated, performance metrics were qualified as "Very Good", "Good", "Fair" and "Unsatisfactory" using thresholds recommended by the modeling literature (Table 5). The calibration assessment includes percent bias,  $r^2$ , and Nash-Sutcliffe efficiency metrics:

- The **percent bias (PBIAS)** quantifies systematic overprediction or underprediction of observations. A bias towards underestimation is reflected in positive values of PBIAS while a bias towards overestimation is reflected in negative values. Low magnitude values of PBIAS indicate better fit, with a value of 0 being optimal.
- The **coefficient of determination (r-Squared)** describes the degree of collinearity between simulated and measured data. The correlation coefficient is an index that is used to investigate the degree of a linear relationship between observed and simulated data. r-Squared describes the proportion of the variance in observed data that is explained by a model. Values for r-Squared range from 0 to 1, with 1 indicating a perfect fit.
- The **Nash-Sutcliffe efficiency (NSE)** is a normalized statistic that determines the relative magnitude of the residual variance compared to the measured data variance (Nash and Sutcliffe, 1970). NSE indicates how well the plot of observed versus simulated data fits the 1:1 line. Values for NSE can range between  $-\infty$  and 1, with  $NSE = 1$  indicating a perfect fit.

**Table 5. Summary of performance metrics used to evaluate hydrology calibration**

Performance Metric	Hydrological Condition	Comparison Type	Performance Threshold for Hydrology Simulation				Reference
			Very Good	Good	Satisfactory	Unsatisfactory	
r-Squared (R <sup>2</sup> )	All Conditions <sup>1</sup>	Compare All Observed vs Simulated Daily Flow Rates that Occur During Selected Season-Conditions	>0.85	0.75 - 0.85	0.60 - 0.75	≤0.60	Moriassi et al. (2015), Donigian (2000)
	Seasonal Flows <sup>2</sup>		>0.75	0.60 - 0.75	0.50 - 0.60	≤0.50	
	Highest 10% of Daily Flow Rates <sup>3</sup>						
	Lowest 50% of Daily Flow Rates <sup>4</sup>						
	Days Categorised as Storm Flow <sup>5</sup>						
	Days Categorised as Baseflow <sup>5</sup>						
Nash-Sutcliffe Efficiency (E)	All Conditions <sup>1</sup>		>0.80	0.70 - 0.80	0.50 - 0.70	≤0.50	
	Seasonal Flows <sup>2</sup>		>0.70	0.50 - 0.70	0.40 - 0.50	≤0.40	
	Highest 10% of Daily Flow Rates <sup>3</sup>						
	Lowest 50% of Daily Flow Rates <sup>4</sup>						
	Days Categorised as Storm Flow <sup>5</sup>						
	Days Categorised as Baseflow <sup>5</sup>						
Percent Bias (PBIAS)	All Conditions <sup>1</sup>		<5%	5% - 10%	10% - 15%	>15%	
	Seasonal Flows <sup>2</sup>		<10%	10% - 15%	15% - 25%	>25%	
	Highest 10% of Daily Flow Rates <sup>3</sup>						
	Lowest 50% of Daily Flow Rates <sup>4</sup>						
	Days Categorised as Storm Flow <sup>5</sup>						
	Days Categorised as Baseflow <sup>5</sup>						

1. All Flows considers all daily time steps in the model time series.
2. Seasonal Flows considers daily flows during a predefined, three-month seasonal period (e.g., Winter, Spring, Summer, and Fall). Winter included the months of July, August, and September. Spring included the months of October, November, and December. Summer included the months of January, February, and March. Fall included the months of April, May, and June.
3. Highest 10% of Flows consider the top 10% of daily flows by magnitude as determined from the flow duration curve.
4. Lowest 50% of Flows consider the bottom 50% of daily flows by magnitude as determined from the flow duration curve.
5. Baseflows and Storm flows were determined from analyzing the daily model time series by applying the USGS hydrograph separation approach (Sloto et al., 1996) This approach parses the volume of the hydrograph at each time step (i.e., daily) into baseflow and stormflow components. Daily model time series were classified as a Storm Flows condition if the stormflow portion of the model hydrograph was greater than zero, and the baseflow recession rate was null. Baseflow recession rate was calculated by dividing baseflow from the following day ( $Q_{t+1}$ ) by baseflow from the current day ( $Q_t$ ) such that both  $Q_t$  and  $Q_{t+1}$  are greater than zero and  $Q_{t+1} / Q_t$  is less than 1.0. If either  $Q_t$  or  $Q_{t+1}$  was zero or  $Q_{t+1} / Q_t \geq 1.0$  then the baseflow recession rate was considered null. All days not classified as Storm Flows condition were considered Baseflows condition.

Figure 6 and Figure 7 presents observed and predicted hydrographs for daily flows and monthly flows for the calibration, validation, and baseline periods, Figure 7 is also normalized by watershed area. Both figures include rainfall hyetographs. Overall trends and timing of flows appear to be in general agreement although the model appears to predict some higher daily peak flows than were observed. Figure 8 presents observed and predicted flow duration curves. The curves appear to be well aligned. The calibration period shows low flows tended to be slightly overestimated. However, the magnitude of the differences is relatively small (< 2 cfs difference). A statistical evaluation of flow prediction using a suite of metrics (Table 5) is presented in Figure 9. Figure 9 is a summary of the more detailed tables presented in Appendix A.

- Every metric achieved a Satisfactory or better for the All category. The All category assesses performance for the full simulation period, including all flow regimes and seasons., The results suggest the LSPC model is reasonably calibrated for flows and can provide a reliable baseline for scenario simulations.
- Most assessments for flow regimes using PBIAS were satisfactory or higher, suggesting that the model does not tend towards a systematic bias towards over- or under-prediction.
- Results for  $R^2$  also suggest that the model performed reasonably well in establishing a linear relationship between model results and observations.
- There appear to be some limitations in seasonal performance. Spring flows appear to be somewhat under-predicted (positive PBIAS) while summer flows are over-predicted (negative PBIAS). However, neither satisfactory result was still achieved in either calibration or validations periods. Fluctuations in low flows are likely in response to processes that are not well captured by LSPC. Causes of low flow fluctuations may include minor discharges and groundwater dynamics. Water use and discharge data were included in the model, but the available data (Table 2, Table 3) did not cover the entire period used for calibration and validation (Table 4). Additionally, LSPC was not coupled to a groundwater model, and spatial variations in groundwater are not well characterized by available data.
- The NSE metric in particular top 10% and low 50% flow regimes show the poorest performance grading. During periods of unsatisfactory NSE results, the residual variance (the variance in the differences between observations and predictions) is larger than the variance of the observed data. NSE is very sensitive to extreme values and reflects the timing of simulated versus observed values. There is potential that using a single rain gauge for the entire watershed affected the predicted timing flows. Satisfactory results for NSE were achieved for the All-conditions category in the calibration and the validation period.

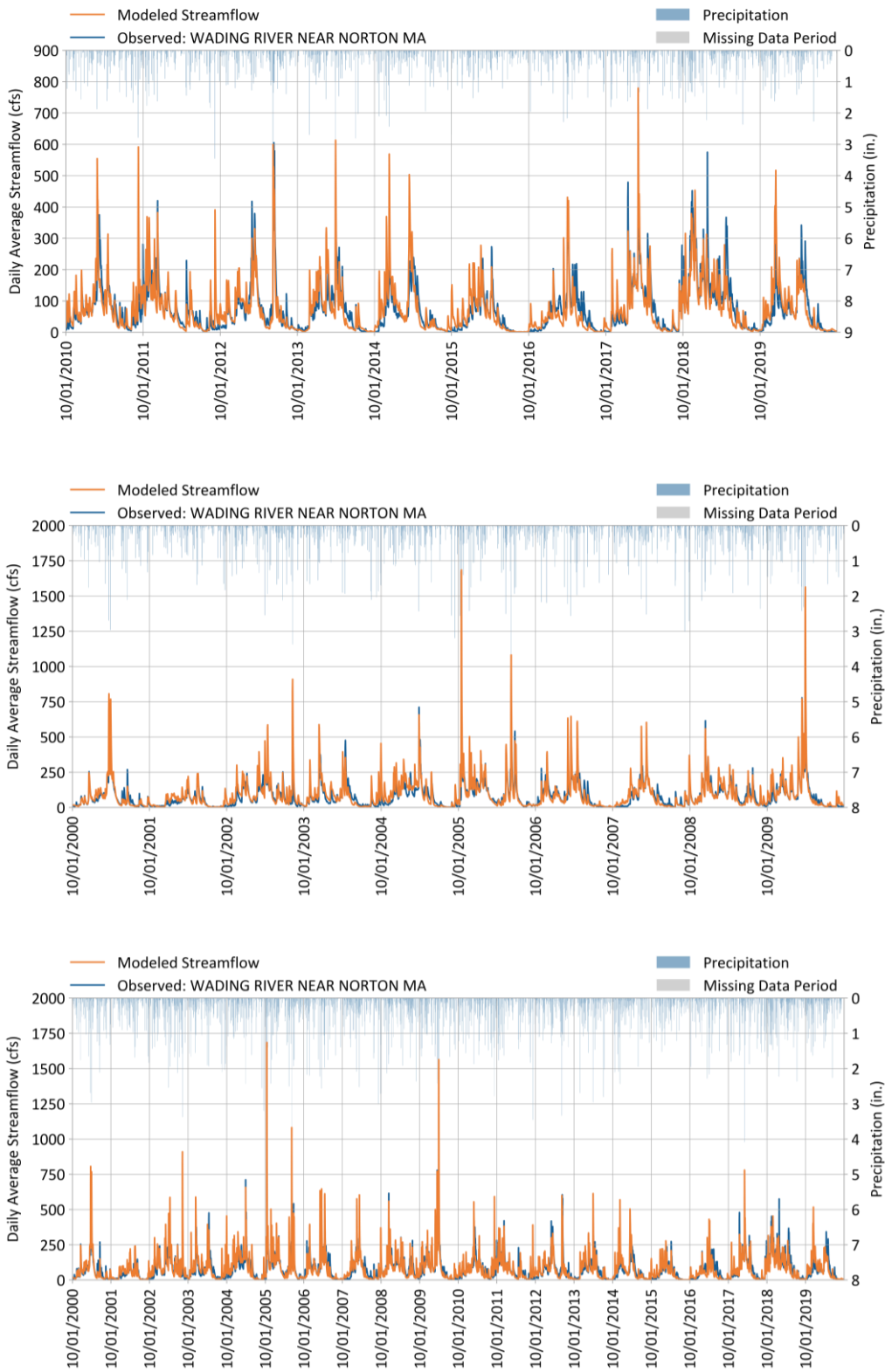


**Figure 6. Comparison of Observed and Predicted Daily Flows for the Calibration (top), Validation (middle), and Baseline (bottom) periods, Wading River, MA.**



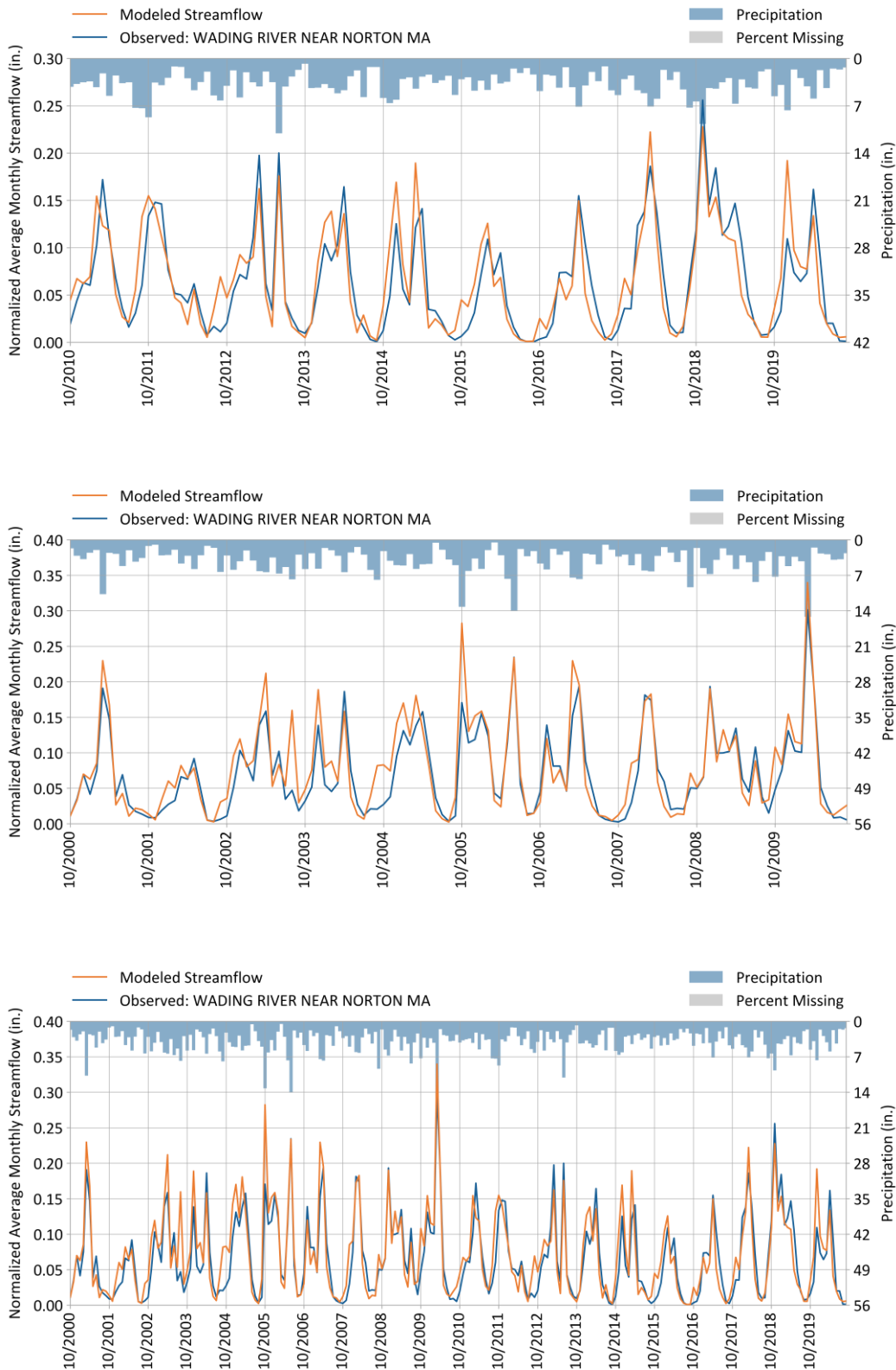


**Figure 7. Comparison of Observed and Predicted Normalized Monthly Streamflow for the Calibration (top), Validation (middle), and Baseline (bottom) periods, Wading River, MA.**

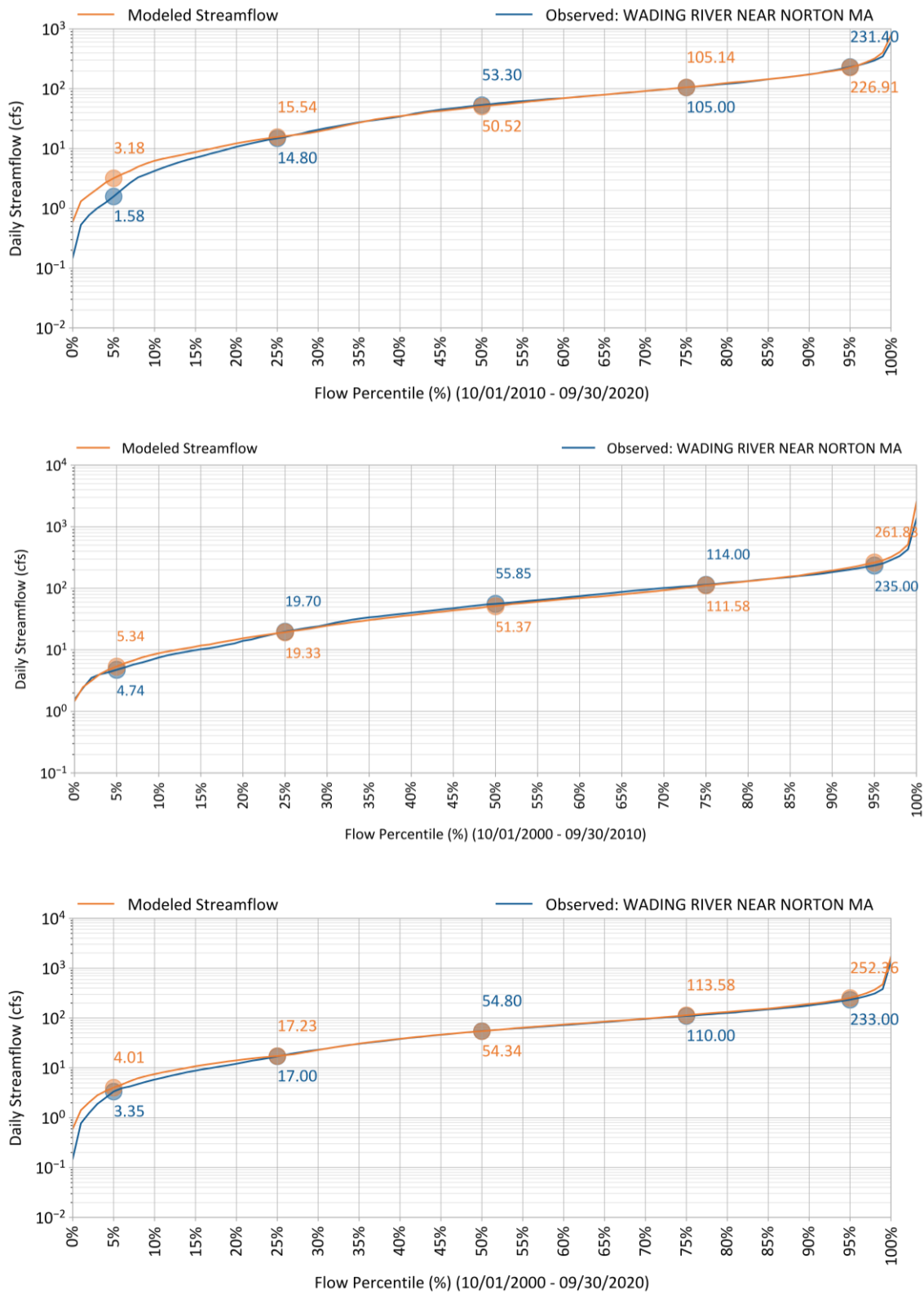


**Figure 8. Comparison of Observed and Predicted Flow Duration Curves for the Calibration (top), Validation (middle), and Baseline (bottom) periods, Wading River, MA.**

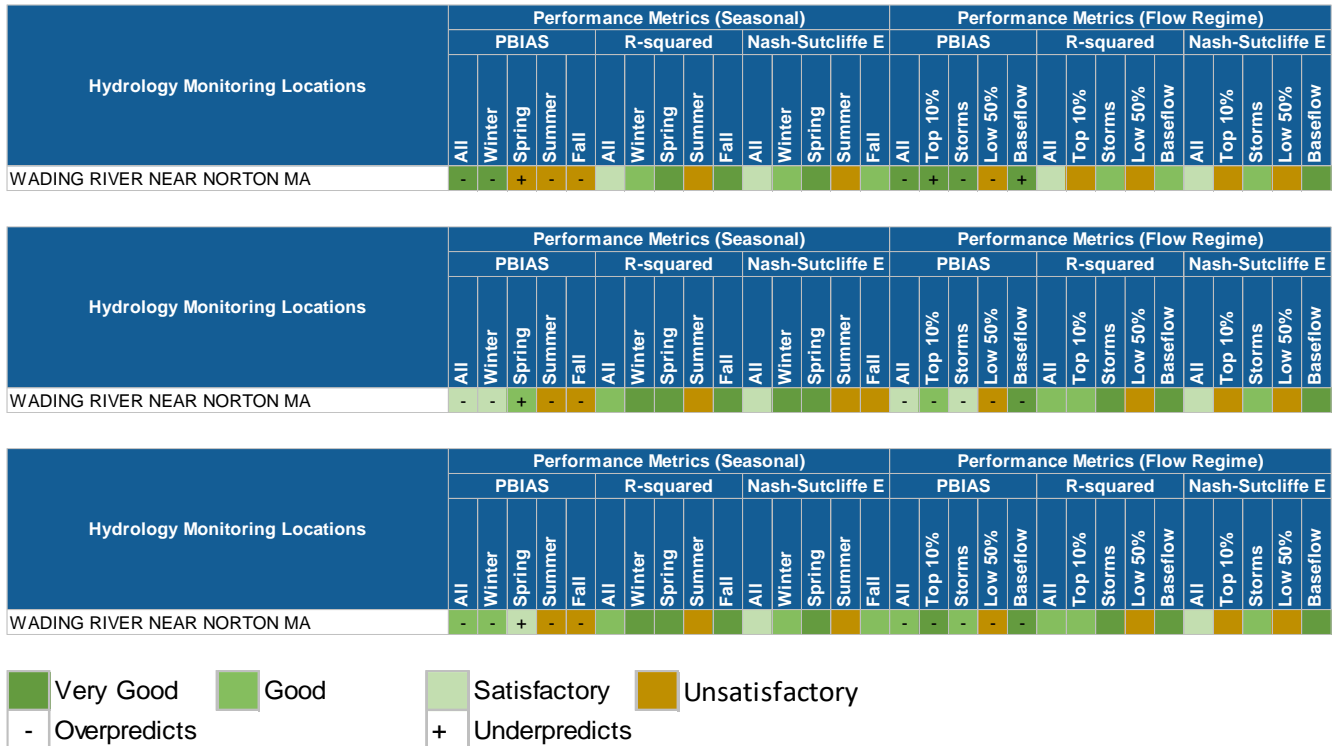


Figure 9. Performance Metric Summary for the Calibration (top), Validation(middle), and Baseline (bottom) periods, Wading River, MA.

### 2.3 HRU Based Water Quality Calibration

The Opti-Tool provides HRU-SWMM models, calibrated to nine major land use categories for New England Region. The SWMM models were calibrated using observed stormwater data from National Stormwater Quality Database (NSQD) and collected locally at the University of New Hampshire for a wide range of storm sizes. Additionally, the models were further calibrated to the long-term annual average pollutant loading rates consistent with the pollutant export rates reported in the small MS4 permits for Massachusetts and New Hampshire. Using the calibrated hydrology model for the Wading River watershed, four pollutants; Total Suspended Solids (TSS), Total Nitrogen (TN), Total Phosphorus (TP), and Zinc (Zn) were calibrated for the HRU categories in the study area. The pollutant build-up and wash-off parameters from the SWMM models were used as a starting point and were adjusted to calibrate the long-term annual average loading rates reported in the Opti-Tool. The model was simulated for 20 years (Oct 2000 – Sep 2020) and annual average loading rates from the model prediction were compared against the pollutant export rates for the similar HRU type in the Opti-Tool. Table 6 presents the summary of unit-area annual average pollutant loading rates from the calibrated Wading River model.

**Table 6. Summary of annual average pollutant loading rate calibrated to HRU type for the study area**

HRU Category	TSS (lb/ac/year)	TN (lb/ac/year)	TP (lb/ac/year)	Zn (lb/ac/year)
Paved Forest	649.15	11.48	1.502	0.714
Paved Agriculture	649.29	11.48	1.502	0.714
Paved Commercial	377.59	15.24	1.794	1.377
Paved Industrial	377.59	15.24	1.794	1.377
Paved Low Density Residential	438.25	14.27	1.503	0.714
Paved Medium Density Residential	438.25	14.27	1.970	0.714
Paved High Density Residential	438.29	14.26	2.381	0.714
Paved Transportation	1,480.46	10.26	1.532	1.760
Paved Open Land	649.29	11.48	1.568	0.987
Developed OpenSpace-A-Low	5.75	0.23	0.020	0.002
Developed OpenSpace-A-Med	6.89	0.25	0.022	0.002
Developed OpenSpace-B-Low	24.73	0.93	0.097	0.016
Developed OpenSpace-B-Med	30.48	1.21	0.126	0.020
Developed OpenSpace-C-Low	57.33	2.26	0.209	0.046
Developed OpenSpace-C-Med	60.04	2.39	0.220	0.049
Developed OpenSpace-D-Low	86.17	3.30	0.305	0.058
Developed OpenSpace-D-Med	100.83	4.04	0.374	0.071
Forested Wetland	27.60	0.52	0.109	0.039
Non-Forested Wetland	27.69	0.52	0.109	0.039
Forest-A-Low	5.97	0.12	0.023	0.009
Forest-A-Med	6.81	0.12	0.025	0.010
Forest-B-Low	26.66	0.52	0.102	0.034
Forest-B-Med	28.60	0.55	0.109	0.036
Forest-C-Low	57.07	1.10	0.204	0.089
Forest-C-Med	59.99	1.17	0.217	0.095
Forest-D-Low	92.09	1.78	0.360	0.133
Forest-D-Med	95.00	1.84	0.373	0.138
Agriculture-A-Low	5.86	0.51	0.088	0.005
Agriculture-A-Med	6.78	0.54	0.093	0.005
Agriculture-B-Low	26.24	2.32	0.409	0.017
Agriculture-B-Med	28.14	2.49	0.439	0.018
Agriculture-C-Low	57.03	5.04	0.773	0.043
Agriculture-C-Med	60.39	5.41	0.829	0.047
Agriculture-D-Low	91.12	8.02	1.366	0.069
Agriculture-D-Med	95.67	8.49	1.447	0.073

## 3 MODELING RESULTS

---

### 3.1 Baseline Unit–Area Analysis

---

After calibration and validation, the 20-year baseline model time series was used to assess the water balance for various land uses (Figure 10) and soil groups (Figure 11). Unsurprisingly, impervious surfaces demonstrate the most substantial deviation from natural conditions such as forests and wetlands. Over 90% of the water balance for impervious surfaces is overland flow. The runoff generated from impervious surfaces is often conveyed to receiving waters including streams, rivers, and lakes where both the quantity and quality of stormwater can impact the health of the systems. Combined, groundwater and interflow represent the portion of the water balance that has been infiltrated into the ground and not removed by evapotranspiration. Impervious surfaces provide no opportunity for infiltration. Interestingly, the water balance suggests that developed open space has a higher proportion of the water balance that is attributed to interflow and groundwater than forests. While infiltration occurs on both land types, a greater proportion in forests is returned to the atmosphere via evapotranspiration.

Wetlands produce the most (~64%) evapotranspiration and relatively little groundwater recharge. This is intuitive as many wetlands are locations of groundwater discharge rather than recharge. After wetlands, forests provide the most evapotranspiration, followed by agriculture, and developed open space. Evapotranspiration differences in soil groups are less pronounced, soils with lower infiltration rates (C, D) have less groundwater recharge than high infiltration soils (A, B). Figure 12 presents the water balance for the three study sub-watersheds representing varying degrees of imperviousness. Increases in imperviousness are associated with increases in overland flow and decreases in evapotranspiration.



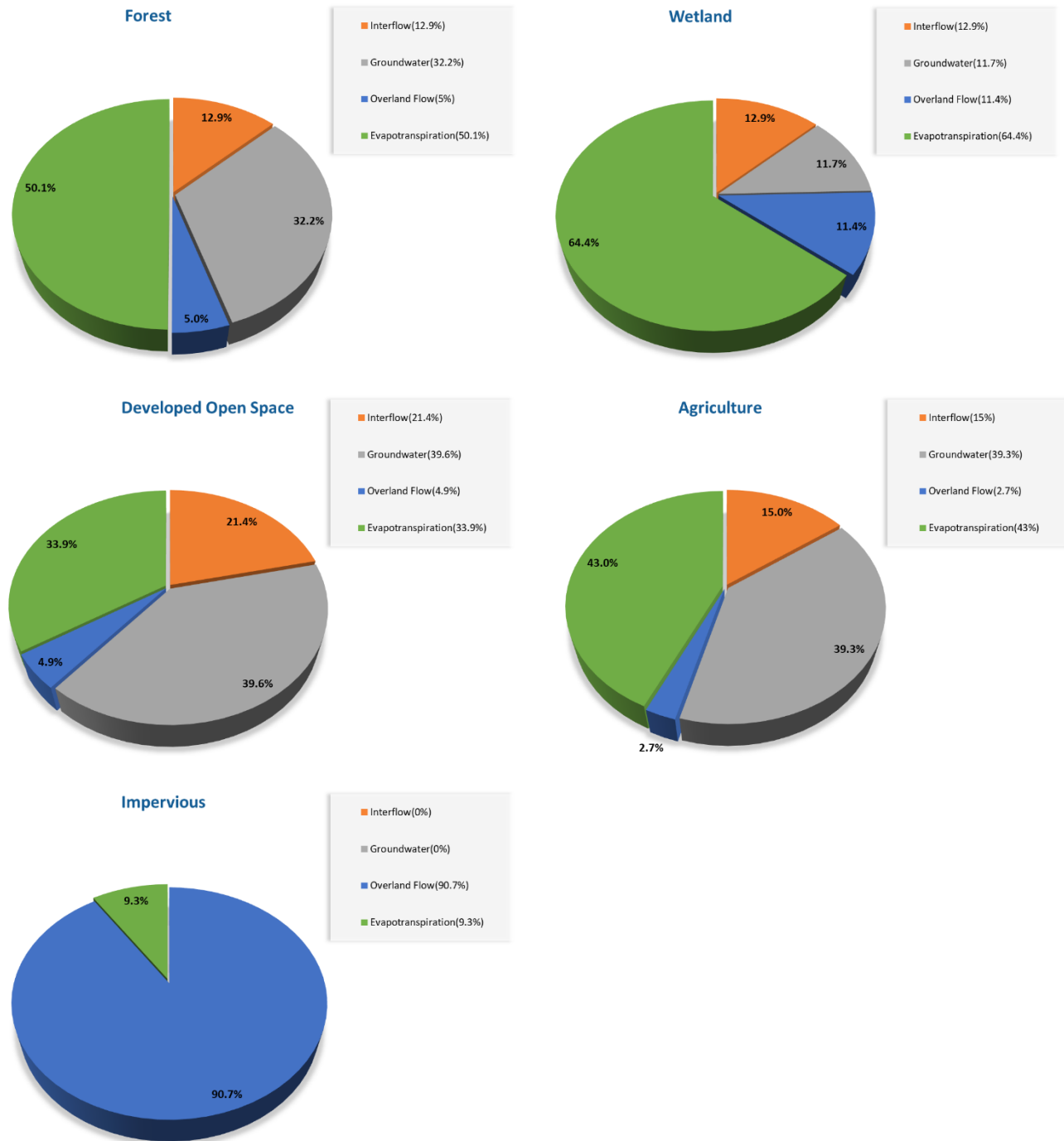


Figure 10. Water Balance for LSPC Hydrological Response Units, Summarized by Land Use. Baseline Simulation 2000-2020.

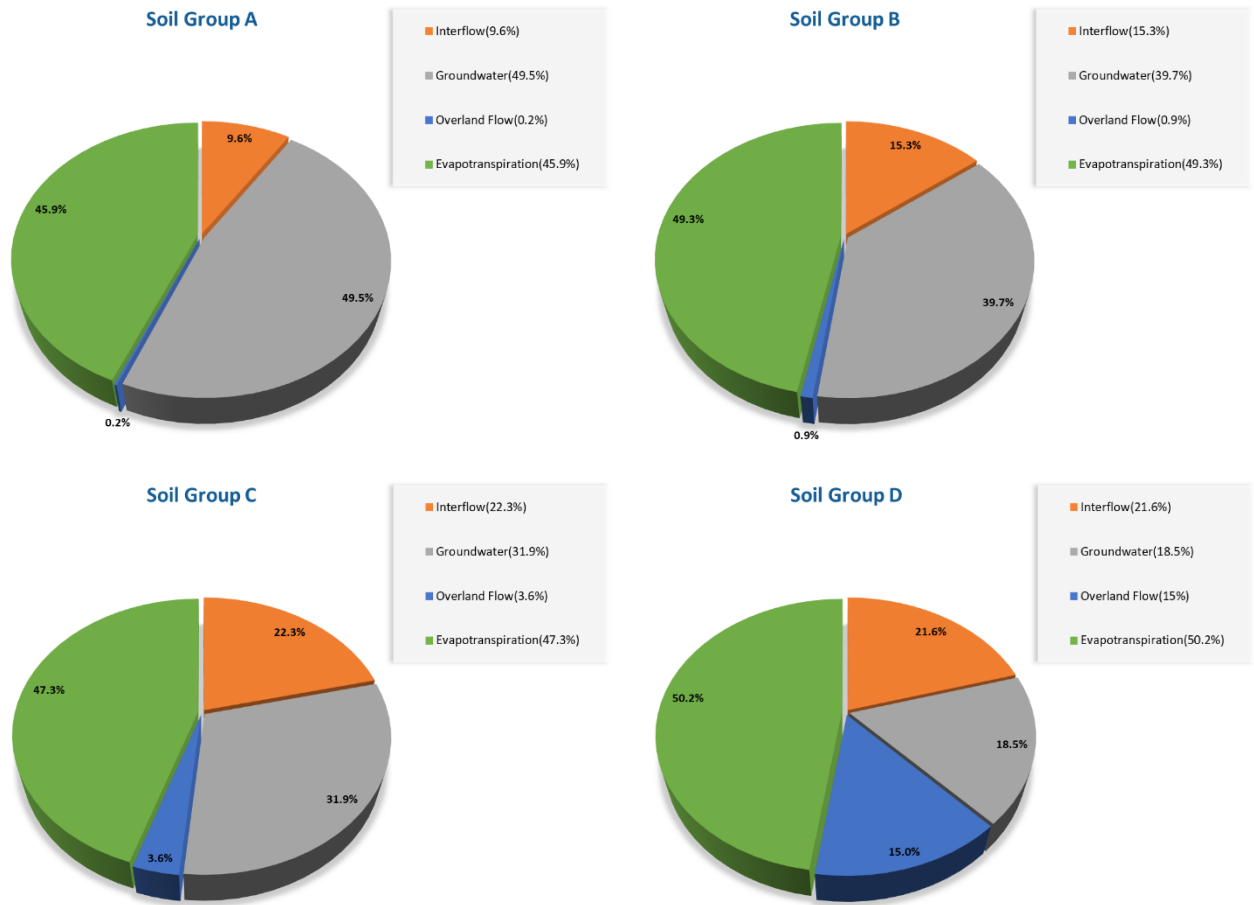
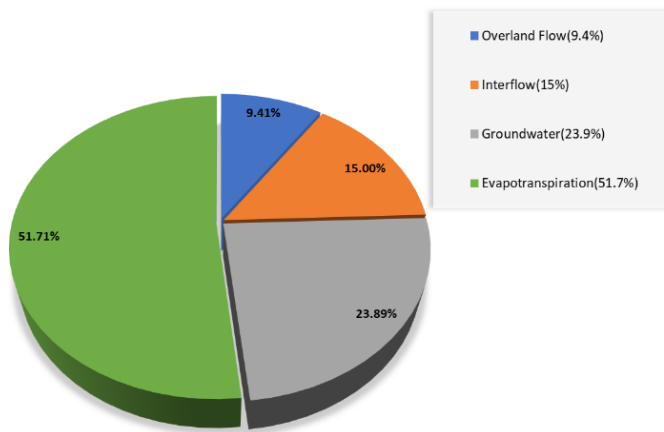
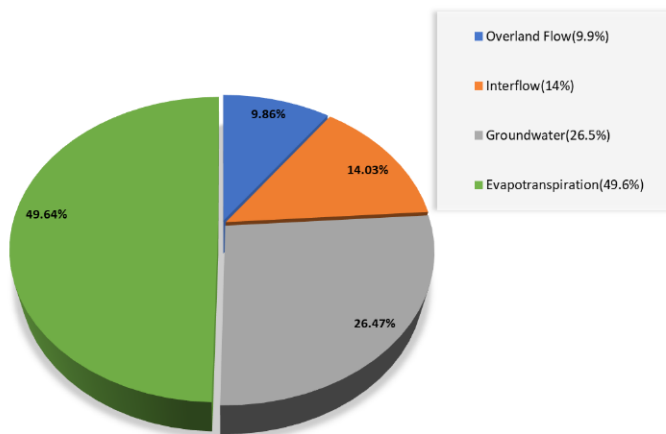


Figure 11. Water Balance for LSPC Hydrological Response Units, Summarized by Soil Group. Baseline Simulation 2000-2020.

**Pilot Tributary (low imperviousness)**



**Lower Hodges (medium imperviousness)**



**Upper Hodges (high imperviousness)**

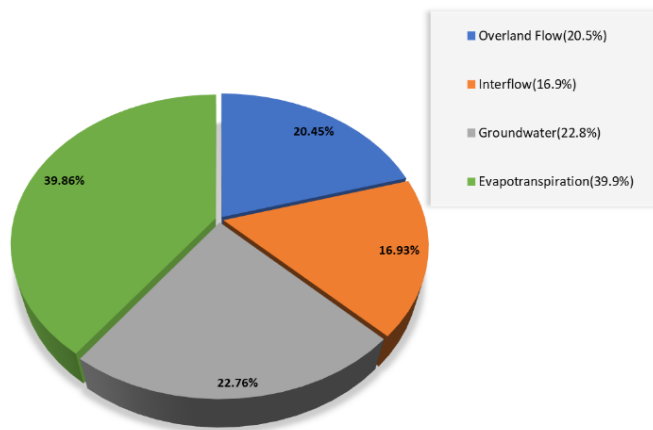


**Figure 12. Water Balance for LSPC sub-watersheds.**

## 3.2 Relationships Between Impervious Cover and Watershed Function

---

Modeling results from the three study sub-watersheds were assessed to improve the understanding between impervious cover and watershed function. Figure 13 presents FDCs for the three sub-watersheds. Since discharge (cubic feet per second [cfs]) is associated with watershed size, a standard FDC and one normalized by watershed area are presented. The normalized FDC suggests that flows across the FDC tend to increase with imperviousness. Both Upper and Lower Hodges have higher normalized flows compared to Pilot Tributary. However, the high impervious watershed (Upper Hodges) FDC does appear to dip below the medium impervious watershed (Lower Hodges) at lower flows. Figure 14 shows that although slight, the two normalized FDCs for Upper and Lower Hodges cross each other, producing an ecosurplus and ecodeficit. The results suggest that initially, as development begins in a watershed, increases across the flow regime may be expected. However as impervious surfaces continue to increase, high flows will continue higher but low flows may begin to become lower. This relationship was further investigated using the Upper Hodges sub-watershed to study the effect of various land-use scenarios (Section 3.2.1).

Figure 15 presents the average monthly discharge for the three study sub-watersheds. When normalized by sub-watershed area, the differences between the most undeveloped sub-watershed (Pilot Tributary) and the more developed sub-watershed appear to increase in the summer months. The differences in ET between in Pilot Tributary and Upper Hodges Book in the overall water balance (Figure 12) are driven by the pronounced increase in ET from the Pilot Tributary in the summer months. The least developed Pilot Tributary has the lowest average 3-day minimum and lowest 3-day maximum flow compared to the other two sub-watersheds (Table 7). Low flows in the area tend to occur in the summer months, and it is perhaps not surprising that given that the least developed sub-watershed has the highest amounts of ET occurring during this time, that this also results in Pilot Tributary having the lowest low flows. However, as discussed in section 3.2.1, a sub-watershed with high amounts of directly connected impervious surfaces (higher than the existing/baseline modeled conditions of Upper Hodges Brook) can begin to have lower flows than pre-developed/forested watersheds. The Richard-Baker Flashiness Index (RBI) was also used to assess relationships between imperviousness and flow regime (Figure 17, Figure 18). Comparisons were mostly unremarkable. While the intercept of the regressions increases as imperviousness decreases, the relationship was not interrogated further. Flashiness may be attributed to both watershed and climatic changes, indeed changes to a watershed's landscape may impact how susceptible it is to changes due to climatic forcing.

While increases in impervious surfaces have been shown to consistently increase the volume and flashiness of stormflows, studies have found diverse, sometimes contrasting responses to base flow (Hopkins et al., 2015). Bhaskar et al. (2016) found that total streamflow and baseflow increased in a watershed with LID practices during urbanization compared to control watersheds. The authors suggest that the flow regime changes may be due to a reduction in evapotranspiration associated with decreased vegetative cover as urbanization occurred and an increase in the point source of recharge. Both increases and decreases to flow regimes can have deleterious effects on both the ecology of a watershed as well as human health (Table 8). It is noted that the impact of SCMs on baseflow is a field of ongoing research, often relying on modeling approaches given the difficulty of monitoring baseflows at the local scale (Li et al., 2017).

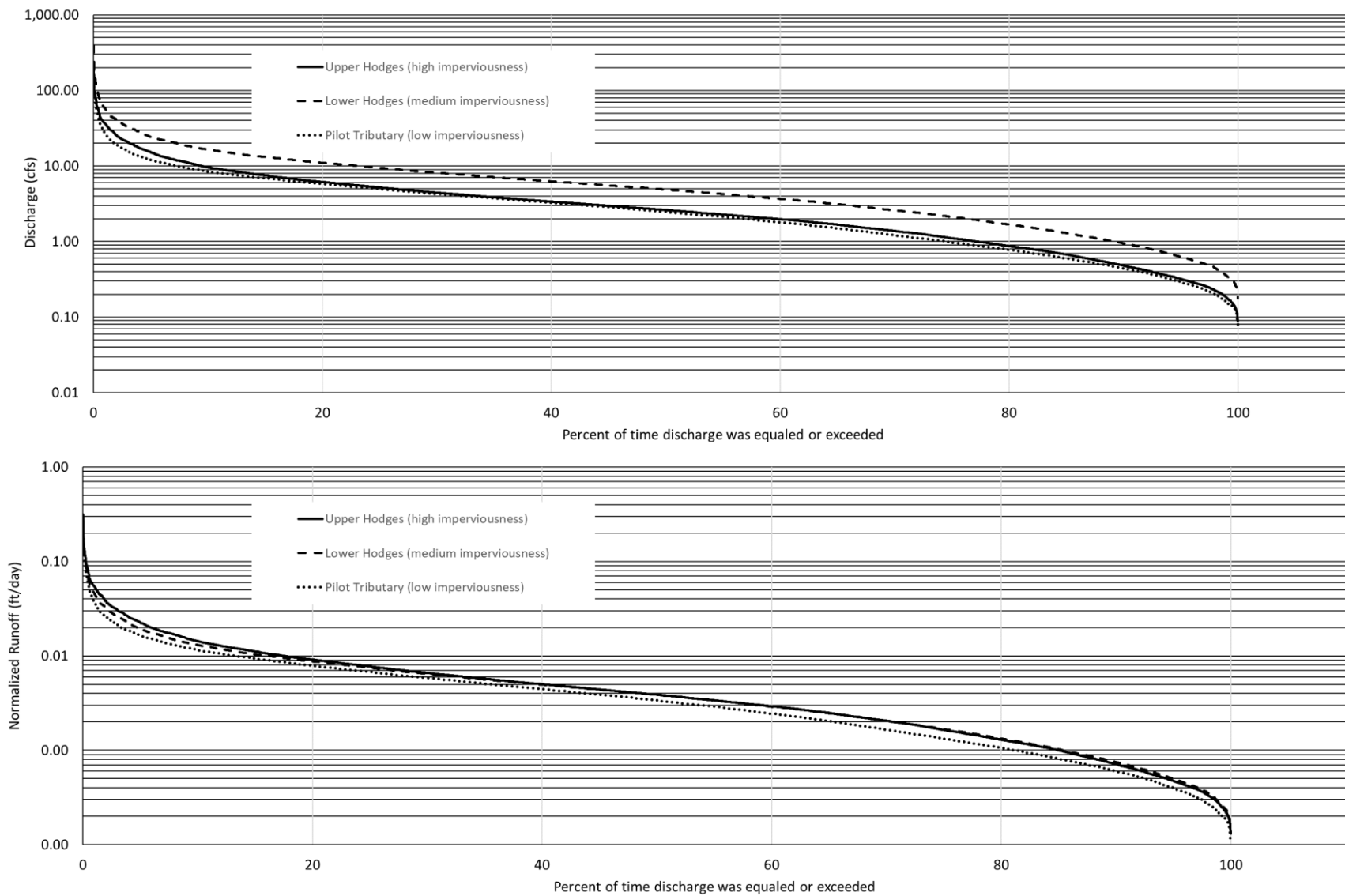


Figure 13. Standard FDC (top) and Normalized FDCs  $\left[\frac{\text{daily flow } ft^3}{\text{watershed area } ft^2}\right]$  (bottom) for the three study watersheds.



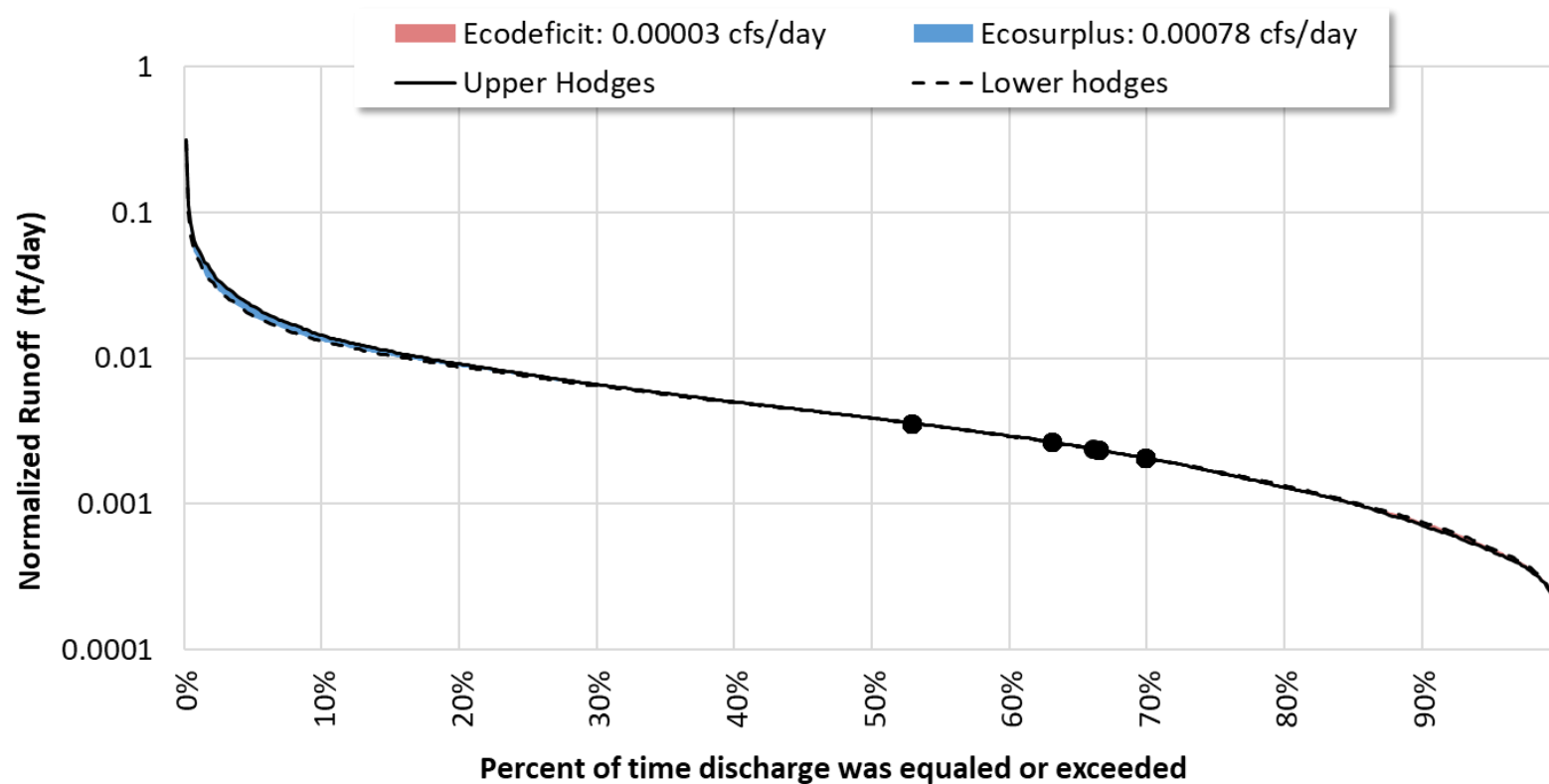


Figure 14. Ecosurplus and Ecodeficit for Upper Hodges compared to Lower Hodges.

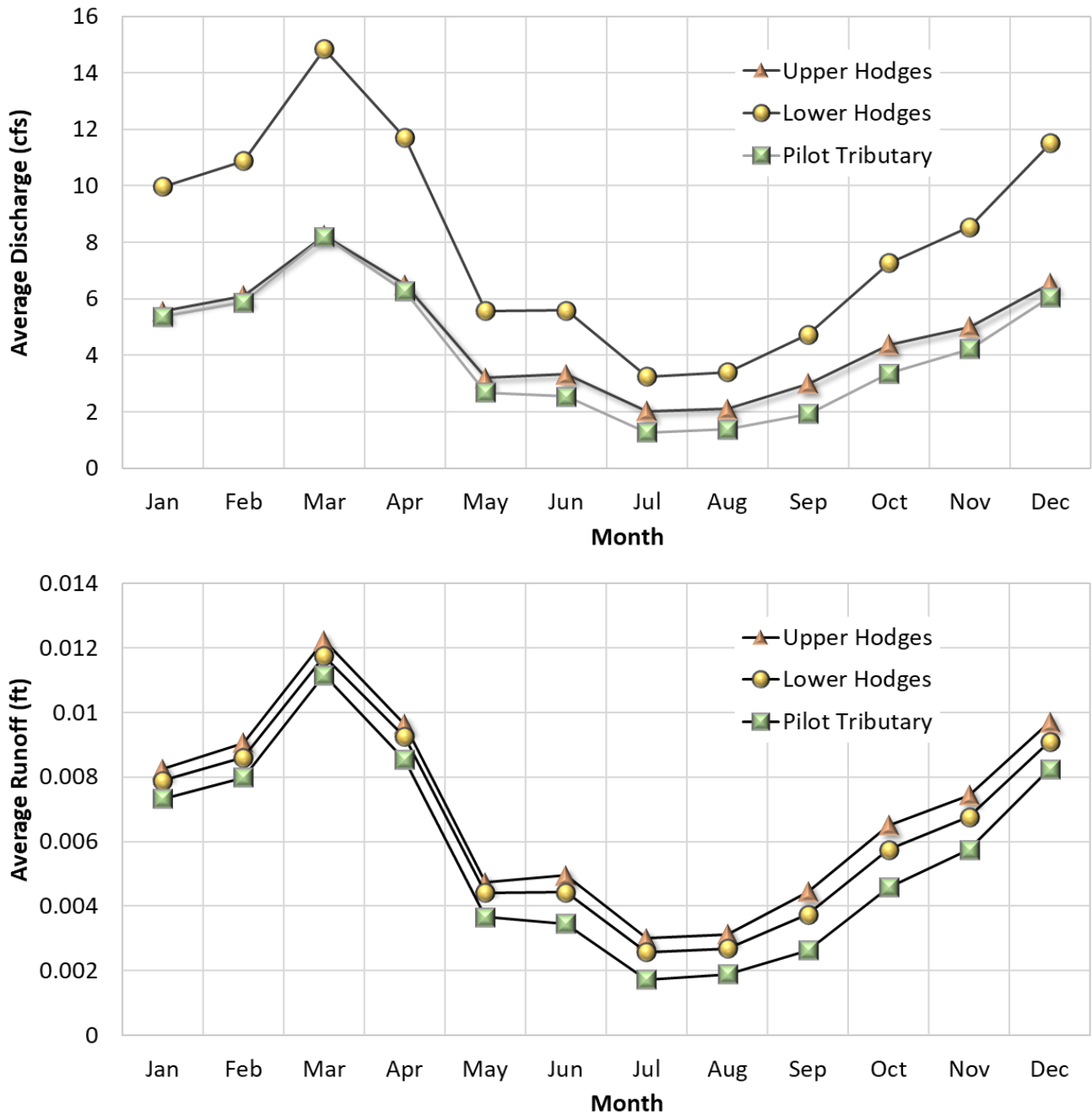


Figure 15. Average monthly discharge and runoff depth for the three study watersheds.

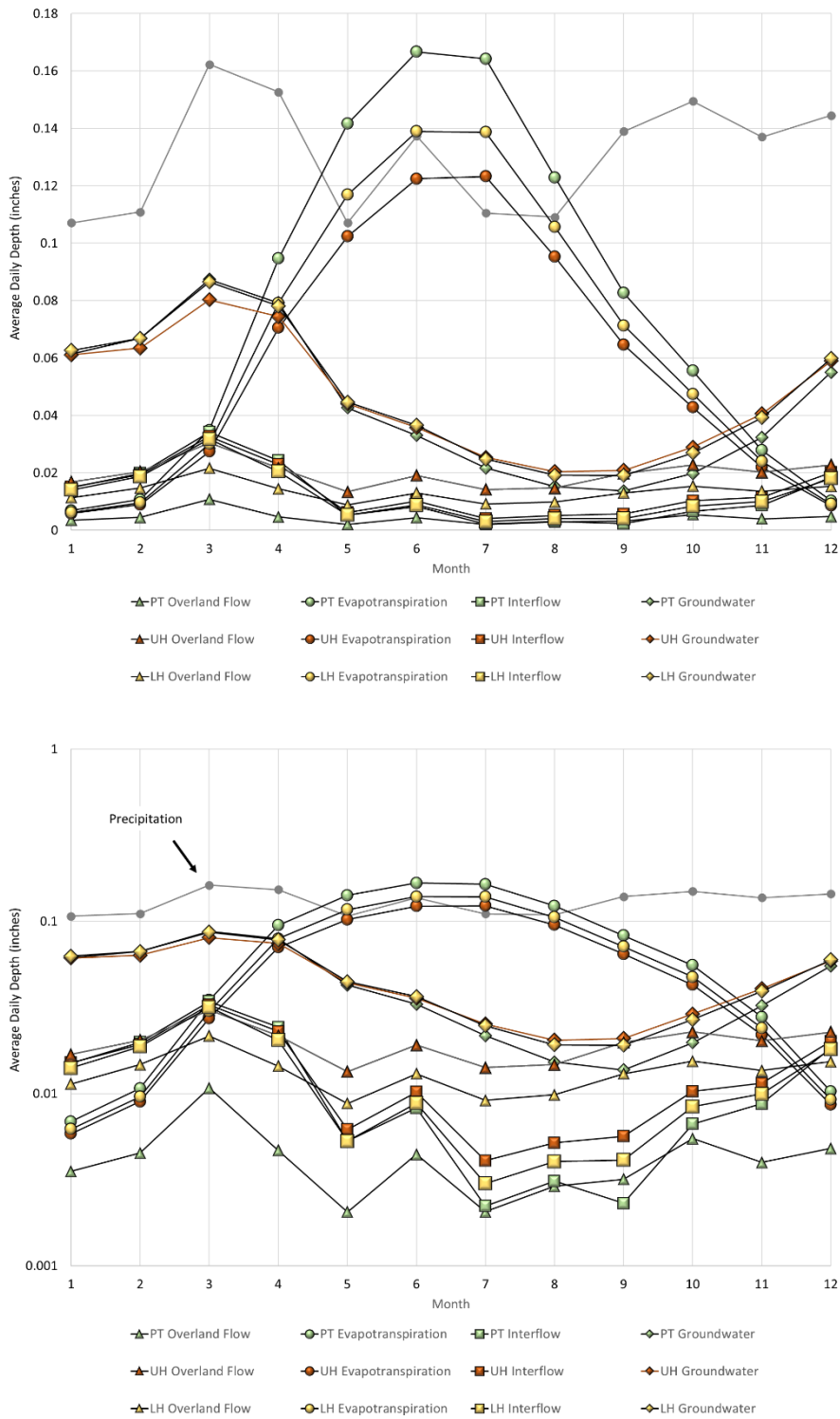
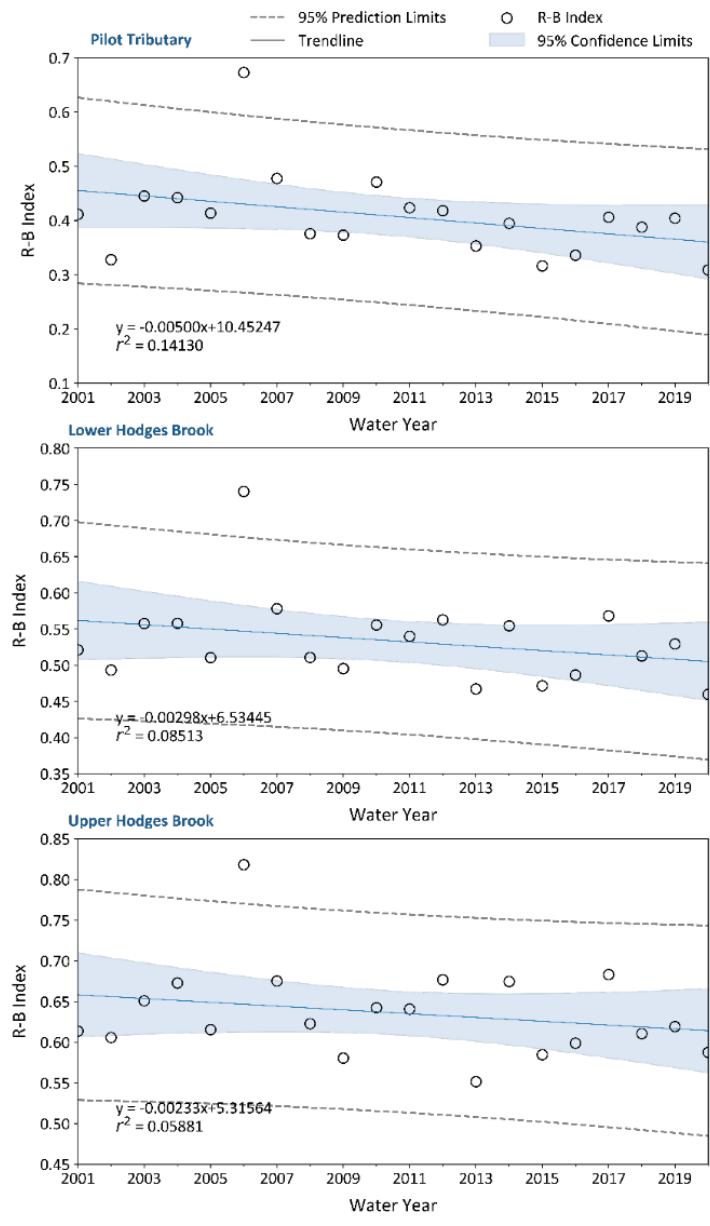


Figure 16. Monthly Water Balance with standard (top) and logarithmic (bottom) for the three study watersheds.

**Table 7. 3-day minimum and maximum flows for the three study watersheds**

Average daily flow normalized by watershed area	Pilot Tributary	Lower Hodges	Difference between Lower Hodges and Pilot Tributary	Upper Hodges	Difference between Upper Hodges and Pilot Tributary
3-day minimum	0.00036	0.00045	23.40%	0.0004	18.39%
3-day maximum	0.05054	0.05565	10.12%	0.0614	21.43%



**Figure 17. Richard Baker Flashiness Index for the 20-year baseline simulation for the three study sub-watersheds.**

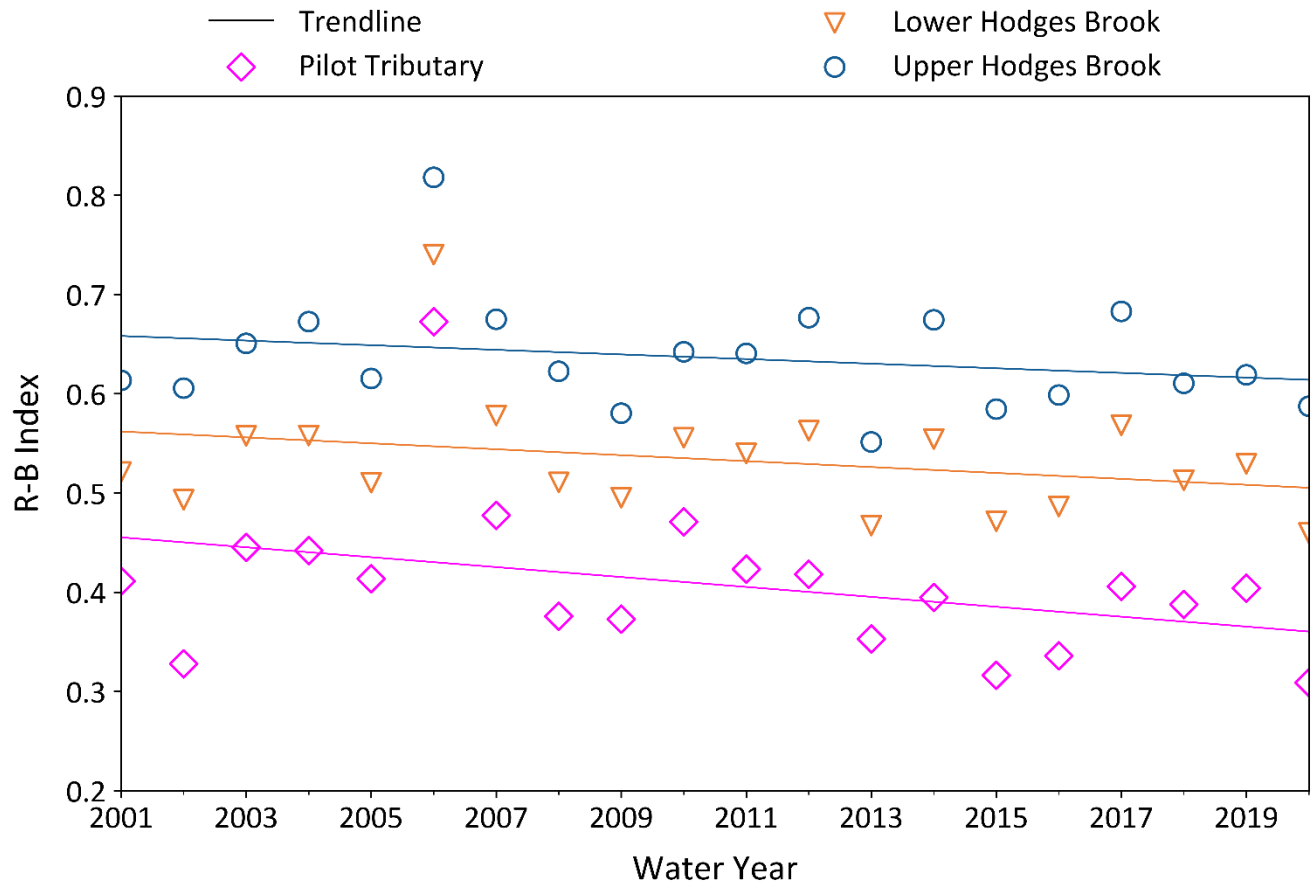


Figure 18. Comparison of Richard Baker Flashiness Index for the 20-year baseline simulation for the three study sub-watersheds.



**Table 8. Ecological and human risks associated with changing water tables/base flow. Adapted from Bhaskar et al., 2016**

Falling water table/baseflow	Rising water table/baseflow
<i>Ecological alteration / risk</i>	<i>Ecological alteration / risk</i>
Increased extreme water temperature	Reduction in extreme water temperature
Increased likelihood of channel drying	Increasing flow permanence and damping of seasonal fluctuations in water depth
Reduced water depth for fish survival and recruitment	Increase in nutrient loads
Reduced water quality due to increased contaminant concentrations	Increase in salinity of surface soil and water
Falling O <sub>2</sub> levels associated with reduced flow velocity	Reduction in species that rely on riffle habitat for feeding or spawning
Altered in-stream species assemblage structure	Altered in-stream species assemblage structure
Reduced nutrient processing in riparian areas	Increased invasion by competitive non-native species
Reduced un-stream processing associated with reduced groundwater upwelling	Altered in-stream and riparian vegetation
Terrestrialization of the riparian vegetation community	
Reduced health of deep-rooted vegetation across the catchment	
<i>Human Risk</i>	<i>Human Risk</i>
Reduced water quality due to increased contaminant concentrations	Flooding of buildings
Reduced access of existing bores to groundwater	Flooding of underground infrastructure
Reduced volume of water for household use and irrigation (where groundwater contributes to water use)	Increasing contamination of ground-ad stream water by septic systems
	Increased leakage of groundwater into wastewater systems leading to wastewater treatment plants treating groundwater

### 3.2.1 Land-use Scenarios

To further investigate relationships between impervious cover and watershed functions, three land-use scenarios were simulated using the Upper Hodges Brook sub-watershed. The Upper Hodges Brook was chosen as it had the most impervious cover of the three study sub-watersheds. Four scenarios were simulated for the sub-watershed (Table 9). Figure 19 presents flow duration curves for the four scenarios and Figure 20 presents the high and low flow sections of those curves. Results support conclusions from others (Bhaskar et al., 2016) that watershed development and associated stormwater management, including disconnecting all impervious surfaces ( $EIA = 0$ ) can result in consistently higher flows across the flow regime compared to pre-development conditions. Figure 21, Figure 22, Figure 23 present water balance and FDCs for baseline conditions compared to  $EIA = TIA$ , pre-developed/forested, and  $EIA = 0$ , respectively. The figures present ecosurplus and ecodeficit in cfs/day as well as millions of gallons/year. Figure 24 presents average and minimum monthly flows for each land use scenario. As ET increases, average flows decrease for all scenarios. The pre-development scenario has the highest ET and the lowest average flows while the  $EIA=TIA$  scenario has the lowest ET and the highest average flows. Interestingly, this relationship changes for low flows, where the most developed scenario ( $EIA=TIA$ ) has the lowest low flows and the disconnected scenario ( $EIA = 0$ ) has the highest low flows. Figure 25 presents three-day minimum and maximum flows by land-use scenario. The  $EIA=TIA$  consistently had the lowest minimum flows while the  $EIA = 0$  (all impervious surfaces disconnected) had the highest low flows. Furthermore,  $EIA=TIA$  had the highest maximum three-day flows while pre-developed conditions had the lowest. Table 10 further supports these conclusions but is based on the average of flows over the simulation period. Figure 26 presents RBI for Upper Hodges Brook calculated for the different land-use scenarios. The impact of land-use change is evident with flashiness increasing with an increase in impervious surfaces. The scenario in which all impervious surfaces are fully disconnected most closely resembles the flashiness and trend of the predevelopment scenario. The Task 5 memo presented evidence that the Wading River watershed was trending to a less-flashy condition. Baseline and  $EIA = TIA$  scenarios suggest that whatever broader trends towards a less-flashy system that may occur in the pre-development scenario are dampened (less steep regression slope/smaller intercept) by the effect of impervious surfaces. Table 11 presents a summary and further comparison of average flows. Care should be taken in making conclusions only from average flows. While it would appear that the pre-development condition has consistently lower flows, Figure 19, Figure 21, Figure 25 provide evidence that the  $EIA=TIA$  scenario results in the lowest of low flow conditions.

**Table 9. Land-use Scenarios simulated using Upper Hodges Brook sub-watershed**

Scenario	Description
Baseline/Existing conditions	Existing land-use and effective impervious surfaces as described in the Task 5 Memo
Pre-development/forested	All land not classified as forest or wetland in the baseline conditions, including impervious surfaces, developed open space, and agriculture was converted to forested land cover but maintained their soil and slope classifications
$EIA=TIA$	Baseline Effective Impervious Area was increased to the Total Impervious Area. Therefore, the effect of the Sutherland Equations discussed in the Task 5 Memo was removed, and all mapped impervious surfaces were assumed to be directly connected to the stream channel. This resulted in an increase of EIA from 15% to 32%.
$EIA=0$	Effective Impervious Area was converted to pervious developed open space. This represents a scenario where all existing impervious surfaces have been disconnected.

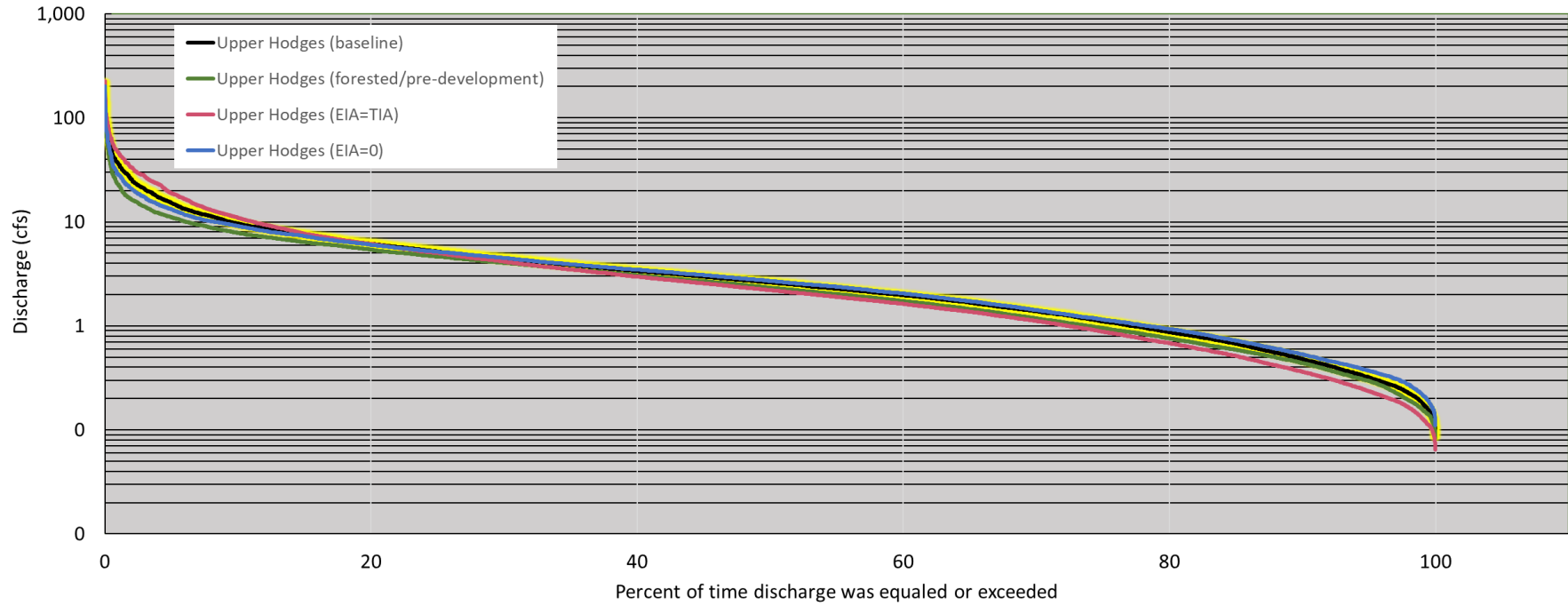


Figure 19. Flow Duration Curves for Upper Hodges Brook watershed for baseline, predevelopment, EIA=TIA, and EIA=0 conditions. Baseline FDC is black with a yellow highlight.,

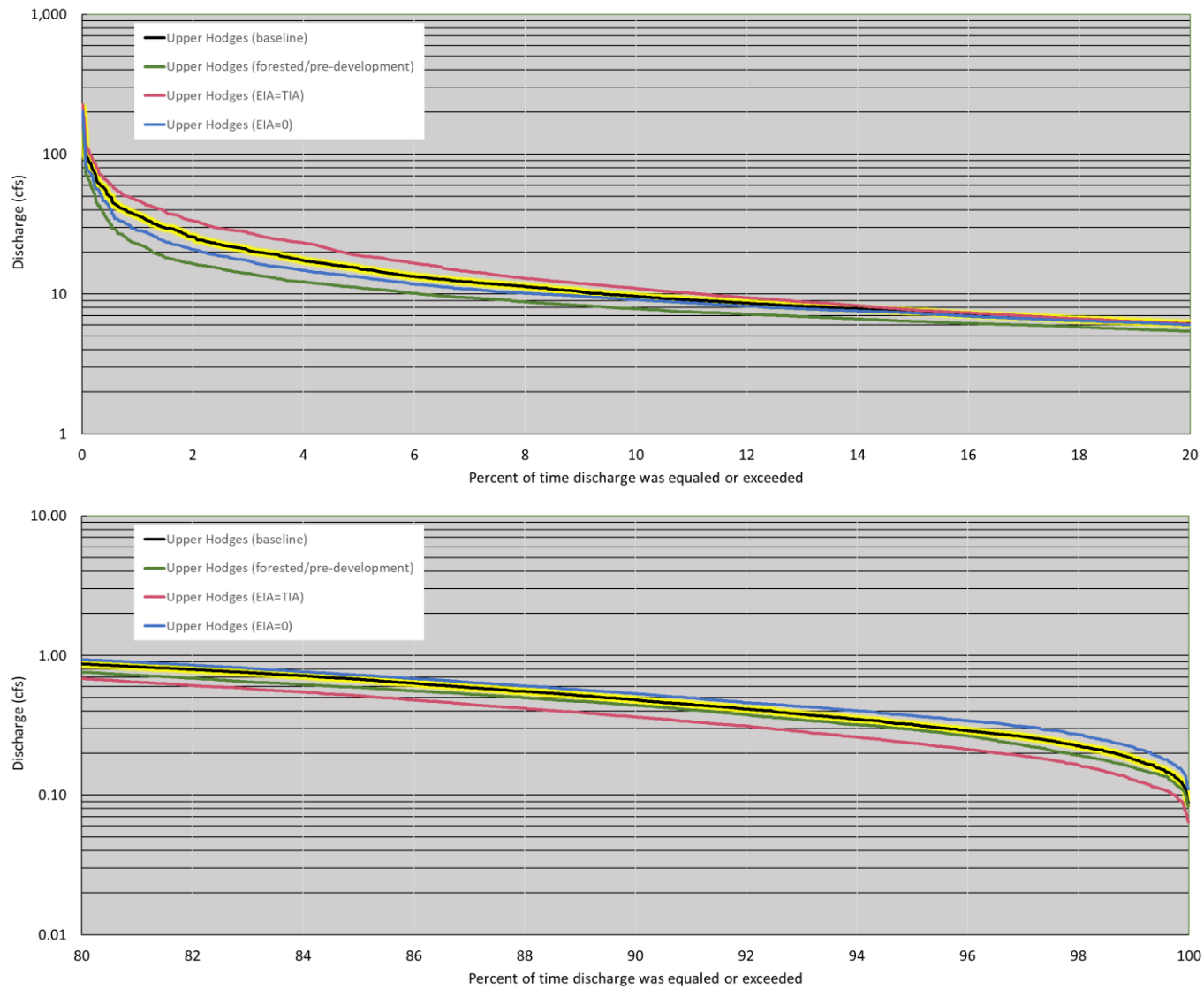


Figure 20. High flow (top) and low flow (bottom) sections of the FDC-presented in Figure 19. Baseline FDC is black with a yellow highlight.

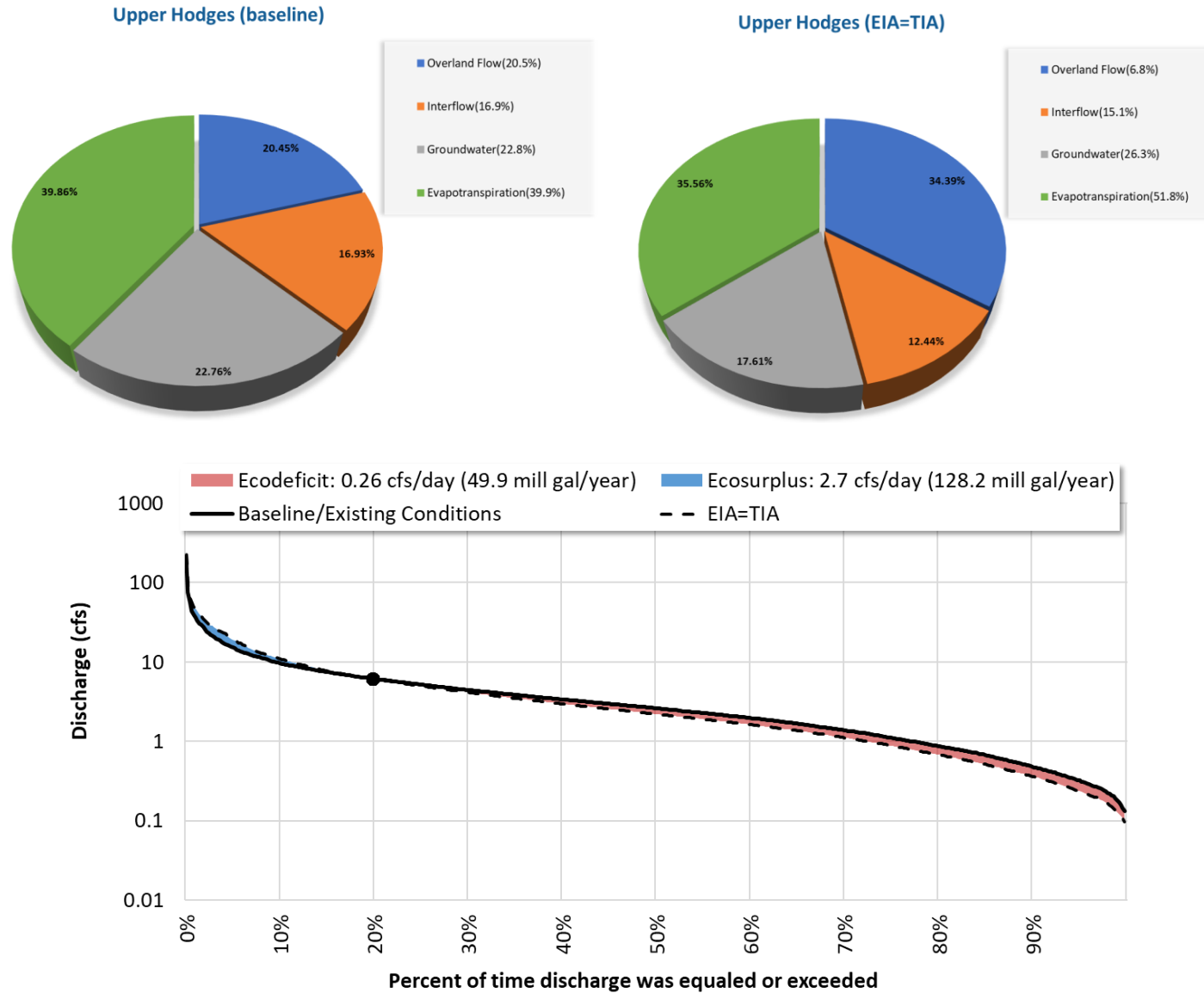


Figure 21. Water balances and Ecosurplus and Ecodeficit for Upper Hodges Brook watershed for baseline and EIA=TIA conditions. EIA=TIA reflects an increase in directly connected impervious surfaces. Black dots indicate places where FDCs cross.



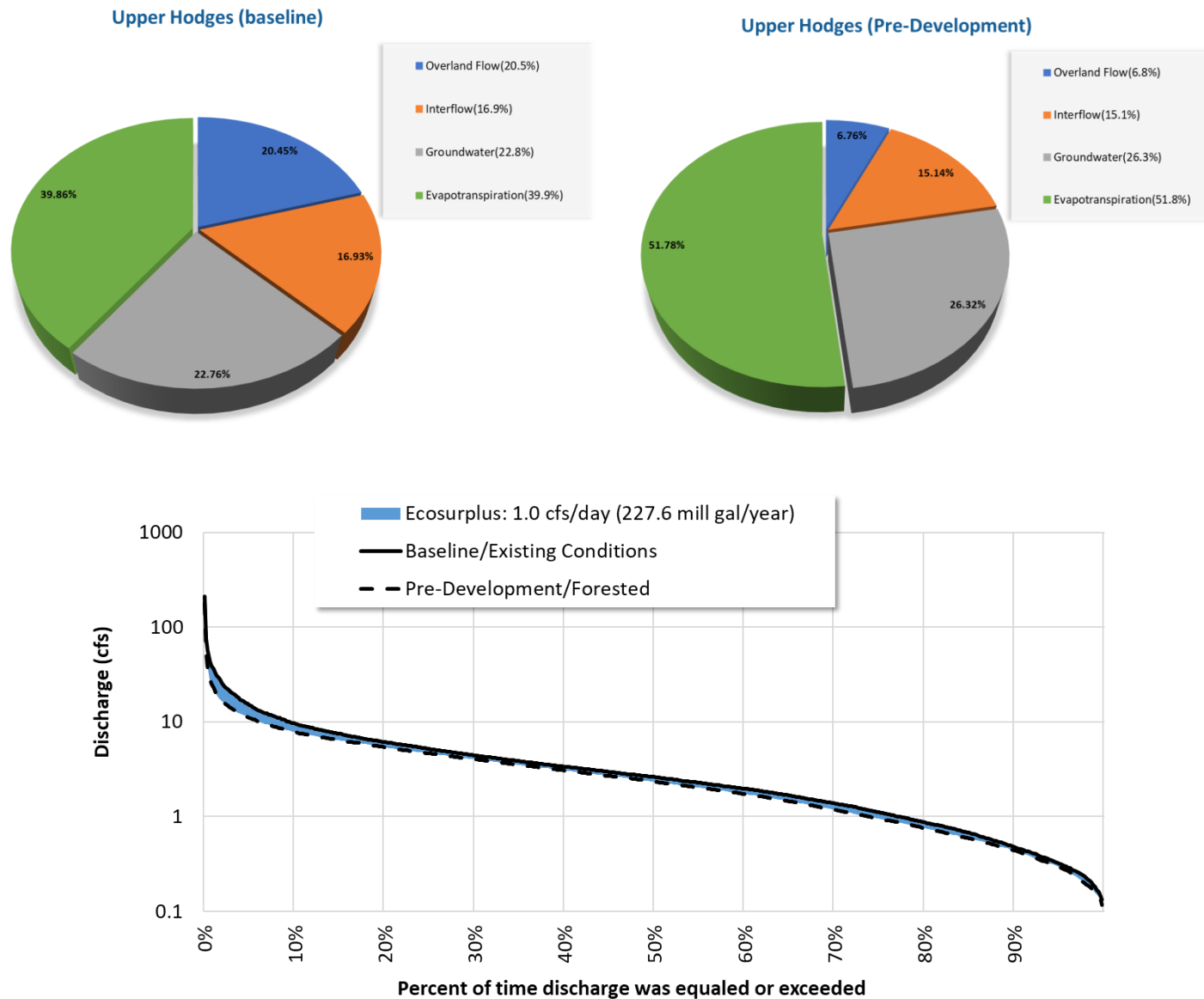


Figure 22. Water balances and Ecosurplus for Upper Hodges Brook watershed for baseline and forested/pre-development conditions. Ecosurplus calculated relative to forested/pre-development conditions.

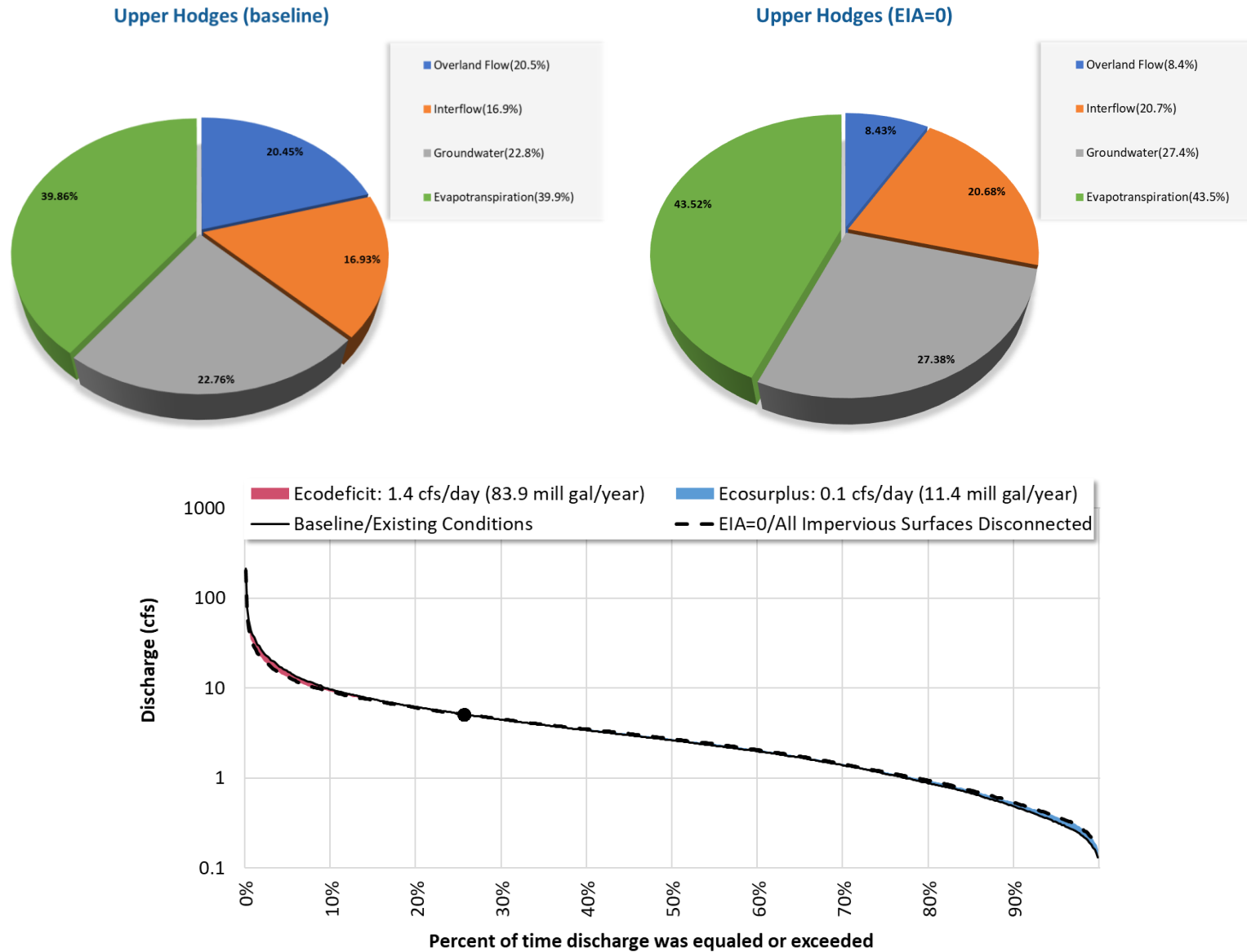


Figure 23. Water balances and Ecosurplus/Ecodeficit for Upper Hodges Brook watershed for baseline and EIA = 0 (all existing impervious surfaces disconnected). Ecosurplus/Ecodeficit calculated relative to baseline/existing condition. Black dots indicate places where FDCs cross

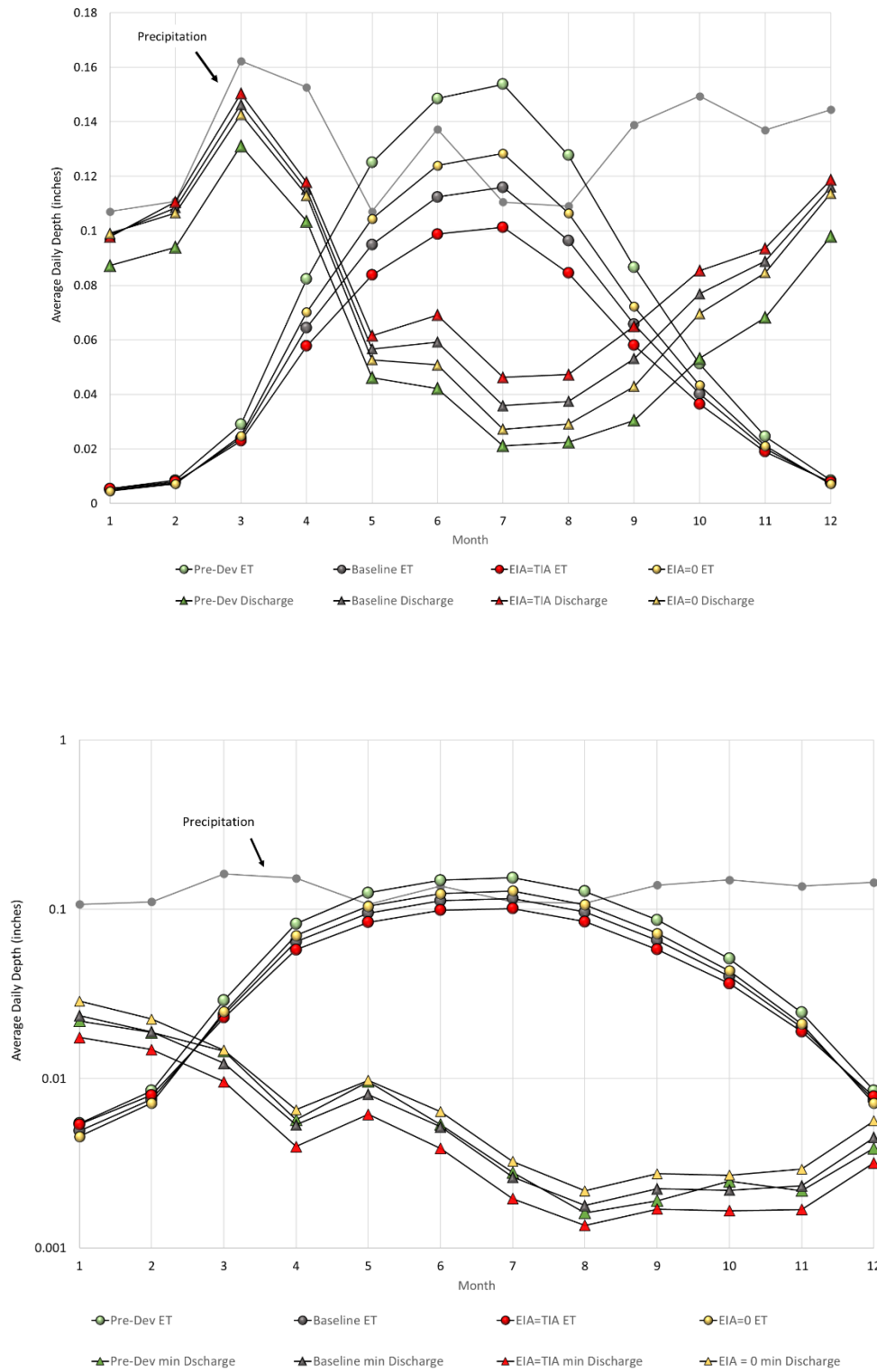


Figure 24. Average (top) and minimum (bottom) monthly flows for land use scenarios. Minimum flows are presented on a logarithmic scale.

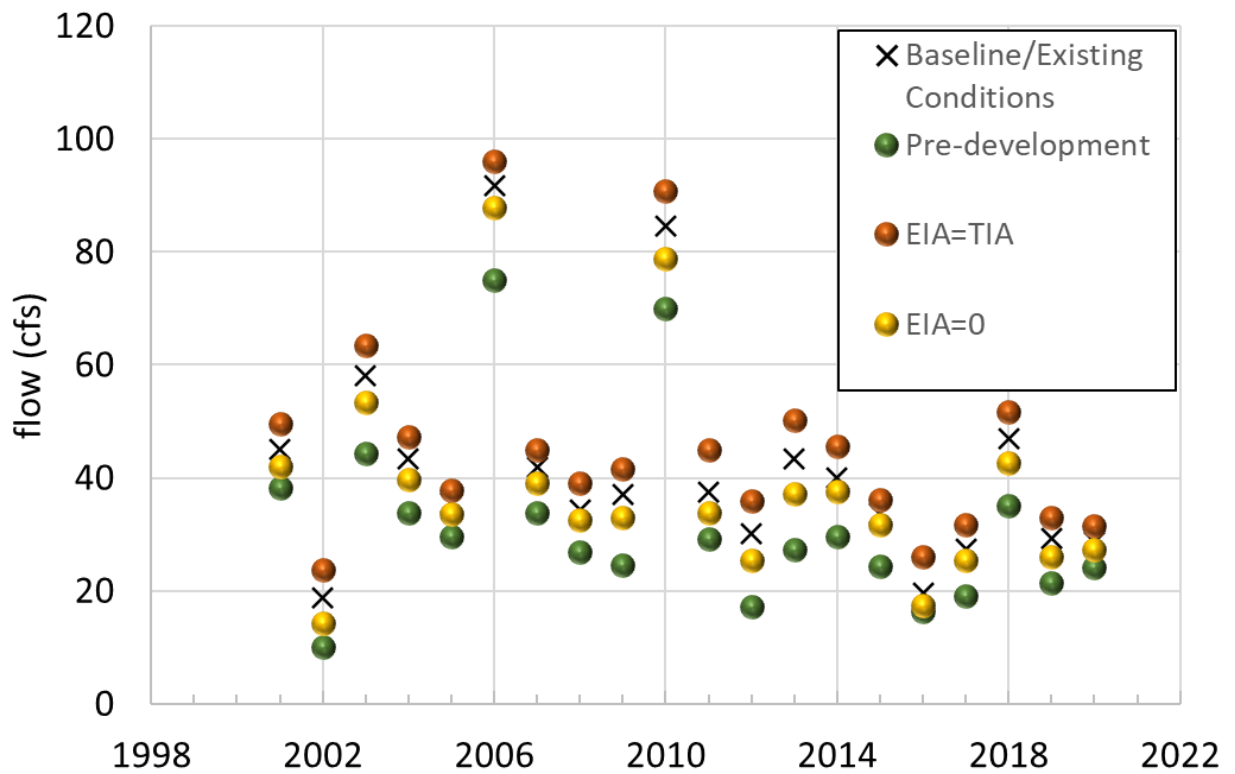
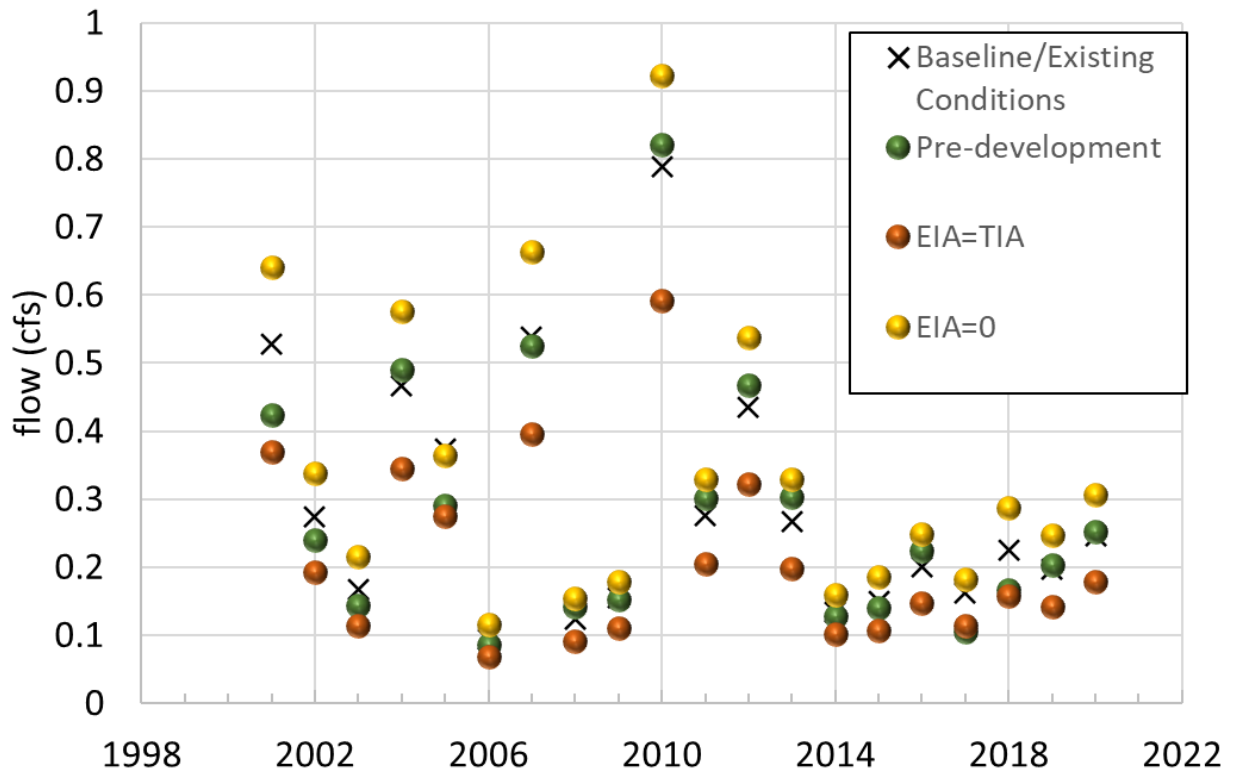
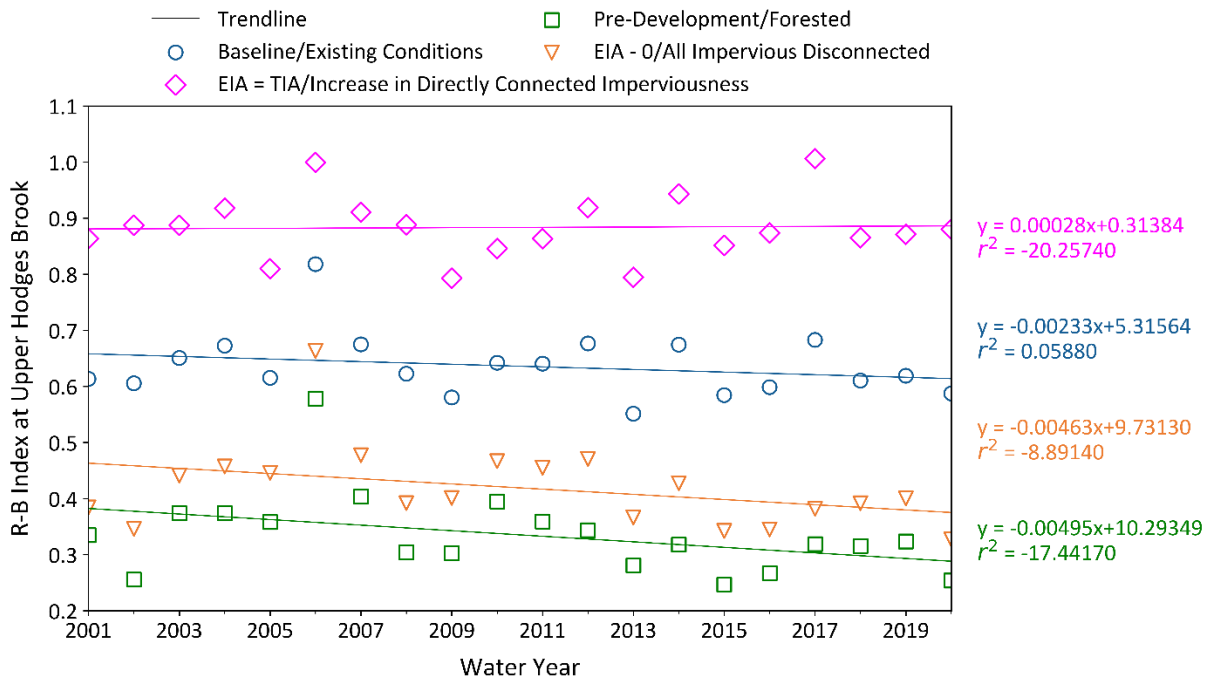


Figure 25. Three-day minimum (top) and maximum (bottom) flow for land-use scenarios.

**Table 10. Comparison of average 3-day minimum and maximum flows for baseline and land-use scenarios**

Average annual flows	Baseline	Pre-development/ Forested		EIA=TIA		EIA = 0	
	cfs	cfs	% diff from baseline	cfs	% diff from baseline	cfs	% diff from baseline
3-day minimum	0.29	0.28	-3.4%	0.21	-27.6%	0.35	20.7%
3-day maximum	41.38	31.51	-23.9%	46.05	11.3%	37.94	-8.3%



**Figure 26. Richard-Baker Flashiness Index for land-use scenarios.**



**Table 11. Summary of average monthly flows and percent differences for land-use scenarios**

Month	Baseline	Pre-development /Forested		All existing impervious directly connected		All existing impervious disconnected	
	Average cfs	Average cfs	% Difference from baseline	Average cfs	% Difference from baseline	Average cfs	% Difference from baseline
January	5.56	4.91	-11.60%	5.52	-0.72%	5.58	0.42%
February	6.11	5.28	-13.50%	6.23	1.93%	5.99	-1.90%
March	8.25	7.39	-10.42%	8.47	2.67%	8.04	-2.52%
April	6.50	5.83	-10.30%	6.65	2.28%	6.36	-2.12%
May	3.20	2.60	-18.79%	3.47	8.56%	2.96	-7.24%
June	3.34	2.37	-29.02%	3.89	16.74%	2.86	-14.36%
July	2.02	1.18	-41.43%	2.60	28.73%	1.52	-24.51%
August	2.11	1.26	-40.29%	2.66	26.30%	1.63	-22.47%
September	2.99	1.71	-42.85%	3.67	22.47%	2.41	-19.38%
October	4.34	3.00	-30.95%	4.82	10.97%	3.92	-9.66%
November	5.01	3.84	-23.34%	5.28	5.35%	4.77	-4.87%
December	6.55	5.52	-15.72%	6.69	2.23%	6.40	-2.17%

### 3.2.2 Pollutant Export

The impact of land-use scenarios on water quality was assessed by quantifying the average annual export of sediment, total phosphorus, total nitrogen, and zinc. Results are relatively straightforward, whereby a scenario of 32% completely connected impervious surfaces results in the highest loadings. Forested conditions and the scenario where all impervious surfaces are managed through disconnection have lower pollutant export rates.

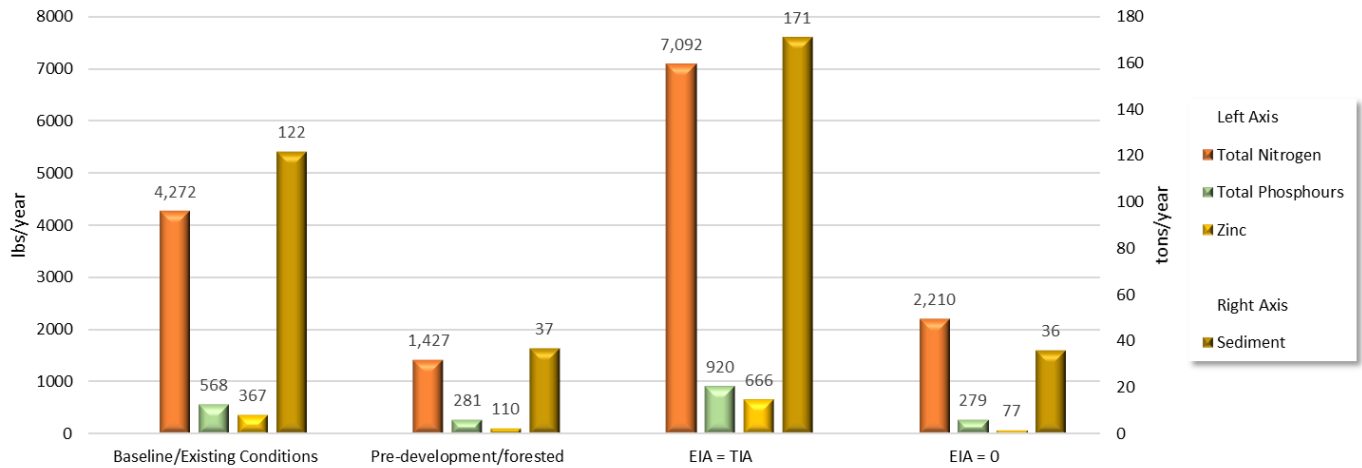


Figure 27. Pollutant export comparisons across land-use scenarios.

### 3.2.3 Climate Change Scenarios

The impact of climate change was assessed using the RCP 4.5 and 8.5 scenarios discussed in section 2.1.4. For the two emission scenarios, twelve models were selected from the period of 2079-2099. This period was selected as a future period to compare to the baseline scenario, which was the 20 years from Oct 2000 – Sep 2020. For both the baseline/existing conditions simulation from 2000-2020 and the future climate simulations from 2079-2099, the HRU distribution remained the same for both, representing the most recently available landcover data, discussed in Task 5 memo. Therefore, any changes to the flow regime may be attributable to changes in the meteorological conditions simulated. Figure 28 presents the ensemble model results for ecodeficits and surpluses. The results suggest that overall, the magnitude of change between deficits and surpluses is similar. The RCP 8.5 scenario produces more extreme ecodeficits than the RCP 4.5 scenario. While RCP 4.5 appears to generally result in slightly ecosurpluses. From the ensemble results, 12 models (Table 12) were selected to represent the range of potential scenarios producing ecodeficits and ecosurpluses. The selected models represent the 20<sup>th</sup>, median, and 80<sup>th</sup> percentile results. For example, for the ecodeficit models for RCP 4.5 miroc-esm-chem-1 was the 20<sup>th</sup> percentile model, producing relatively little ecodeficits, termed the ‘wet’ model, bcc-csm-1-m-1 produced the median, or 50<sup>th</sup> percentile result and was termed the ‘median’ model, and mpi-esm-mr-1 was the 80<sup>th</sup> percentile model producing a relatively high ecodeficit and was termed the ‘dry’ model. Figure 29 and Figure 30 presents the FDCs from the models that produced the 20<sup>th</sup>, median, and 80<sup>th</sup> percentile ecodeficits and ecosurpluses, respectively, for the two RCPs. The FDCs are further compared to the baseline model results in Figure 31 Figure 32, Figure 33, and Figure 34. Ecosurplus and ecodeficits are presented in both cfs/day and millions of gallons per year (mgy). Table 13 presents a summary of ecosurpluses and ecodeficits for the two emission scenarios. For the ecodeficit models, ecodeficits ranged from a low 20<sup>th</sup> percentile (wet) of 470.5 mgy to an 80<sup>th</sup> percentile (dry) 1,829.1 mgy for an RCP 4.5 scenario. For RCP 8.5, the 20<sup>th</sup> percentile ecodeficit increased to 703.2 mgy and the 80<sup>th</sup> percentile ecodeficit increased to 2,281.8 mgy.

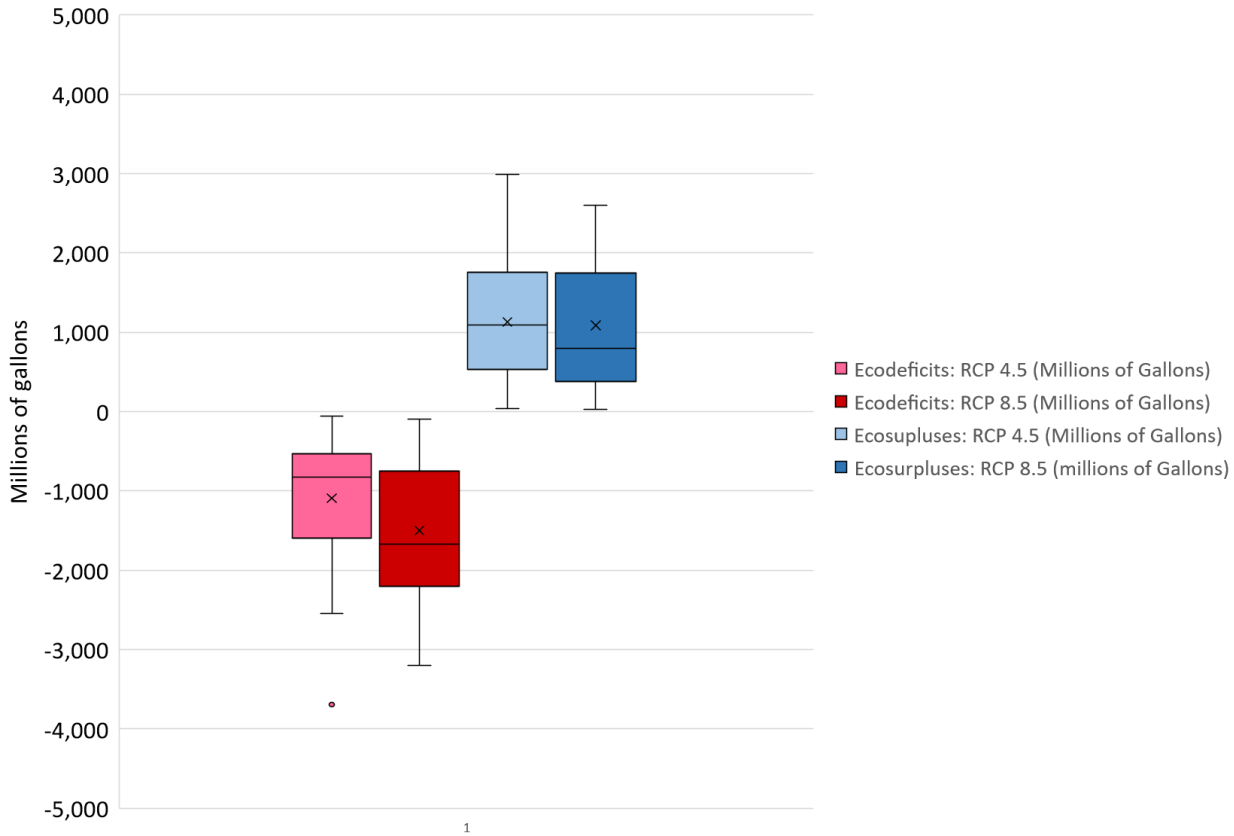


Figure 28. Ensemble results for ecosurplus and ecodificits.

Table 12. Selected models from ensemble results

RCP	Scenario	Ecosurplus Model	Ecodificit Model
RCP 4.5	Dry	hadgem2-cc-1	mpi-esm-mr-1
	Median	bcc-csm1-1-m-1	bcc-csm1-1-m-1
	Wet	bcc-csm1-1-1	miroc-esm-chem-1
RCP 8.5	Dry	inmcm4-1	miroc-esm-1
	Median	cesm1-cam5-1	cesm1-cam5-1
	Wet	cesm1-bgc-1	mri-cgcm3-1

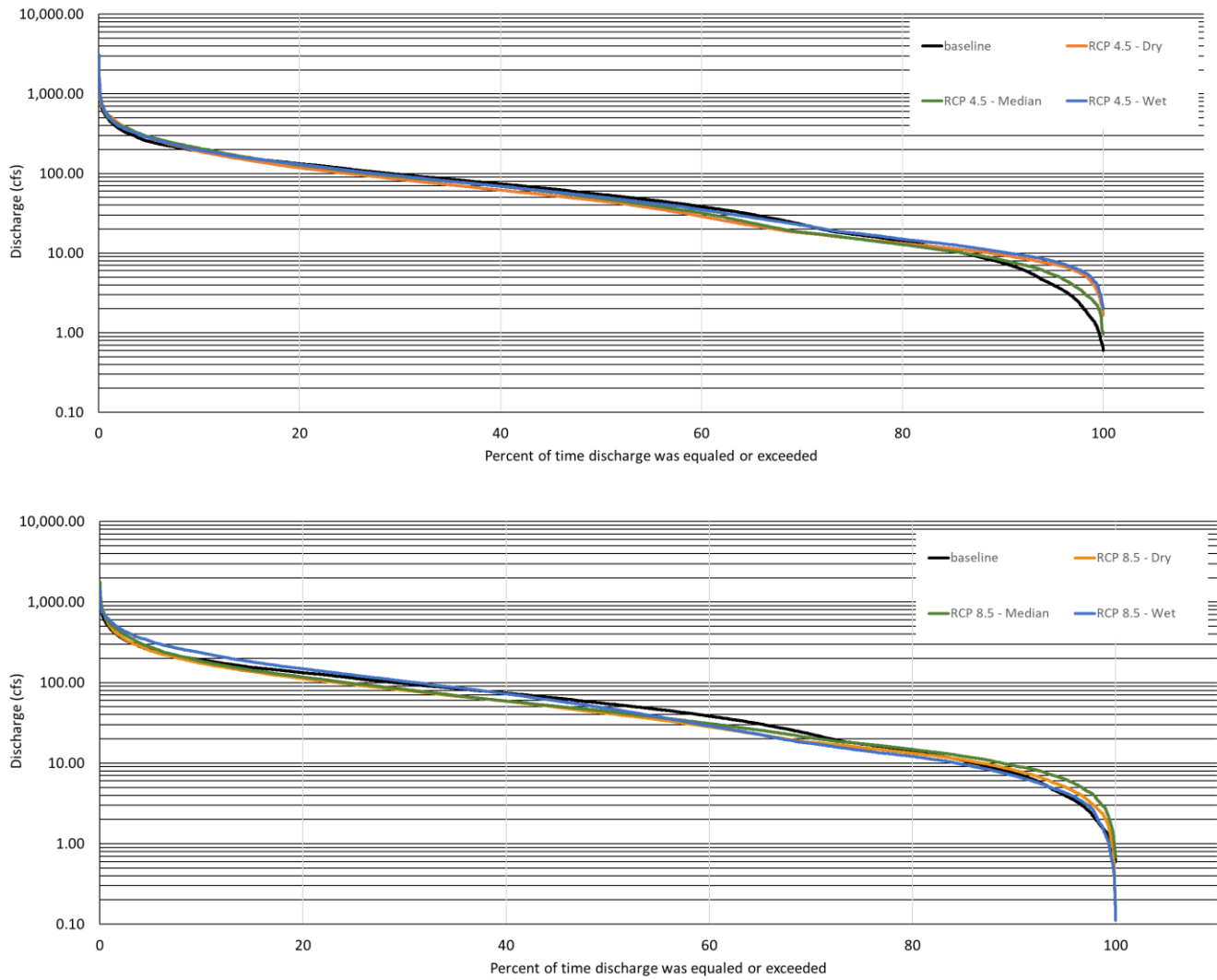


Figure 29. Ecodeficit FDCs at the Wading River USGS Gage (01109000) under baseline and climate change scenarios for RCP 8.5 (top) and RCP 4.5 (bottom).

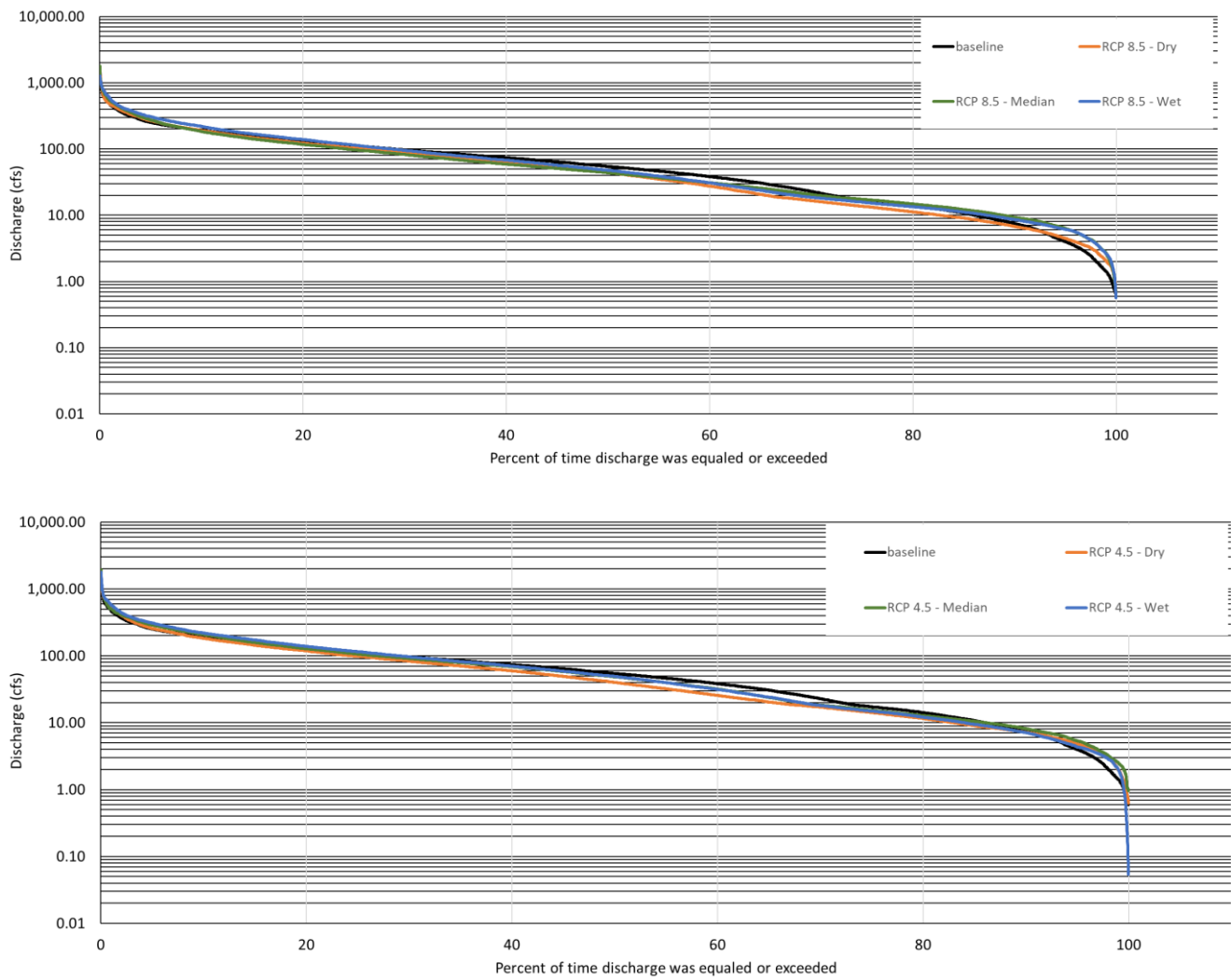


Figure 30. Ecosuplus FDCs at the Wading River USGS Gage (01109000) under baseline and climate change scenarios for RCP 8.5 (top) and RCP 4.5 (bottom).

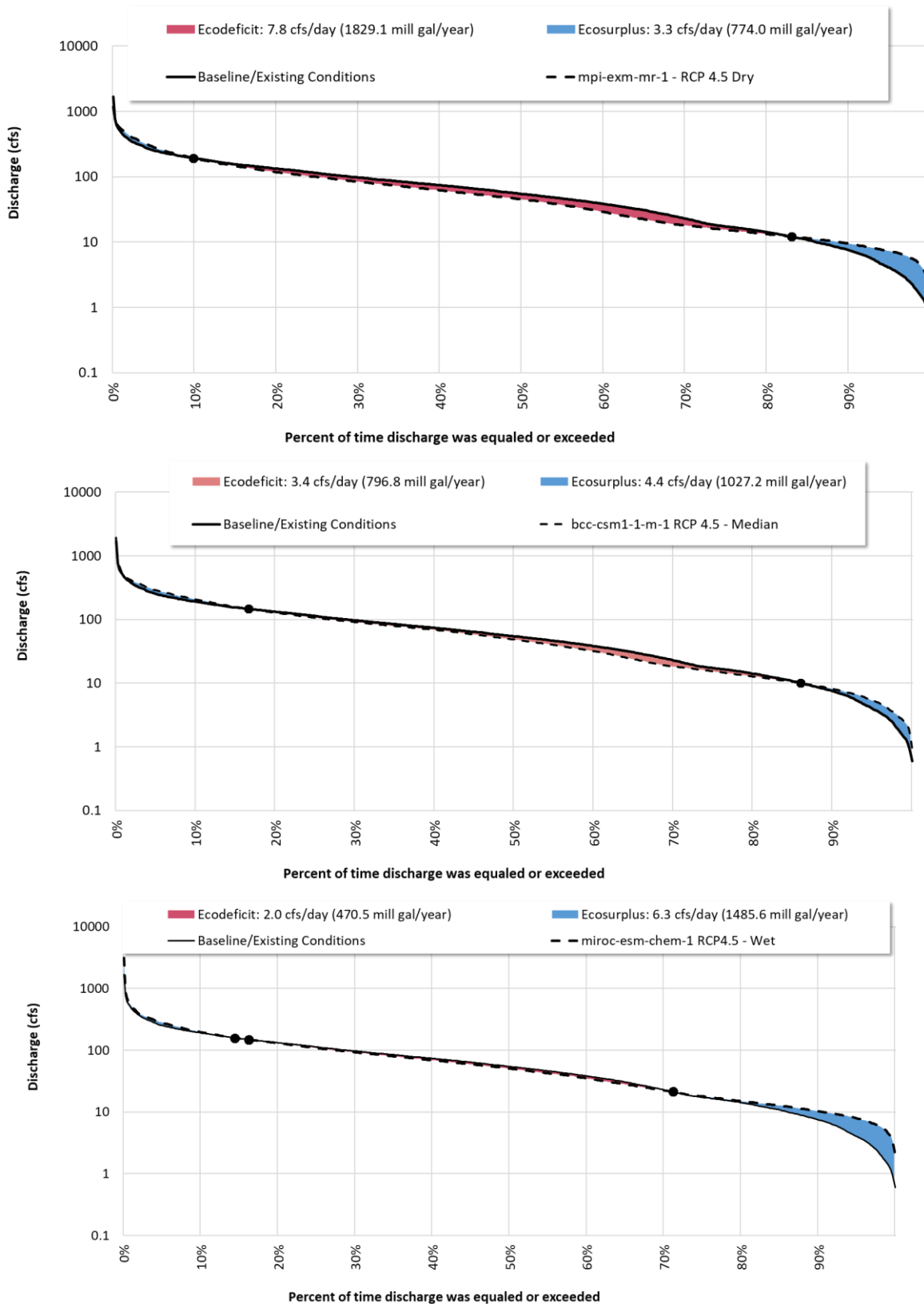


Figure 31. Results for the wet, median, and dry models for ecodeficits based on an RCP 4.5 scenario. Results are for the Wading River USGS Gage (01109000) under comparing baseline (2000-2020) to future climate scenarios (2079-2099).



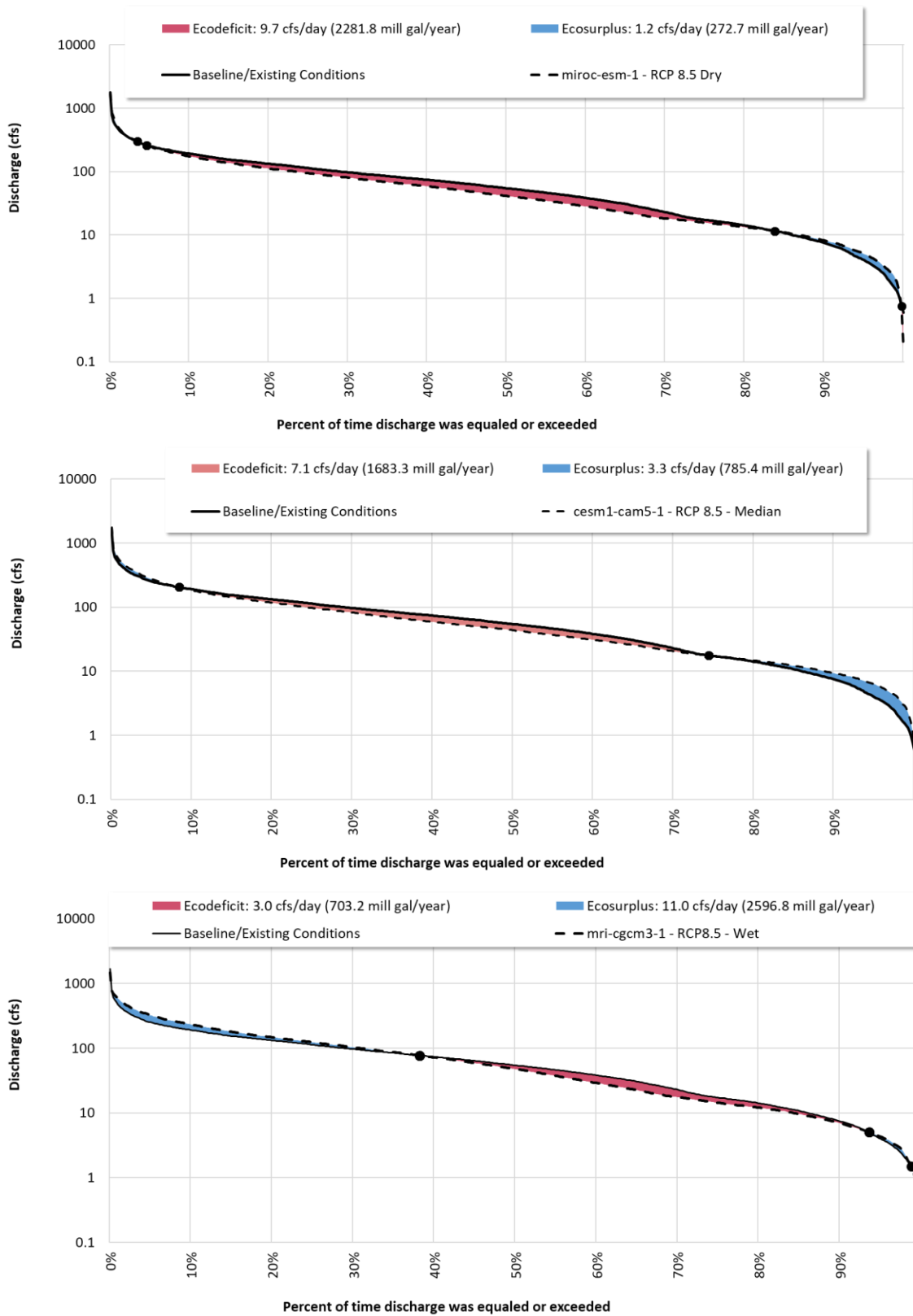


Figure 32. Results for the wet, median, and dry models for ecodéficits based on an RCP 8.5 scenario. Results are for Wading River USGS Gage (01109000) comparing baseline (2000-2020) to future climate scenarios (2079-2099).

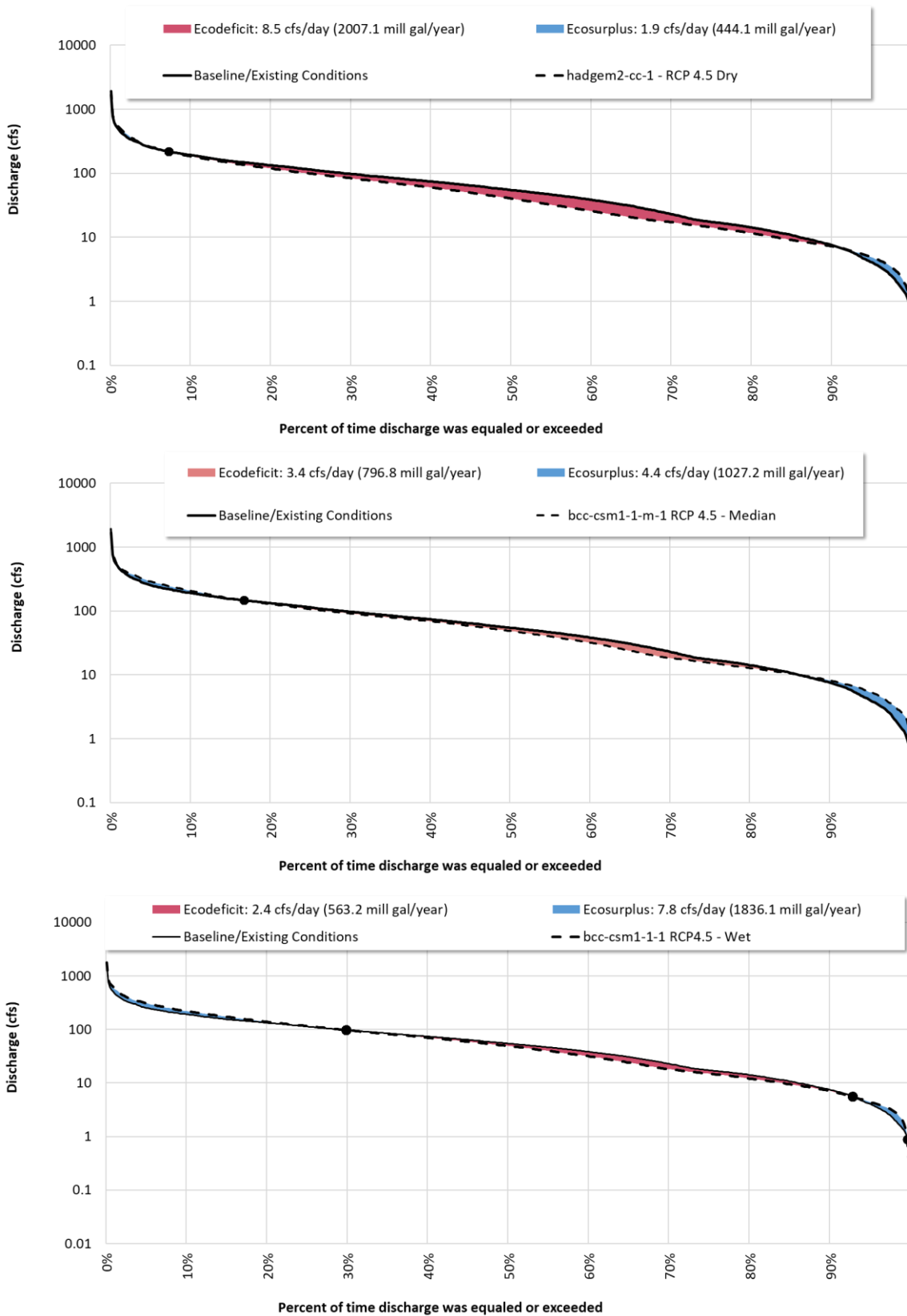
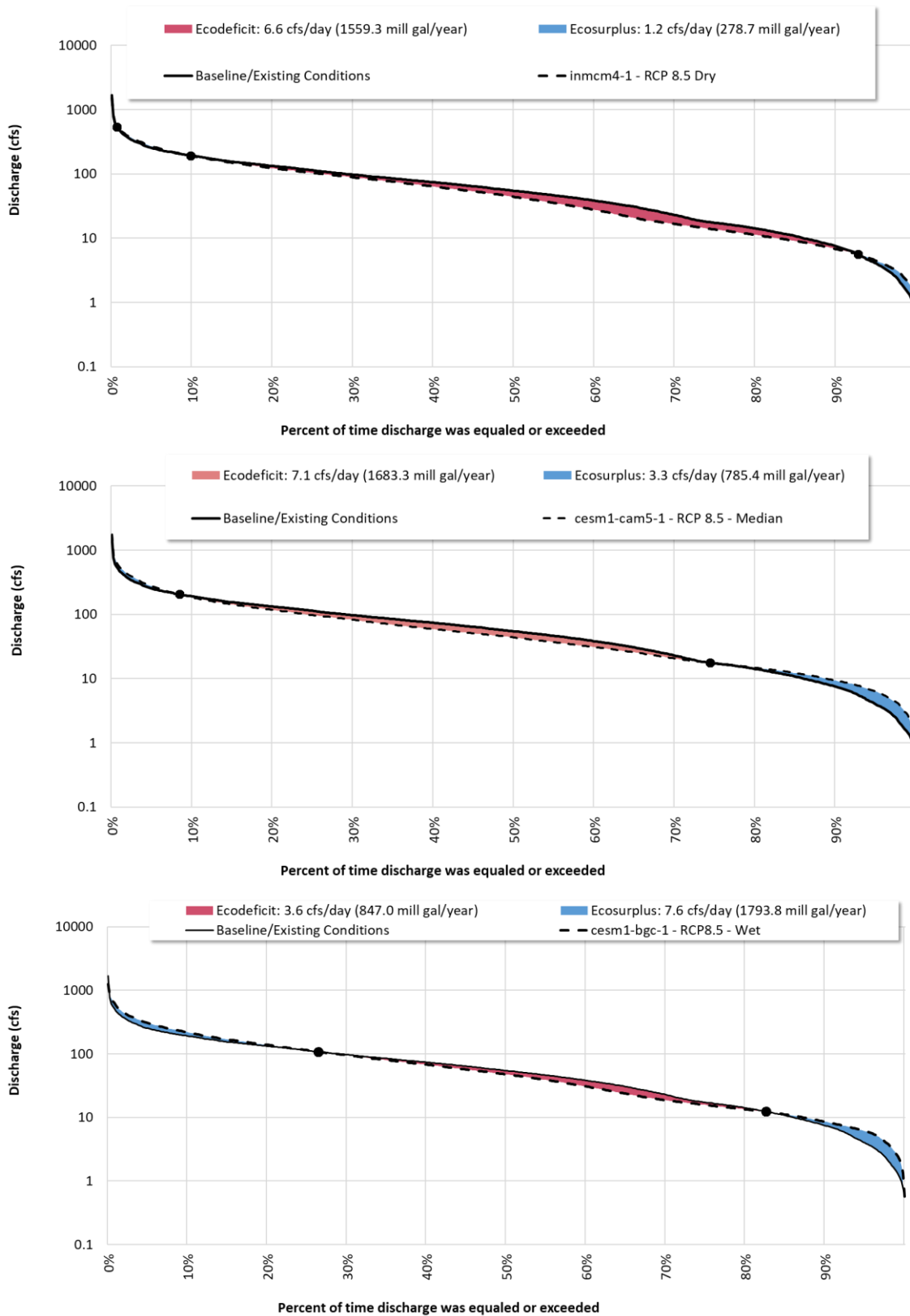


Figure 33. Results for the wet, median, and dry models for ecosurpluses based on an RCP 4.5 scenario. Results are for Wading River USGS Gage (01109000) comparing baseline (2000-2020) to future climate scenarios (2079-2099).



**Figure 34. Results for the wet, median, and dry models for ecosurpluses based on an RCP 8.5 scenario. Results are for the Wading River USGS Gage (01109000) comparing baseline (2000-2020) to future climate scenarios (2079-2099).**

**Table 13. Summary of ecosurpluses and ecodeficits (millions of gallons per year) for RCP 8.5 and 4.5 scenarios**

Scenario	Ecodeficit models					
	Ecodeficits			Ecosurplus		
	Dry	Median	Wet	Dry	Median	Wet
RCP 4.5	1,829.1	796.8	470.5	774.0	1,027.2	1,485.6
RCP 8.5	2,281.8	1,683.3	703.2	272.7	785.4	2,596.8
Scenario	Ecosurplus models					
	Ecodeficits			Ecosurplus		
	Dry	Median	Wet	Dry	Median	Wet
RCP 4.5	2,007.1	796.8	563.2	444.1	1,027.2	1,836.1
RCP 8.5	1,559.3	1,683.3	847.0	278.7	785.4	1,793.8

For the ecosurplus models, the result ranges from a 20<sup>th</sup> percentile ecosurplus of 441.1 mgly to an 80<sup>th</sup> percentile 1,836.1 mgly for the RCP 4.5 scenario. For the RCP 8.5 scenario, ecosurpluses for the 20<sup>th</sup> and 80<sup>th</sup> percentiles are almost lower to 278.2 and 1,793.8 mgly, respectively. Overall, these results support the conclusions of Demaria et al (2016) who found that future climate scenarios may result in a decrease in the magnitude of low flow conditions in the northeast. Table 14 presents the analysis of average 3-day low flows and high flows for the RCP 4.5 and 8.5 model simulations compared against the baseline simulation. While FDC analysis helps to understand the overall trends, analysis of 3-day low and high flows provides greater information on extreme (drought vs flood) conditions. General trends in the data show the lowest flows (average 3-day minimum flow) became higher, which is expected given the prevalence of ecosurpluses at low flows on the climate change FDCs. Additionally, the high flows also became higher. The analysis removed two years from the observed annual 3-day maximum flow dataset. These were high flows resulting from tropical storm Tammy in October of 2005 and a nor'easter in March of 2010. The high flows from these two storms resulted in 2005 and 2010 having annual maximum high flows almost 3 times higher than the average from high flows across the other years (2000-2020). The two years were therefore removed to provide a better comparison of historical and future high flows that were not impacted by rare, extreme, historical events. Uncertainty surrounding future climate predictions is well documented and a field of active research. The results suggest that assuming no change to land use, future climate conditions will result in both low and high flows increasing in the Wading River. Table 15 shows that generally, the selected climate models have more days with a relatively high precipitation amount ( $\geq 0.5$  in) compared to the baseline. Table 16 shows how seasonal rainfall trends change. More precipitation generally occurs in the winter months. Interestingly, most models also have additional rain in August, which is typically the period for the lowest flows in the watershed.

Table 17 provides information on possible future drought conditions by quantifying changes in the maximum amount of consecutive dry days that occur. Late spring and early summer appear to become drier while winter becomes wetter. Table 18, Table 19, and Table 20 present an analysis of future temperatures. Overall, the maximum, minimum, and average temperatures are expected to increase throughout the year. While the percent change to maximum temperatures does not appear to have a strong seasonal influence, the winter is expected to see large increases in minimum and average temperatures.

**Table 14. Percent change in 3-day minimum and maximum flows for RCP 8.5 and 4.5 scenarios compared to baseline simulation**

Model	RCP	Scenario	Average annual 3-day minimum (cfs)	Average annual 3-day maximum (cfs)
Baseline	NA	Historical	3.75	500.44
Ecodeficit Model	RCP45	Dry	38.53%	-12.37%
Ecodeficit Model	RCP45	Median	18.16%	-10.44%
Ecodeficit Model	RCP45	Wet	70.85%	6.64%
Ecodeficit Model	RCP85	Dry	38.10%	18.15%
Ecodeficit Model	RCP85	Median	51.23%	26.23%
Ecodeficit Model	RCP85	Wet	15.88%	13.29%
Ecosurplus Model	RCP45	Dry	-2.50%	27.88%
Ecosurplus Model	RCP45	Median	18.16%	15.40%
Ecosurplus Model	RCP45	Wet	8.02%	20.76%
Ecosurplus Model	RCP85	Dry	0.25%	24.95%
Ecosurplus Model	RCP85	Median	51.23%	26.23%
Ecosurplus Model	RCP85	Wet	19.08%	20.34%

**Table 15. Dry days and days with precipitation for the selected future climate scenarios compared to the historical, observed conditions.**

Model	RCP	Scenario	Maximum Consecutive Dry Days	Average No. Rain Days				
				≥0.01 in	≥0.10 in	≥0.50 in	≥1.00 in	≥2.00 in
Baseline	NA	Historical	8.4	128.0	78.2	29.9	12.6	2.4
Ecodeficit Model	RCP45	Dry	9.3	126.1	78.3	29.3	12.9	2.3
Ecodeficit Model	RCP45	Median	9.2	125.5	77.6	29.1	12.5	2.3
Ecodeficit Model	RCP45	Wet	8.7	126.8	77.0	31.2	13.9	3.4
Ecodeficit Model	RCP85	Dry	9.6	122.0	76.2	31.6	14.0	3.0
Ecodeficit Model	RCP85	Median	9.3	128.6	78.2	32.1	13.8	2.7
Ecodeficit Model	RCP85	Wet	8.5	126.0	79.3	34.6	15.3	3.4
Ecosurplus Model	RCP45	Dry	9.1	126.1	76.1	31.2	13.0	2.4
Ecosurplus Model	RCP45	Median	9.2	125.5	77.6	29.1	12.5	2.3
Ecosurplus Model	RCP45	Wet	9.5	130.2	77.0	31.1	13.9	2.4
Ecosurplus Model	RCP85	Dry	8.7	125.6	75.8	29.2	12.5	2.5
Ecosurplus Model	RCP85	Median	9.3	128.6	78.2	32.1	13.8	2.7
Ecosurplus Model	RCP85	Wet	8.8	132.8	82.2	33.2	15.1	2.7

Note: For maximum consecutive dry days, red shading indicates an increase in dry days. For rain days, red shading indicates a decrease in days greater than or equal to the associated depth, blue shading indicates an increase in days with precipitation greater than or equal to the associated depth.

**Table 16. Percent change for average annual and monthly precipitation for future climate scenarios compared to the historical, observed conditions.**

Model	RCP	Scenario	Percent Change of Average Monthly Precipitation (inches) by Scenario												
			Annual	Jan	Feb	Mar	Apr	May	Jun	Jul	Aug	Sep	Oct	Nov	Dec
NA	NA	Historical	46.9	3.3	3.2	4.9	4.6	3.5	4.1	3.5	3.1	4.1	4.4	3.9	4.2
Ecodeficit Model	RCP45	Dry	-1%	44%	16%	-8%	9%	-1%	-26%	-29%	36%	-14%	-7%	3%	-15%
Ecodeficit Model	RCP45	Median	-2%	36%	37%	-18%	-29%	-25%	-17%	1%	0%	-6%	-2%	1%	18%
Ecodeficit Model	RCP45	Wet	4%	17%	18%	-11%	-34%	-9%	14%	4%	33%	15%	-1%	12%	12%
Ecodeficit Model	RCP85	Dry	5%	20%	14%	-4%	-23%	2%	-2%	38%	-12%	-1%	-15%	51%	3%
Ecodeficit Model	RCP85	Median	4%	34%	7%	-8%	-15%	-13%	-43%	10%	72%	23%	6%	-13%	16%
Ecodeficit Model	RCP85	Wet	10%	47%	81%	33%	-33%	-3%	-30%	-14%	-3%	9%	-3%	35%	21%
Ecosurplus Model	RCP45	Dry	0%	19%	32%	-2%	-19%	7%	-20%	-2%	-2%	-4%	-39%	-9%	49%
Ecosurplus Model	RCP45	Median	-2%	36%	37%	-18%	-29%	-25%	-17%	1%	0%	-6%	-2%	1%	18%
Ecosurplus Model	RCP45	Wet	2%	28%	38%	-5%	3%	-17%	-34%	-18%	31%	-18%	5%	7%	20%
Ecosurplus Model	RCP85	Dry	-2%	30%	9%	-15%	5%	-4%	-31%	-14%	39%	-10%	-22%	16%	-1%
Ecosurplus Model	RCP85	Median	4%	34%	7%	-8%	-15%	-13%	-43%	10%	72%	23%	6%	-13%	16%
Ecosurplus Model	RCP85	Wet	9%	66%	54%	14%	-14%	-16%	-37%	39%	5%	18%	-29%	21%	8%

Note: Red shading indicates a decrease in precipitation, blue shading indicates an increase in precipitation

**Table 17. Percent change for average maximum consecutive dry days for the future climate scenarios compared to the historical, observed conditions.**

Model	RCP	Scenario	Percent Change for Average No. Maximum Consecutive Dry Days by Scenario												
			Annual	Jan	Feb	Mar	Apr	May	Jun	Jul	Aug	Sep	Oct	Nov	Dec
Baseline	NA	Historical	8	11	10	9	8	7	7	8	9	9	7	9	8
Ecodeficit Model	RCP45	Dry	11%	-33%	-16%	6%	6%	11%	31%	27%	6%	11%	73%	21%	21%
Ecodeficit Model	RCP45	Median	9%	-21%	-14%	-8%	5%	42%	38%	23%	25%	16%	36%	1%	-2%
Ecodeficit Model	RCP45	Wet	4%	-9%	-12%	-12%	2%	45%	30%	18%	-19%	-13%	36%	12%	2%
Ecodeficit Model	RCP85	Dry	15%	-27%	-15%	-17%	17%	82%	36%	40%	57%	18%	30%	4%	-9%
Ecodeficit Model	RCP85	Median	11%	-13%	5%	12%	-1%	26%	61%	29%	-24%	-19%	37%	38%	10%
Ecodeficit Model	RCP85	Wet	1%	-17%	-33%	-22%	11%	19%	41%	22%	5%	14%	33%	-19%	-9%
Ecosurplus Model	RCP45	Dry	8%	-34%	-29%	-8%	28%	28%	40%	33%	15%	14%	75%	-6%	-10%
Ecosurplus Model	RCP45	Median	9%	-21%	-14%	-8%	5%	42%	38%	23%	25%	16%	36%	1%	-2%
Ecosurplus Model	RCP45	Wet	13%	-28%	-17%	-21%	-11%	38%	5%	60%	2%	50%	83%	36%	-3%
Ecosurplus Model	RCP85	Dry	4%	-21%	-23%	-29%	-6%	20%	47%	36%	-6%	1%	66%	11%	-5%
Ecosurplus Model	RCP85	Median	11%	-13%	5%	12%	-1%	26%	61%	29%	-24%	-19%	37%	38%	10%
Ecosurplus Model	RCP85	Wet	4%	-21%	-26%	-12%	-8%	18%	47%	21%	1%	-10%	52%	10%	16%

Note: Red shading indicates an increase in dry days, blue shading indicates a decrease in dry days

**Table 18. Percent change in average maximum daily temperature for the selected future climate scenarios compared to the historical, observed conditions**

Model	RCP	Scenario	Average Maximum Daily Temperature (F) / Percent Change by Scenario												
			Annual	Jan	Feb	Mar	Apr	May	Jun	Jul	Aug	Sep	Oct	Nov	Dec
Baseline	NA	Historical	65	48	46	53	63	72	78	81	79	75	67	60	54
Ecodeficit Model	RCP45	Dry	3%	-1%	-2%	5%	3%	3%	4%	2%	3%	5%	3%	3%	5%
Ecodeficit Model	RCP45	Median	1%	-4%	0%	2%	0%	3%	2%	3%	3%	3%	-2%	-2%	-2%
Ecodeficit Model	RCP45	Wet	2%	-5%	4%	7%	3%	4%	3%	3%	5%	4%	0%	1%	-4%
Ecodeficit Model	RCP85	Dry	10%	9%	18%	14%	11%	10%	9%	8%	9%	9%	8%	9%	3%
Ecodeficit Model	RCP85	Median	7%	3%	8%	3%	6%	8%	7%	6%	9%	8%	5%	7%	8%
Ecodeficit Model	RCP85	Wet	5%	7%	11%	4%	9%	3%	5%	4%	4%	6%	2%	3%	2%
Ecosurplus Model	RCP45	Dry	5%	-2%	5%	5%	8%	2%	3%	4%	7%	4%	6%	9%	5%
Ecosurplus Model	RCP45	Median	1%	-4%	0%	2%	0%	3%	2%	3%	3%	3%	-2%	-2%	-2%
Ecosurplus Model	RCP45	Wet	1%	-5%	6%	4%	2%	-1%	2%	2%	3%	3%	-1%	-2%	-5%
Ecosurplus Model	RCP85	Dry	4%	4%	11%	8%	7%	4%	3%	2%	3%	6%	2%	6%	0%
Ecosurplus Model	RCP85	Median	7%	3%	8%	3%	6%	8%	7%	6%	9%	8%	5%	7%	8%
Ecosurplus Model	RCP85	Wet	5%	7%	8%	4%	7%	6%	6%	5%	7%	7%	4%	-2%	3%

Note: Red shading indicates an increase in temperature, blue shading indicates a decrease in temperature.



**Table 19. Percent change in average minimum daily temperature for the selected future climate scenarios compared to the historical, observed conditions**

Model	RCP	Scenario	Average Minimum Daily Temperature (F) / Percent Change by Scenario												
			Annual	Jan	Feb	Mar	Apr	May	Jun	Jul	Aug	Sep	Oct	Nov	Dec
Baseline	NA	Historical	38	12	18	24	37	47	55	64	62	52	40	29	21
Ecodeficit Model	RCP45	Dry	6%	67%	-1%	11%	7%	2%	3%	1%	5%	5%	4%	15%	-3%
Ecodeficit Model	RCP45	Median	5%	36%	8%	14%	1%	-1%	3%	2%	4%	2%	4%	12%	3%
Ecodeficit Model	RCP45	Wet	9%	46%	27%	28%	11%	0%	6%	6%	7%	3%	7%	12%	2%
Ecodeficit Model	RCP85	Dry	24%	110%	46%	51%	26%	13%	20%	14%	17%	16%	15%	32%	27%
Ecodeficit Model	RCP85	Median	14%	87%	46%	25%	1%	1%	5%	8%	11%	7%	13%	33%	34%
Ecodeficit Model	RCP85	Wet	14%	70%	34%	27%	9%	6%	8%	8%	6%	6%	12%	28%	33%
Ecosurplus Model	RCP45	Dry	10%	70%	10%	16%	5%	4%	7%	4%	7%	-1%	10%	21%	30%
Ecosurplus Model	RCP45	Median	5%	36%	8%	14%	1%	-1%	3%	2%	4%	2%	4%	12%	3%
Ecosurplus Model	RCP45	Wet	7%	48%	0%	24%	6%	5%	5%	4%	6%	7%	7%	10%	1%
Ecosurplus Model	RCP85	Dry	5%	66%	22%	27%	5%	-4%	3%	-2%	1%	-1%	1%	16%	2%
Ecosurplus Model	RCP85	Median	14%	87%	46%	25%	1%	1%	5%	8%	11%	7%	13%	33%	34%
Ecosurplus Model	RCP85	Wet	13%	85%	40%	24%	6%	3%	9%	6%	8%	6%	8%	25%	29%

Note: Red shading indicates an increase in temperature, blue shading indicates a decrease in temperature.

**Table 20. Percent change in average daily temperature for the selected future climate scenarios compared to the historical, observed conditions**

Model	RCP	Scenario	Average Daily Temperature (F) / Percent Change by Scenario												
			Annual	Jan	Feb	Mar	Apr	May	Jun	Jul	Aug	Sep	Oct	Nov	Dec
Baseline	NA	Historical	51.1	29.6	31.7	38.1	48.1	58.1	66.5	72.7	71.0	63.7	53.5	43.7	35.1
Ecodeficit Model	RCP45	Dry	5%	11%	3%	8%	5%	4%	4%	2%	3%	5%	2%	6%	6%
Ecodeficit Model	RCP45	Median	3%	6%	1%	6%	3%	2%	3%	3%	3%	3%	2%	1%	4%
Ecodeficit Model	RCP45	Wet	6%	10%	10%	15%	9%	5%	6%	4%	6%	4%	4%	5%	2%
Ecodeficit Model	RCP85	Dry	16%	27%	27%	27%	20%	14%	13%	11%	13%	13%	13%	17%	15%
Ecodeficit Model	RCP85	Median	11%	18%	18%	12%	7%	8%	7%	7%	10%	10%	10%	13%	19%
Ecodeficit Model	RCP85	Wet	9%	17%	18%	11%	11%	6%	8%	5%	6%	7%	5%	10%	14%
Ecosurplus Model	RCP45	Dry	7%	11%	4%	7%	9%	5%	6%	5%	8%	6%	8%	12%	13%
Ecosurplus Model	RCP45	Median	3%	6%	1%	6%	3%	2%	3%	3%	3%	3%	2%	1%	4%
Ecosurplus Model	RCP45	Wet	4%	3%	4%	10%	6%	2%	4%	4%	4%	6%	2%	2%	0%
Ecosurplus Model	RCP85	Dry	6%	14%	12%	14%	10%	5%	5%	2%	4%	4%	2%	5%	3%
Ecosurplus Model	RCP85	Median	11%	18%	18%	12%	7%	8%	7%	7%	10%	10%	10%	13%	19%
Ecosurplus Model	RCP85	Wet	9%	20%	17%	9%	10%	8%	7%	6%	8%	8%	8%	8%	14%

Note: Red shading indicates an increase in temperature.

### 3.3 Carbon Sequestration

Carbon sequestration is the process of capturing and storing atmospheric carbon dioxide (CO<sub>2</sub>) which is the most commonly produced greenhouse gas. Carbon is sequestered in vegetation such as grasslands or forests, as well as in soils as organic carbon. The activities that involve land conservation or restoration and some agricultural Nature-Based Solutions (NBS) and green infrastructure BMPs can sequester carbon.

Forests, grasslands, peat swamps, and other terrestrial ecosystems collectively store much more carbon than does the atmosphere (Lal 2002). By storing this carbon in wood, other biomass, and soil, ecosystems keep CO<sub>2</sub> out of the atmosphere, where it would contribute to climate change. Beyond just storing carbon, many systems also continue to accumulate it in plants and soil over time, thereby “sequestering” additional carbon each year. Disturbing these systems with fire, disease, or vegetation conversion (e.g., land use/land cover (LULC) conversion) can release large amounts of CO<sub>2</sub>. Other management changes, like forest restoration or alternative agricultural practices, can lead to the storage of large amounts of CO<sub>2</sub>. Therefore, how we manage terrestrial ecosystems is critical to regulating our climate (Brill et. al., 2021).

The Natural Capital Project’s InVEST (Integrated Valuation of Ecosystem Services and Tradeoffs) open-source software uses a relatively simple terrestrial ecosystem biomass and soil carbon model to calculate net annual carbon balance (positive or negative) following a change from one land use/land cover (LULC) type



to another and based on global datasets of LULC, soil carbon, and other parameters. Stock-change or gain-loss methods to estimate avoided CO<sub>2</sub> emissions or CO<sub>2</sub> removals (Table 21) are typically based on information regarding activity data (i.e., hectares of protected area) and emission factors (i.e., tons of avoided CO<sub>2</sub>).

**Table 21. Carbon benefits and associated activities, indicators, and calculation methods (Brill et.al., 2021)**

Benefit	Habitat Intervention	Activity	Indicator	Calculation Method
Improved carbon sequestration	Land restoration, wetland, and mangrove restoration	Plant/restore native vegetation, introduce grazing management systems	CO <sub>2</sub> removals by above and below-ground biomass and soil	Stock-change or gain-loss methods
	Agricultural management	Agricultural NBS (introduce grazing management systems, plant vegetation buffers)	CO <sub>2</sub> removals by above and below-ground biomass and soil	Stock-change or gain-loss methods
Reduced/avoided carbon emissions	Land (forest, grassland) protection	Avoided habitat conversion (forest, grassland)	Avoided CO <sub>2</sub> emissions from above- and belowground biomass and soil	Stock-change or gain-loss methods
	Agricultural management	Agricultural NBS (activities relating to rice management like restoring/improving soil health)	Avoided CH <sub>4</sub> emissions from soil (rice fields)	Stock-change or gain-loss methods
	Wetland protection	Avoided habitat conversion	Avoided CH <sub>4</sub> emissions from the soil at wetlands	Stock-change or gain-loss methods

Given a range of data, carbon storage data should be set equal to the average carbon storage values for each LULC class. The ideal data source for all carbon stocks is a set of local field estimates, where carbon storage for all relevant stocks has been directly measured. These can be summarized to the LULC map, including any stratification by age or other variables. For this analysis, the default sample dataset from InVEST carbon model (Table 22) was used and a crosswalk table (Table 23) was developed for mapping the LULC classification of the carbon pool dataset with the HRU classification of the Wading River model. The results from the InVEST Carbon model are presented in Table 24. The results show that the existing land use/land cover condition has reduced 58%, 27%, and 20% of the Carbon pool compared to the predevelopment/forested condition for Upper Hodges Brook, Lower Hodges Brook, and Pilot Tributary sub-watersheds, respectively.

The model limitations include; (1) the land use/land cover types are not gaining or losing carbon over time whereas in reality with age the same LULC could be accumulating more carbon, (2) carbon storage is fixed for a given LULC type and does not account for the age, so the storage varies only across the LULC types, (3) the model does not capture the movement of carbon from above-ground biomass to other dead organic material, (4) the carbon sequestration is assumed to be linear change over the time while most sequestration follows a non-linear path such that carbon is sequestered at a higher rate in the first few years and a lower rate in subsequent years.

**Table 22. Carbon pool default dataset by land use/land cover type in InVEST carbon model**

LUCODE	Land Use / Land Cover Name	Carbon (megagrams/ha)			
		Above ground biomass	Below ground biomass	Soil organic matter	Dead organic matter
1	Residential 0-4 units/acre	15	10	60	1
2	Residential 4-9 units/acre	5	3	20	0
3	Residential 9-16 units/acre	2	1	5	0
4	Residential >16 units/acre	0	0	0	0
5	Vacant	10	20	10	5
6	Commercial	0	0	0	0
7	Commercial/Industrial	0	0	0	0
8	Industrial	0	0	0	0
9	Industrial & Commercial	0	0	0	0
10	Residential & Commercial	0	0	0	0
51	Upland Forest open	75	45	85	20
52	Upland Forest Semi-closed mixed	90	60	110	30
53	Forest Closed hardwood	180	120	120	55
54	Forest Closed mixed	200	130	130	65
55	Upland Forest Semi-closed conifer	90	60	95	29
56	Conifers 0-20 yrs	10	7	76	2.5
57	Forest closed conifer 21-40 yrs	88	59	96	29
58	Forest closed conifer 41-60 yrs	165	110	115	50
59	Forest closed conifer 61-80 yrs	225	150	124	65
60	Forest closed conifer 81-200 yrs	300	200	135	85
61	Forest closed conifer older than 200 yrs	375	250	150	100
62	Upland Forest Semi-closed hardwood	80	50	100	25
66	Hybrid poplar	75	25	90	2
67	Grass seed rotation	1	1	10	0
68	Irrigated annual crop rotation	2	1	10	0
71	Grains	3	2	10	0
72	Nursery	10	3	90	1
73	Berries & Vineyards	8	5	20	0
74	Double cropping	5	2	10	0
75	Hops	5	4	20	0
76	Mint	2	1	10	0
77	Radish seed	2	1	10	0
78	Sugar beet seed	2	1	10	0

LUCODE	Land Use / Land Cover Name	Carbon (megagrams/ha)			
		Above ground biomass	Below ground biomass	Soil organic matter	Dead organic matter
79	Row crop	3	2	10	0
80	Grass	1	1	10	0
81	Burned grass	0	1	10	0
82	Field crop	3	2	8	1
83	Hayfield	5	4	23	1
84	Late field crop	5	3	15	0
85	Pasture	5	4	25	1
86	Natural grassland	6	6	20	2
87	Natural shrub	8	8	25	3
88	Bare/fallow	1	1	10	0
89	Flooded/marsh	10	5	20	0
90	Irrigated perennial	5	5	15	0
91	Turfgrass	1	1	10	0
92	Orchard	125	5	115	1
93	Christmas trees	13	28	95	2
95	Conifer Woodlot	275	30	95	10
98	Oak savanna	100	20	115	50
101	Wet shrub	7	3	25	0
102	Unknown	0	0	0	0

**Table 23. Cross-walk table for mapping HRU categories with land use/land cover type in Carbon pool dataset**

HRUCODE	HRU Description	LUCODE	Land Use / Land Cover Name
1000	Paved Forest	10	Residential & Commercial
2000	Paved Agriculture	10	Residential & Commercial
3000	Paved Commercial	10	Residential & Commercial
4000	Paved Industrial	10	Residential & Commercial
5000	Paved Low Density Residential	10	Residential & Commercial
6000	Paved Medium Density Residential	10	Residential & Commercial
7000	Paved High Density Residential	10	Residential & Commercial
8000	Paved Transportation	10	Residential & Commercial
9000	Paved Open Land	10	Residential & Commercial
10110	Developed OpenSpace-A-Low	91	Turfgrass
10120	Developed OpenSpace-A-Med	91	Turfgrass
10210	Developed OpenSpace-B-Low	91	Turfgrass
10220	Developed OpenSpace-B-Med	91	Turfgrass
10310	Developed OpenSpace-C-Low	91	Turfgrass
10320	Developed OpenSpace-C-Med	91	Turfgrass
10410	Developed OpenSpace-D-Low	91	Turfgrass
10420	Developed OpenSpace-D-Med	91	Turfgrass
11000	Forested Wetland	89	Flooded/marsh
12000	Non-Forested Wetland	101	Wet shrub
13110	Forest-A-Low	51	Upland Forest open

HRUCODE	HRU Description	LUCODE	Land Use / Land Cover Name
13120	Forest-A-Med	51	Upland Forest open
13210	Forest-B-Low	51	Upland Forest open
13220	Forest-B-Med	51	Upland Forest open
13310	Forest-C-Low	51	Upland Forest open
13320	Forest-C-Med	51	Upland Forest open
13410	Forest-D-Low	51	Upland Forest open
13420	Forest-D-Med	51	Upland Forest open
14110	Agriculture-A-Low	79	Row crop
14120	Agriculture-A-Med	79	Row crop
14210	Agriculture-B-Low	79	Row crop
14220	Agriculture-B-Med	79	Row crop
14310	Agriculture-C-Low	79	Row crop
14320	Agriculture-C-Med	79	Row crop
14410	Agriculture-D-Low	79	Row crop
14420	Agriculture-D-Med	79	Row crop
15000	Water	102	Unknown

**Table 24. InVEST carbon model results for three pilot sub-watersheds**

Total Carbon (megagrams)	Upper Hodge Brook	Lower Hodge Brook	Pilot Tributary
Predevelopment/Forested Condition	109,290	82,405	99,350
Existing Land Use/Land Cover Condition	45,628	60,065	79,233
Change in Carbon for Existing Condition	-63,662	-22,340	-20,117
Percent Change in Carbon for Existing Condition	-58%	-27%	-20%

Note: 1 megagram = 1.102 US ton

### 3.4 Conclusions

Within the study watershed, the pre-development/forested condition had lower flows across the FDC compared to the existing and fully disconnected conditions. Substantially increasing connected impervious surfaces resulted in the lowest FDC flows falling below pre-development conditions. The results appear to be largely driven by changes to ET and infiltration. A developed watershed with disconnected impervious surfaces conveyed stormflows into groundwater via infiltration but also had lower ET than the pre-development condition. As a watershed is subject to increasing amounts of directly connected impervious surfaces, ET is further reduced, as are opportunities for infiltration. Unsurprisingly, high flows increased with impervious surfaces, creating ecosurpluses. While disconnected impervious surfaces mitigated high flows, they remained elevated above pre-development conditions. The FDC for a fully disconnected scenario showed the maximum reduction in high flows as well as the largest increase in low flows.

## 4 UPDATES TO OPTI-TOOL

This subtask involved updating the user interfaces and developing VBA source codes for the Opti-Tool to adopt the functionality of groundwater/aquifer and FDC evaluation factor for the optimization from the EPA SUSTAIN version 1.2 model needed to meet the project goals. Currently, Opti-Tool is designed to optimize the treatment of overland flow, it does not include groundwater components comparable to those found in the EPA SUSTAIN model. Water that infiltrates to 'active groundwater storage' can move laterally

and contribute to baseflow, percolate to the deeper groundwater or leave the groundwater through plant uptake. Adding the functionality of a SUSTAIN aquifer unit into the Opti-Tool provides tracking and attenuating infiltration for the water balance.

## 4.1 SCM Groundwater Recharge

The following steps were carried out to add the Aquifer module in Opti-Tool:

- Reviewed the functionality of GI SCM groundwater recharge linkage to local surface waters in SUSTAIN version 1.2 developed for EPA Region 10.
- Reviewed the GI SCM interfaces and VBA source codes for the current version of Opti-Tool developed for EPA Region 1.
- Developed user interfaces to incorporate the EPA SUSTAIN's Aquifer module into the Opti-Tool spreadsheet.
- Developed VBA source codes to integrate the groundwater/aquifer component for tracking baseflow and infiltrated water from GI SCM controls in Opti-Tool.

The *Implementation Level* interface was modified to add *Aquifer Information* (Figure 35) that requires the basic information including the aquifer name, initial storage, recession coefficient, seepage coefficient, and groundwater pollutant concentration (Figure 37). The user may define multiple aquifer systems depending on the size of the watershed (Figure 36) under the *Watershed Information* user input interface.



Figure 35. Aquifer information option in Opti-Tool.

Key Information

Number of Subwatersheds:  Number of BMPs:

Number of Land Uses:

Number of Pollutants:

Number of Aquifers:

Figure 36. The number of aquifers option under Watershed Information window.

Add Aquifer Information

Aquifer ID:  Pollutant ID:

Aquifer Name:  Groundwater Conc (mg/l):

Initial Storage (ac-ft):

Recession Coefficient (1/hr):

Seepage Coefficient (1/hr):

Figure 37. Aquifer Information user interface window.

The aquifers are assigned to corresponding BMPs (Figure 38) or Conveyance (Figure 39) or Junction (Figure 40) by selecting Aquifer ID from the pulldown list on the respective interface window. The following notes describe implications for assigning aquifers to Junctions, BMPs, and Conveyance:

- Assigning an aquifer to Junctions: When an aquifer is assigned to a Junction, the groundwater component in the time series files that are added to the Junction are routed to aquifer storage.
- Assigning aquifer to BMPs: When an aquifer is assigned to a BMP, the groundwater component in the time series file that is added to the BMP is routed to the aquifer storage and the flow component that infiltrates into the background soil from the BMP is also added to the assigned aquifer storage.
- Assigning aquifer to Conveyance: When an aquifer is assigned to a stream/conduit, the released groundwater from the aquifer is routed to the conveyance. The aquifer to stream/conduit assignment is a one-to-one relationship. In other words, one aquifer can only be assigned to one conveyance, and only an individual stream/conduit can receive routed water from a single aquifer.

The groundwater inflow data in the HRU time series files are written in the column immediately following the surface runoff flow data. Once the contributing land uses (i.e., HRUs) are linked to an aquifer through either receiving junctions or BMPs, the groundwater inflow data in the time series are routed to the aquifer storage. If no aquifer is defined and linked, that column is ignored. The flow released from the aquifer to receiving streams/conduits is computed using the recession coefficient. In the case when the groundwater flow component in the time series files represents already routed flow (e.g., baseflow outflow from LSPC),

the recession coefficient should be set to 1 to allow the groundwater flow directly added to the receiving conduit without further attenuation.

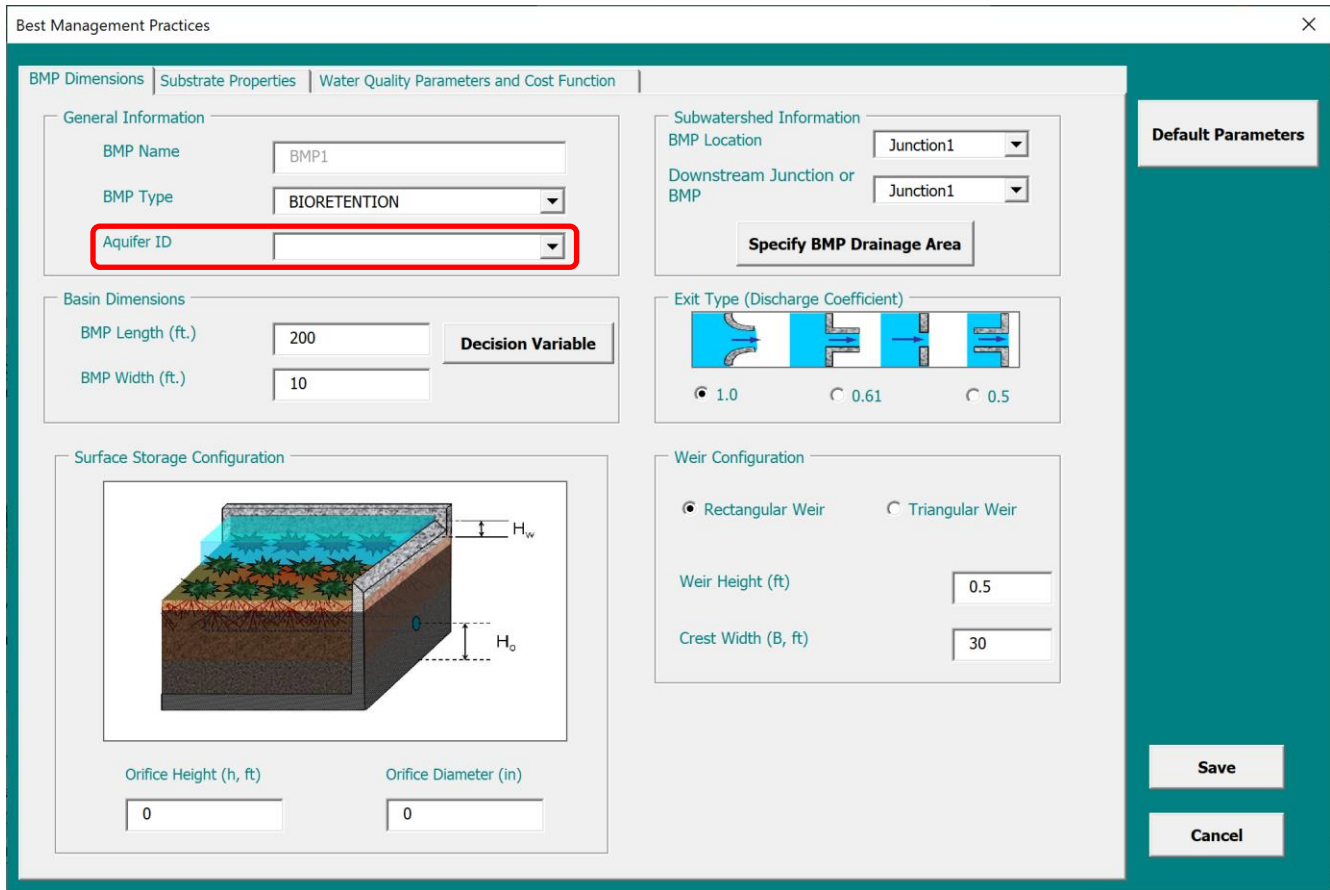


Figure 38. Aquifer selection under BMP Information user interface window.

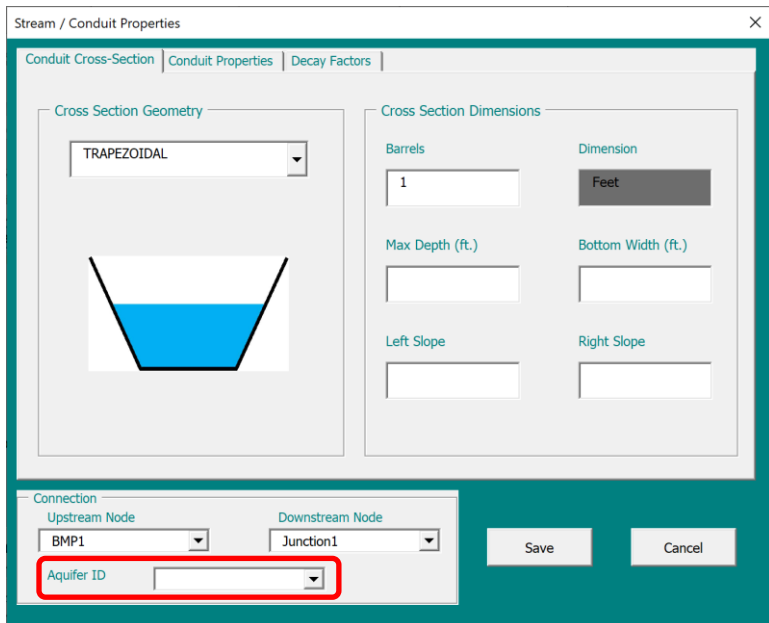
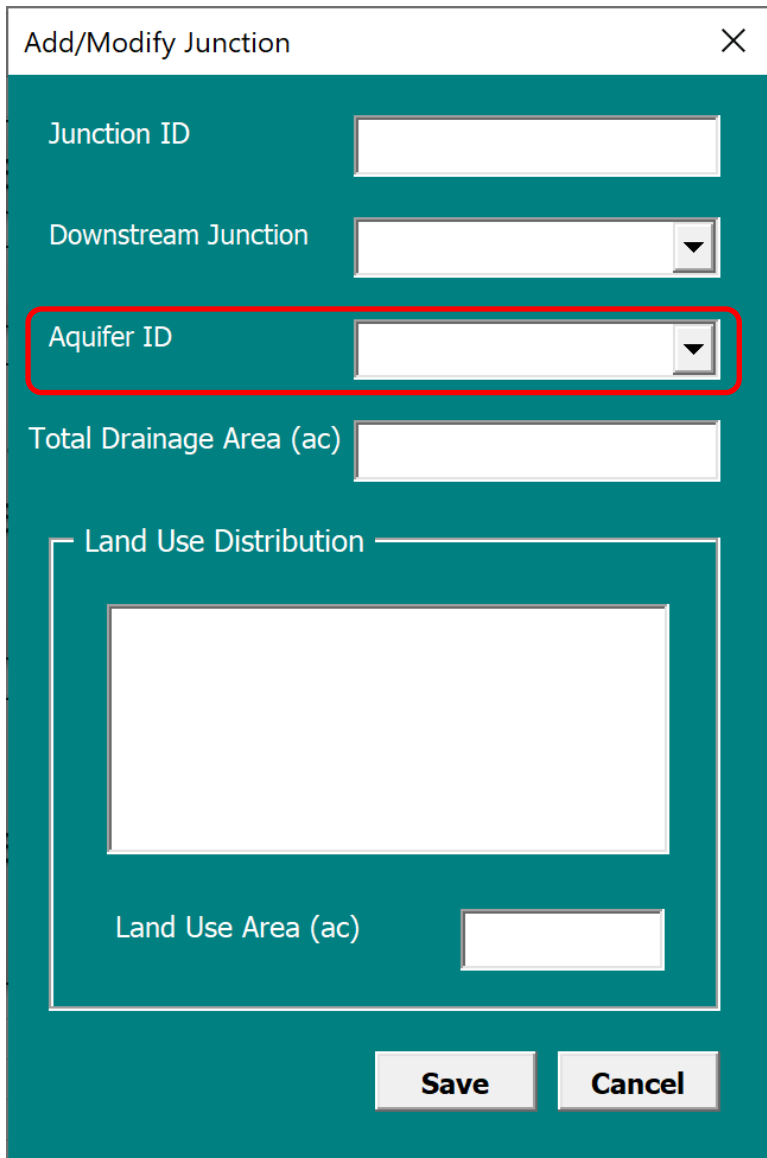


Figure 39. Aquifer selection under Stream/Conduit Properties user interface window.





The image shows a software dialog box titled "Add/Modify Junction" with a close button (X) in the top right corner. The dialog has a teal background and contains several input fields and a section for land use distribution. The fields are:

- Junction ID: A text input field.
- Downstream Junction: A dropdown menu.
- Aquifer ID: A dropdown menu, which is highlighted with a red rectangular border.
- Total Drainage Area (ac): A text input field.
- Land Use Distribution: A section containing a large empty rectangular area and a "Land Use Area (ac)" text input field below it.

At the bottom of the dialog are two buttons: "Save" and "Cancel".

Figure 40. Aquifer selection under Junction Properties user interface window.

## 4.2 Flow Duration Curve Evaluation

Following steps were carried out to add the Aquifer module in Opti-Tool:

- Reviewed the FDC evaluation factor used in the EPA SUSTAIN version 1.2 model.
- Updated the user interfaces to add the FDC evaluation factor as an option in the current version of Opti-Tool (Figure 41).
- Developed VBA source code in Opti-Tool to integrate the FDC evaluation factor for optimization simulations to identify optimal and most cost-effective management strategies to address impacts associated with the key critical flow regimes.

Management Objectives

Assessment Method: Cost-Effectiveness Curve

Assessment Point: Location (BMP or Junction): OUTLET

Evaluation Factor:

Factor Name: Flow

Factor Type: Flow Duration Curve

Factor Value 1: 0

Factor Value 2: 100

Notes:

FactorValue 1 -- if FactorType = MAC: Maximum #Days;  
 -- if FactorType = FEF: Flow Threshold (cfs)  
 -- if FactorType = FDC: Low flow limit (cfs)  
 -- all other FactorType : -99

FactorValue 2 -- if FactorType = FEF: Minimum inter-exceedance time (hr)  
 if = 0 then daily running average flow exceeding frequency  
 if = -1 then daily average flow exceeding frequency  
 otherwise minimum inter-exceedance time for simulation interval  
 -- if FactorType = FDC: High flow limit (cfs)  
 -- all other FactorType : -99

Save Cancel

**Figure 41. Flow Duration Curve selection under Optimization Setup user interface window.**

The FDC Evaluation Factor is computed as the area between the evaluated condition and pre-developed condition FDCs, measured between the user-defined upper and lower percentile flow limits. In Figure 42, the green line shows the predevelopment FDC, the blue line shows the existing condition FDC, and the brown line is the FDC with BMPs. The dashed lines show the user-defined upper and lower flow limits (or thresholds) that bound the FDC comparison. That range is determined using the predevelopment condition FDC, hence the green-colored dashed line. The orange highlighted area between the red and green lines AND that falls within the upper and lower limits is the area computed for the FDC Evaluation Factor. When using the FDC evaluation factor for optimization, the objective is to minimize the area between the two curves bounded by the green and brown lines AND ALSO bounded by the upper and lower percentile thresholds; flows outside of the target range are not considered.

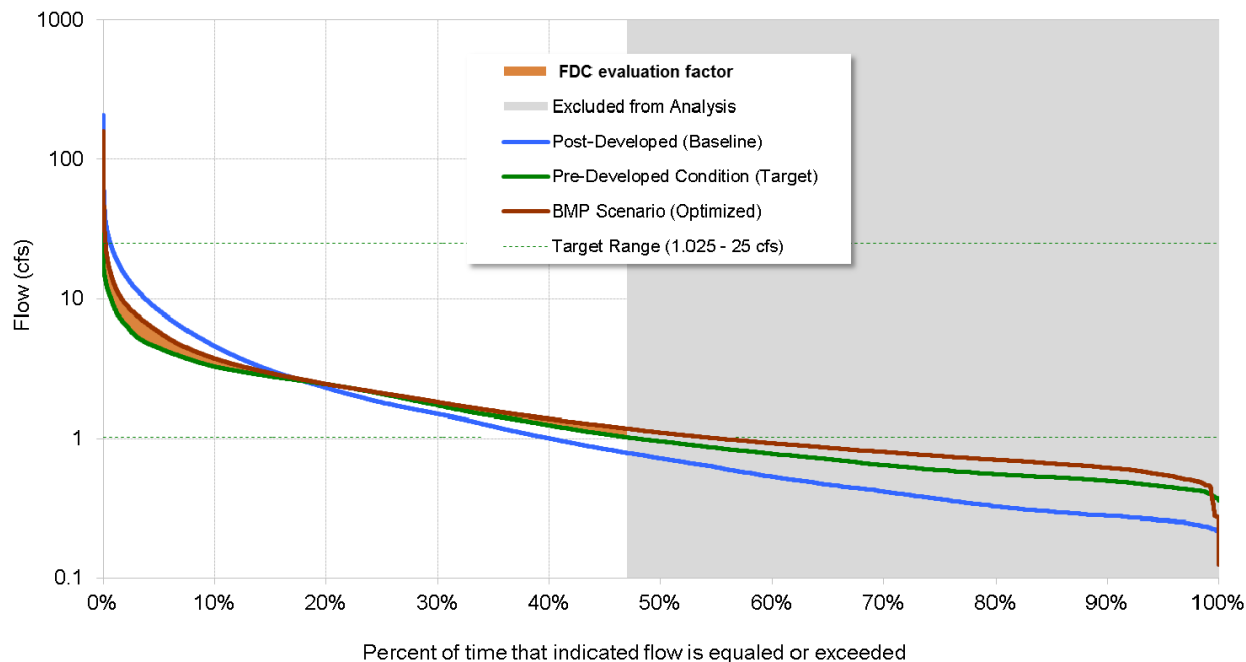


Figure 42. Flow Duration Curve evaluation factor.

## 5 NEXT STEPS

Task 7 of the FDC 1 project includes performing GIS-based screening to identify SCM opportunities within selected three sub-watersheds and optimizing those opportunities to identify the most cost-effective types and sizes that achieve the FDC objective. Management strategies that may include both structural controls and non-structural practices such as land-use conversion will be identified as a suite of innovative GI SCMs for disconnecting impervious cover.

### 5.1 GIS Screening to Identify SCM Opportunities

The approach to identifying the SCM opportunities will be based on the approach used in EPA Region 1's Tisbury, MA Impervious Cover Disconnection Project [LINK](#). A GIS spatial data analysis will be performed to identify potential stormwater control technologies that would be technically feasible based on the available GIS data at this time. Management categories will include consideration of the following physical characteristics:

- Land use
- Impervious cover
- Landscape slope
- Hydrologic soil group
- Distance to impervious cover

Management categories will preferably be considered for areas with pervious cover based on the suitability of site conditions for BMPs to treat stormwater runoff from impervious cover and reduce pollutant loads. The suitability of site conditions is assessed using a combination of thresholds and attributes describing the physical characteristics represented in the GIS data. Table 25 presents the proposed matrix of suitability criteria and management categories for this study.

**Table 25. Site suitability criteria for stormwater management categories**

Land Use	Within 200 feet of impervious surface	Landscape Slope (%)	Within FEMA Hazard Areas	Within Wellhead Protection Zone	Within Active River Area	Within Wetland	Within 25 feet of Structure?	Soil Group	Management Category	SCM Type(s) in Opti-Tool
Pervious Area	Yes	<= 15	Yes	Yes	Yes	Yes	Yes	All	SCM with complicating characteristics	--
			No	No	No	No	No	A/B/C	Infiltration	Surface Infiltration Basin (e.g., Rain Garden)
		D	Biofiltration	Biofiltration (e.g., Enhanced Bioretention with ISR and underdrain option)						
	> 15	--	--	--	--	--	--	SCM with complicating characteristics	--	
No	--	--	--	--	--	--	--	No SCM opportunity	--	
Impervious Area	<= 5	<= 5	Yes	Yes	Yes	Yes	Yes	All	SCM with complicating characteristics	--
			No	No	No	No	No	A/B/C	Infiltration	Infiltration Trench
		D	Shallow filtration	Porous Pavement						
	> 5	--	--	--	--	--	--	SCM with complicating characteristics	--	

## 5.2 SCM Modeling with FDC Optimization Objective

---

The proposed hydrograph attenuation approach, which is being called the Multi-Objective Inclusive Solution Technique (MOIST) and presented in detail in previous technical memo 5 will be used for modeling the management scenarios. The MOIST approach will be adapted for application in the Opti-Tool for the Wading River watershed. A series of progressively increasing storms will be used to build a composite optimized solution matrix. An alternative set of future storms will be used to stress test system resiliency of both the baseline model and optimized management plans. Other features such as extreme wet and drought periods can also be mined from the time series and used for staging and testing model scenarios. Future climate time series will also be pushed through the optimized SCM footprints to assess the resiliency of the proposed plans toward mitigating future climate change impacts.

## 5.3 Final Project Report

---

We will compile all technical memorandums developed under each subtask and will prepare a draft written project report that documents all work performed during Phase 1 of this project. We will address the comments received on the draft report from the TSC and the EPA Project Team. The final project report will also describe how the work conducted under Phase 1 will be applied to accomplish the objectives of Phase 2 work to develop wise water resource management strategies for future watershed development activities.

## 5.4 Outreach Materials

---

We will prepare outreach materials that provide brief project information summaries for efficiently conveying key messages, lessons learned, and valuable water resource management information to watershed management practitioners including local, state, and federal government representatives. Outreach materials will be developed to effectively communicate key findings including discussion of relationships between watershed function, land use development and water resource impacts in low-order stream systems, and larger down-gradient waters resources (e.g., lakes, coastal waters, aquifers, etc.). The information summaries will be designed with accompanying graphics and tables to convey water resource impacts associated with inadequately managed IC conversion and the potential quantitative benefits of feasible watershed restoration activities/strategies identified in this study.

## 6 REFERENCES

- Barbaro, J.R., Sorenson, J.R., 2013. Nutrient and sediment concentrations, yields, and loads in impaired streams and rivers in the Taunton River Basin, Massachusetts, 1997–2008: U.S. Geological Survey Scientific Investigations Report 2012–5277.
- Bent, G.C., Waite, A.M., 2013. Equations for Estimating Bankfull Channel Geometry and Discharge for Streams in Massachusetts. USGS Scientific Investigations Report 2013–5155.
- Bhaskar, Aditi Seth, Beesley, L., Fletcher, T.D., Hamel, P., 2016. Will it rise or will it fall ? Managing the complex effects of urbanization on base flow. *Freshw. Sci.* <https://doi.org/10.1086/685084>
- Bhaskar, Aditi S., Hogan, D.M., Archfield, S.A., 2016. Urban base flow with low impact development. *Hydrol. Process.* 30, 3156–3171. <https://doi.org/10.1002/hyp.10808>
- Demaria, E.M.C., Palmer, R.N., Roundy, J.K., 2016. Regional climate change projections of streamflow characteristics in the Northeast and Midwest U.S. *J. Hydrol. Reg. Stud.* 5, 309–323. <https://doi.org/https://doi.org/10.1016/j.ejrh.2015.11.007>
- Donigian, A.S., 2000. HSPF Training Workshop Handbook and CD. Lecture #19. Calibration and Verification Issues. Prepared for U.S. Environmental Protection Agency. Washington DC.
- Hayhoe, C.P., Wake, T.G., Huntington, L., Luo, M.D., Schrawtz, J., Sheffield, E., Wood, E., Anderson, B., Bradbury, A., Degaetano, T.J., Wolfe, D., 2006. Past and Future Changes in Climate and Hydrological Indicators in the U.S. Northeast. *Clim. Dyn.* 28, 381–707. <https://doi.org/10.1007>
- Hopkins, K.G., Morse, N.B., Bain, D.J., Bettez, N.D., Grimm, N.B., Morse, J.L., Palta, M.M., Shuster, W.D., Bratt, A.R., Suchy, A.K., 2015. Assessment of regional variation in streamflow responses to urbanization and the persistence of physiography. *Environ. Sci. Technol.* 49, 2724–2732. <https://doi.org/10.1021/es505389y>
- Hwang, S., Graham, W.D., 2014. Assessment of Alternative Methods for Statistically Downscaling Daily GCM Precipitation Outputs to Simulate Regional Streamflow. *JAWRA J. Am. Water Resour. Assoc.* 50, 1010–1032. <https://doi.org/https://doi.org/10.1111/jawr.12154>
- International Institute for Applied Systems Analysis, 2009. Representative Concentration Pathways (RCP) Database, version 2.0 [WWW Document]. URL <http://www.iiasa.ac.at/web-apps/tnt/RcpDb/>.
- Jewell, T.K., Nunno, T.J., Adrian, D.D., 1978. Methodology for Calibrating Stormwater Models. *J. Environ. Eng. Div.* 104, 485–501. <https://doi.org/10.1061/JEEGAV.0000772>
- Leopold, L.B., 1994. *A view of the river*. Harvard University Press, Cambridge, MA.
- Li, C., Fletcher, T.D., Duncan, H.P., Burns, M.J., 2017. Can stormwater control measures restore altered urban flow regimes at the catchment scale? *J. Hydrol.* 549, 631–653. <https://doi.org/10.1016/j.jhydrol.2017.03.037>
- Moriasi, D.N., Gitau, M.W., Pai, N., Daggupati, P., 2015. Hydrologic and water quality models: Performance measures and evaluation criteria. *Trans. ASABE* 58, 1763–1785. <https://doi.org/10.13031/trans.58.10715>
- Nash, J.E., Sutcliffe, J. V., 1970. River flow forecasting through conceptual models part I—A discussion of principles. *J. Hydrol.* 10, 282–290.
- Sloto, R.A., and Crouse, M.Y., 1996, HYSEP: A Computer Program for Streamflow Hydrograph Separation and Analysis: U.S. Geological Survey Water-Resources Investigations Report 1996–4040, 46 p., <https://pubs.er.usgs.gov/publication/wri964040>.